INFORMATION TO USERS

This manuscript has been reproduced from the microfilm master. UMI films the text directly from the original or copy submitted. Thus, some thesis and dissertation copies are in typewriter face, while others may be from any type of computer printer.

The quality of this reproduction is dependent upon the quality of the copy submitted. Broken or indistinct print, colored or poor quality illustrations and photographs, print bleedthrough, substandard margins, and improper alignment can adversely affect reproduction.

In the unlikely event that the author did not send UMI a complete manuscript and there are missing pages, these will be noted. Also, if unauthorized copyright material had to be removed, a note will indicate the deletion.

Oversize materials (e.g., maps, drawings, charts) are reproduced by sectioning the original, beginning at the upper left-hand corner and continuing from left to right in equal sections with small overlaps.

Photographs included in the original manuscript have been reproduced xerographically in this copy. Higher quality 6" x 9" black and white photographic prints are available for any photographs or illustrations appearing in this copy for an additional charge. Contact UMI directly to order.

ProQuest Information and Learning
300 North Zeeb Road, Ann Arbor, MI 48106-1346 USA
800-521-0600

UMI®

DISSERTATION

CONTROL OF AMINO ACID STARVATION-INDUCED APOPTOSIS IN CHO CELL CULTURES

Submitted by

Laurent Simon

Chemical and Bioresource Engineering

In partial fulfillment of the requirements

for the Degree of Philosophy of Science

Colorado State University

Fort Collins, Colorado

Fall 2001

ProQuest Information and Learning Company
300 North Zeeb Road
P.O. Box 1346
Ann Arbor, MI 48106-1346

COLORADO STATE UNIVERSITY

October 27, 2001

WE HEREBY RECOMMEND THAT THE DISSERTATION PREPARED UNDER OUR SUPERVISION BY LAURENT SIMON ENTITLED CONTROL OF AMINO ACID STARVATION-INDUCED APOPTOSIS IN CHO CELL CULTURES BE ACCEPTED AS FULFILLING IN PART REQUIREMENTS FOR THE DEGREE OF DOCTOR OF PHILOSOPHY.

Committee on Graduate Work

Adviser

Department Head/Director

ABSTRACT OF DISSERTATION

CONTROL OF AMINO ACID STARVATION-INDUCED APOPTOSIS IN CHO CELL CULTURES

This research was dedicated to the study of amino acid starvation-induced apoptosis in CHO cell cultures. The two mechanisms of cell death reported in the literature are necrosis and apoptosis. Necrosis is a passive process that occurs when the cells are exposed to extreme environmental or physiologic stresses. In apoptosis or programmed cell death (PCD), the cells are induced to commit suicide under normal physiological conditions. The study of apoptosis is very important to biotechnology due to the extensive use of animal cell cultures for the production of useful proteins. However, the productivity of recombinant mammalian cells is limited by the rate at which cells die right after reaching a maximum cell density. For mammalian cells, PCD is a way of life and can be induced in response to several stress related phenomena including starvation-induced conditions during the declining phase of a batch culture. In order to control starvation-induced apoptosis in a fed-batch reactor, a mathematical model of mammalian cell culture kinetics is paramount. However, classical kinetic models do not distinguish between death by necrosis or apoptosis. In this work, we extended classical kinetic models to account for apoptotic cell death in real-time. Neural network based sensitivity analysis identified glutamine and asparagine as two major amino acids that play a key role in the suppression of apoptosis.

Advanced process control concepts are usually tested using a simulated system. This works shows that a non-classical control algorithm can be implemented in a discrete fashion on real processes with satisfactory results. Kalman filters and model predictive controllers were implemented to delay starvation-induced apoptosis in CHO cell cultures. The off-line measured concentrations of viable and total cells, lactate, and glucose were used to update the state estimates. A NN was then used to approximate the concentration of apoptotic cells in the bioreactor based on the concentrations of viable cells, glutamine and asparagine. This information was then fed to a model predictive controller that was activated when the apoptotic cells reached a concentration of 1.0×10^5 cells/ml.

Laurent Simon
Department of Chemical
and Bioresource Emgineering
Colorado State University
Fort Collins, Colorado, 80523
Fall 2001

ACKNOWLEDMENTS

I would like to thank my advirer. Dr. M. Nazmul Karim for his advice. and support. Special thanks also go to Dr. James C. Linden. Dr. Brian Batt. and Dr. Vince G. Murphy for serving on my committee. I am also thankful to my family and friends for their encouragement. and to the UNCF-Merck Graduate Science Research Dissertation Fellowship for financial support.

TABLE OF CONTENTS

LIST OF TABLES

LIST OF FIGURES

Chapter 1

INTRODUCTION

1.1 Motivation

Apoptosis - programmed cell death (PCD) - is a mode of cell death essential to the homeostasis and development of multicellular organisms. The regulation of apoptosis is of interest for the optimization of biological processes. Animal cell cultures are widely used in biotechnology for the development of therapeutic and diagnostic agents (Dickson, 1998). Mammalian cells produce a variety of complex proteins such as Hepatitis B virus surface antigen, glycoprotein D of the Herpes Simplex virus, tissue type plasminogen activator, monoclonal antibodies, and interferon-gamma (Hu and Himes, 1989). The complex structural nature of these therapeutic proteins and their requirement for post-translational modifications makes mammalian cells a good host for complete expression of the proteins (Dickson, 1998). However, as noted by Murray et al. (1996), the productivity of recombinant mammalian cell lines in batch culture is limited by the rate at which cells die right after reaching a maximum cell density. Because of apoptosis, maintaining cell viability in mammalian cells is a challenge. For hybridoma, myeloma, and CHO cells, PCD is a way of life and can be induced in response to several stress conditions including starvation-induced conditions during the decline phase of batch culture (Singh et al., 1994; Franek et al., 1992; Mercille and Massie, 1994). A major branch of apoptosis research focuses on the identification of the molecular components of

PCD including sensors and triggers as well as different mechanisms to regulate PCD. The tumor suppressor *p53* is regarded as a sensor of apoptosis (Donehower and Bradley, 1993). *p53* has been identified as a DNA-binding protein and transcriptional activator that may be instrumental to DNA repair because it accumulates after the cell's DNA has been damaged (Donehower and Bradley, 1993). Consequently, *p53* may serve as a sensor of DNA damage. The motivation for this research is twofold. From an industrial point of view, the goal is to prolong the stationary phase in cultivations by preventing apoptosis as much as possible (up regulation) so that the recombinant protein of interest can be produced for a longer period, thus giving a higher titer of protein. This will ultimately minimize the down-stream processing cost. The second goal is to understand starvation-induced apoptosis as a result of changes in key amino acids in the medium.

1.2 Outline and Summary of Contributions

The initial work outlined in Section 1.2.1 is a study of programmed cell death (PCD) as a result of amino acid limitation. The applications of a neural network to model PCD were investigated and a connection between amino acid starvation and the onset of apoptosis was established. Apoptotic cell death is a nonlinear function of viable cells and key amino acids. Section 1.2.2 describes the applications of model predictive controllers (MPCs) to a nonlinear process: the control of dissolved oxygen in a shear sensitive environment. Also, key acids that played a role on the onset of apoptosis and an expression for the concentrations of apoptotic cells in terms of these amino acids had to be determined. Section 1.2.3 describes a neural network based sensitivity analysis approach to select the relevant amino acids. The methodology was also tested on an industrial

process to explain the protein yield based on fermentation states. A simulation was run to test the hypothesis that glutamine and asparagine would control PCD (Section 1.2.4). Kalman filters was used to monitor the concentration of apoptotic CHO cells (predicted by a neural network) in a 3-l bioreactor. MPC was implemented to calculate the inlet flow rates of glucose, glutamine and asparagine (Section 1.2.5).

1.2.1 Modeling and Understanding of Apoptosis in CHO Cells

The study of apoptosis has become critical for mammalian cell culture based processes. Development of the field is reviewed and the relevance of apoptotic research on productivity of bioreactors is underlined in the present work. Most studies include extreme starvation of cells on one amino acid. No model is explicitly formulated, which impedes further development in terms of controlling apoptosis with a fed-batch scheme. In this paper, a NN is used to model starvation-induced apoptosis on glutamine and asparagine. The initial conditions are also used in the model since, in actual implementation, the initial concentrations may be different from that of the training and testing phases. The inputs to the network are the differences in concentration of viable cells, glutamine, and asparagine from their initial values. A bias plot showed that the NN performed very well on training and testing data.

The main contribution of this work is that it establishes a clear connection between the concentration of certain amino acids and apoptosis. It provides a justification for the use of these key amino acids to control starvation-induced apoptosis. Instead of deriving kinetic models, NN can be used to approximate the concentration of apoptotic cells. The

outlined methodology makes it more suitable for control of programmed cell death in a bioreactor.

1.2.2 Identification and Control of Dissolved Oxygen in Hybridoma Cell Culture in a Shear Sensitive Environment

The productivity of mammalian cells can be enhanced by facilitating adequate oxygen transfer into the cultivation medium. However, current methods of controlling dissolved oxygen (DO) fail to account for alterations in medium composition during the course of the fermentation. These changes, which directly affect gas solubility and overall mass transfer coefficient, may be significant and deteriorate the controller's performance in the long run. In this paper, the applications of Generalized Predictive Controllers (GPC) to DO control were investigated in a shear sensitive environment and compared to PID and Model Predictive Controllers (MPC). Input and output data for system identification were initially generated by varying the composition of oxygen fed into the bioreactor from 0 to 0.21 mole % while keeping the total inlet gas flow rate at 8.75 vvm. The process was identified using an AutoRegressive model with eXogeneous inputs (ARX) model and tested on different data sets. The model parameters were then correlated with the overall mass transfer coefficients. In simulation tests, the output of the PID controller switched from minimum to maximum values while more continuous control signals were obtained with the MPC and GPC controllers. When tested in a cell-free medium, all three controllers were able to track setpoint changes with some chattering observed in the control signals. The GPC outperformed the MPC and PID controllers when applied to the cultivation of hybridoma cells.

The main contribution of this paper is the applications of GPC to monitor the overall mass coefficients in real time. This work can be extended to monitor meaningful biological parameters without the use of expensive sensors.

1.2.3 Data-based Analysis of Bioprocesses

Bioprocesses offer a particular modeling challenge in view of their complexity and nonlinearity. These processes are very difficult to model and, as a result, difficult to control. Data mining has been used in an attempt to understand the biological nature of various processes. Two case studies are described in this article. The first one deals with the modeling of apoptosis based on the concentrations of viable cells, glutamine and asparagine. An autoregressive exogenous model accurately predicted the concentration of apoptotic cells using 1, 2, and 5-step ahead predictions. The second case study investigated the applications of artificial NNs to model the dynamics of an industrial bioprocess. The inputs to the model were the optical density of the cell culture, specific growth rate, pH, temperature, stirring rate, dissolved oxygen concentration, working volume, volume of added base, concentration of glucose, and the conductance of the cultivation sample. The output variable was the yield of protein in the bioreactor. This procedure assumes that the optical density of the cell culture correlates very well with the concentration of viable cells. By combining correlation map, partial correlation and NN based sensitivity analyses, it was possible to prune the number of input variables, which increased the performance of the NN.

The main contributions can be summarized as follows: an input-output model (ARX) was used to model apoptotic cells as a function of the concentration of viable cells,

glutamine and asparagine. This work illustrate the use of statistical techniques such as correlation map, partial correlation and NN based sensitivity analyses to identify process variables affecting industrial fermentation processes.

1.2.4 Control of Starvation-induced Apoptosis in CHO Cell Cultures

The application of the Unscented Kalman Filter was investigated to control starvation-induced programmed cell death – apoptosis – in CHO cells. Neural network (NN) based sensitivity analysis identified glutamine and asparagine as two major amino acids that play a key role in the suppression of apoptosis. Dynamic equations that accounted for the dependence of apoptotic cells on the concentrations of viable cells, glutamine and asparagine were derived. These state equations were highly nonlinear and included nine state variables. An oxygen mass balance was written in the liquid phase. It served as the output equation for the Unscented Kalman Filter. Using the oxygen uptake rate as the observer, it was possible to estimate the states. A model predictive controller was then implemented once the apoptotic cells reached a concentration of 1.1×10^4 cells/ml in the bioreactor, taking into account the operating range of the flow cytometer and measurement error. The manipulated variables were the flow rates of glucose, glutamine and asparagine. Simulation results show that the controller was able to keep the apoptotic cells at a concentration of 1.1×10^4 cells/ml.

The main contributions of this work are: 1) a framework was developed for real-time control of apoptosis based on easily measurable quantities such as the concentration of dissolved oxygen; 2) model predictive control was used to control apoptosis; 3) classical cell growth models were extended to include the concentration of apoptotic cells

as a function of key amino acids that were found to delay the onset of apoptosis; 4) a NN sensitivity analysis was used to select anti-apoptotic amino acids, which were used to control PCD. Although a lack of other nutrients, such as glucose, can cause apoptotic death in some mammalian cells, previous research designed to investigate cell death had focused more closely on the effect of amino acids on apoptosis.

1.2.5 Advanced Process Control in CHO Cell Culture Processes: Experimental Studies

Advanced process control concepts are usually tested using a simulated system. This article shows how a non-classical control algorithm can be implemented in a discrete fashion on real processes with satisfactory results. Kalman filters and model predictive controllers were implemented to delay starvation-induced apoptosis in CHO cell cultures. Apoptosis was mostly caused by deprivation of glutamine and asparagine in the medium. The concentrations of the state variables were estimated every 15 hours by forward integration of the first-principle mathematical model of the process. The off-line measured concentrations of viable and total cells, lactate, and glucose were used to update the state estimates. A NN was then used to approximate the concentration of apoptotic cells in the bioreactor based on the concentrations of viable cells, glutamine and asparagine. This information was then fed to a model predictive controller that was activated when the apoptotic cells reached a concentration of 1.0×10^5 cells/ml. This value is different from the set point of 1.0×10^4 cells/ml chosen for the simulation. Implementation issues are discussed including the integration of off-line measurements, computational methods, and flow delivery constraints into discrete fed-batch control of complex biological processes.

This work employed a novel methodology to control apoptosis in real-time. A model predictive controller was used to control apoptotic cells at a concentration 1.0×10^5 cells/ml. The maximum concentration of apoptotic cells was reduced from 1.5×10^5 cells/ml to 1.1×10^5 cells/ml. A higher protein productivity was also obtained: 0.054 mg/(viable cells .h) for the fed-batch as compared to 0.014 mg/(viable cells .h) for the batch operation. This contribution proves that it is possible to increase protein production by minimizing the concentration of apoptotic cells.

1.2.6 References

Dickson, AJ. 1998. Apoptosis regulation and its applications to biotechnology. Science 16:339-342.

Donehower, LA, Bradley, A. 1993. The tumor suppressor p53. Biochemica et Biophysica Acta 1155:181-205.

Franek, F, Vomastek, T, Dolnikova, J. 1992. Fragmented DNA and apoptotic bodies document the programmed way of cell death in hybridoma cultures. Cytotechnology 9:117-123.

Hu, WS, Himes, VB 1989. Considerations of mammalian cell metabolism in bioreactors. In: Pages 33-46 Springer-Verlag New York, Inc., New York, NY.

Mercille, S, Massie, B. 1994. Introduction of apoptosis in nutrient-deprived cultures of hybridoma and myeloma cells. Biotechnology and Bioengineering 44:1140-1154.

Murray, K, Ang, CE, Gull, K, Hickman, JA, Dickson, AJ. 1996. NS0 myeloma cell death: influence of bcl-2 overexpression. Biotechnology and Bioengineering 51:298-304.

Singh, RP, Al-Rubeai, M, Gregory, CD, Emery, AN. 1994. Cell death in bioreactors: A role for apoptosis. Biotechnology and Bioengineering 44:720-726.

Chapter 2

MODELING AND UNDERSTANDING OF APOPTOSIS IN CHO CELLS

2.1 Introduction

2.1.1 Overview of Apoptosis

The study of apoptosis - programmed cell death (PCD) - is very important to biotechnology. The use of animal cells for the development of industrial therapeutics or diagnosis reagents is so widespread that Biotechnology is often referred to as the use of animal-cell cultures for the production of useful protein products (Dickson, 1998). Mammalian cells produce a variety of complex proteins such as Hepatitis B virus surface antigen, glycoprotein D of the Herpes Simplex virus, tissue type plasminogen activator, monoclonal antibody, and interferon-gamma (Hu and Himes, 1989). The complex structural nature of these therapeutic proteins and their requirement for post-translational modifications makes mammalian cells a good host for complete expression of the proteins (Dickson, 1998). However, as noted by Murray *et al.*, the productivity of recombinant mammalian cell lines in batch culture is limited by the rate at which cells die right after reaching a maximum cell density (Murray et al., 1996). Thus, because of apoptosis, maintaining cell viability in mammalian cells is a challenge. For hybridoma, myeloma, and CHO cells, PCD is a way of life and can be induced in response to several stress

conditions, including starvation, during the decline phase of batch culture (Singh et al., 1994; Franek et al., 1992; Mercille and Massie, 1994).

The two mechanisms of cell death reported in the literature are necrosis and apoptosis (Wyllie et al., 1980). Necrosis, also called accidental cell death or pathological cell death, is a passive process that occurs when the cells are exposed to extreme physiologic or environmental stresses. The physiological stresses may be due to a lack of oxygen, a mechanical damage, or an exposure of the cells to toxic chemicals. Under these conditions, the cells are no longer able to maintain homeostatis, which leads to a cellular edema, extracellular ions and the eventual osmotic lysis of the cell. The contents of the cytoplasm leak out, leading to an intensive inflammation of surrounding tissues (Van Furth and Van Zwet, 1988). In necrotic death, the cells respond to pathologic changes initiated outside of the cells. These changes can be elicited by a large series of factors that trigger a change in the permeability of the plasma membrane. The cells play a passive role in initiating the process of death. On the contrary, in PCD the cells participate actively in the death mechanism (Wyllie et al., 1980).

Apoptotic cells are induced to commit suicide under normal physiological conditions. PCD is crucial to the normal development and homeostatis of multicellular organisms and can be used to kill cells infected by virus and cancerous cells (Reed, 1994; Oltvai and Korsmeyer, 1994; Nunez and Clarke, 1994; Korsmeyer, 1995). PCD occurs normally at different stages of morphogenesis - in the growth and development of metazoans and in normal turnover in adult tissue. Once initiated, PCD leads to a cascade of biochemical and morphological events that result in irreversible degradation of the genomic DNA and fragmentation of the cell (Wyllie et al., 1980; Cohen, 1993; Steller,

1995). The chromatin condenses and migrates to the nuclear membrane. Internucleosomal cleavage, that leads to laddering of DNA at the junction of nucleosomes, is noticed (Reed, 1994). The cytoplasm shrinks without membrane rupture. Blebbing of plasma and nuclear membranes is observed. The cell contents are then packaged in vesicles called apoptotic bodies which are immediately engulfed by phagocytic cells (Savill et al., 1989). Epitopes appear on the plasma membrane marking the cells as a phagocytic membrane.

According to Denmeade and Isaacs, the overall cell cycle, which controls cell number, can be divided into a system with different compartments (Denmeade and Isaacs, 1996). Initially, cells metabolically active in the G_o phase can undergo mitosis (M phase) by the following pathway: the G_o cells enter the G_1 phase in which the number of organelles and cell size double. The fully developed cells undergo DNA synthesis and chromosomal replication in the S phase before entering the G_2 phase followed by mitosis (M phase). Cells belonging to the G_o phase can also die directly by necrosis or enter the apoptotic pathway: G_o -> D_1 -> F ->D_2-> apoptotis.

The period of DNA fragmentation (F phase) can also be used to divide the sequences of events that lead to PCD (Berges et al., 1993). During the D_1 phase of apoptosis, genes previously expressed by the cells are repressed, while other genes previously repressed are expressed (Furuya and Isaacs, 1993; Smeyne et al., 1993; Deng and Podack, 1993). In the study conducted by Deng and Podack (1993), apoptosis was suppressed in a cytotoxic T-cell line by expression of interleukin 2-mediated gene and deregulation of the protooncogene bcl-2. As a result of these epigenetic changes, the double-stranded DNA fragments during the F phase (Denmeade and Isaacs, 1996). The

nuclear morphology of the cell changes while the plasma and lysosomal membranes remain intact. The mitochondria are still functional at this stage (Denmeade and Isaacs, 1996). The D_2 phase follows the F phase. In the D_2 phase, proteases are activated, including the interleukin-1 beta converting enzyme (ICE)-like proteases that hydrolyzes poly(ADP-ribose) polymerase (Lazebnik et al., 1994). The lamins of the nuclear membrane are degraded by other ICE-like proteases. Even the nucleus itself is subject to fragmentation.

It is important to note that cells in any phase of the cycle can be induced to undergo apoptosis (Denmeade and Isaacs, 1996). As a result, the different phases of the cell cycle do not provide any information about the accumulation of apoptotic cells in the bioreactor. Therefore, from a control viewpoint, the cell cycle cannot be used as an observer or measurement to control PCD. An efficient control strategy should, instead, be based on the concentration of apoptotic cells, the accumulation of pro-apoptotic molecules in the bioreactor, or the genes necessary to activate the death machinery. Targeting the genes necessary to stop (or induce) PCD would result in a better control of apoptotic death since, as described in the next paragraph, these genes are responsible for the activation of the death machinery. However, this procedure would be difficult to implement in real-time.

Metabolic engineering approaches to control apoptosis focuses on three types of genes. The first type of gene (Type-I gene) generates the signal transduction necessary to activate the death machinery in healthy and undamaged cells. The same gene can simulate cell proliferation and PCD depending on the differentiation status of the cell (Denmeade and Isaacs, 1996). Transforming growth factor-β (TGF-β1) is such a gene (Martikainen et al., 1990). Type-II genes encode proteins involved in determining the sensitivity of the

cell to PCD activated by radiation, viral infection, chemotherapy or any other pathological damage to the cell. *p*53 and *bcl*-2 are type-II genes. *p*53 increases the sensitivity of the cells to activation of PCD while *bcl*-2 decreases the sensitivity of the cells to apoptosis caused by damaging chemicals such as alkylating or mitogenic agents (Fig. 4.1) (Denmeade and Isaacs, 1996).

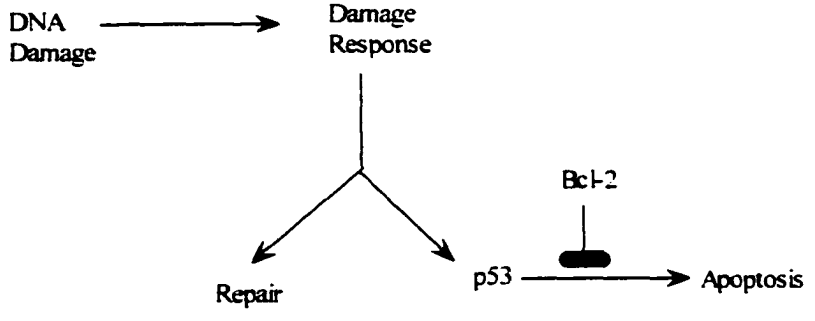

Figure 2.1 DNA damage leads to apoptosis.

This distinction helps to explain the use of *bcl*-2 gene to delay the onset of apoptosis in mammalian cells (Singh et al., 1997). According to Nunez and Clarke, *bcl*-2 genes regulates cell death and survival (Nunez and Clarke, 1994). The third type of gene (Type-III gene) involved in apoptosis, encodes proteins that form the machinery needed for the process of cell death itself (Denmeade and Isaacs, 1996). Loss of function of type-III genes would stop the cell from undergoing apoptosis regardless of the treatment used.

In *Caenorhabditis elegans*, two genes have been identified to play a key role in the onset of apoptosis: CED-3, which is a cysteine protease or caspase that cleaves certain

proteins after aspartic residues (Ashkenazi and Dixit, 1998) and CED-4 (Hengartner and Horvitz, 1994). A member of this family, caspase-3 is a key mediator of apoptosis in mammalian cells. CED-9, also found in *C. elegans*, has been shown to inhibit apoptosis (Hengartner and Horvitz, 1994). The role of CED-4 is to bind to CED-3 and promote its activation, whereas CED-9 binds to CED-4 and prevents it from activating CED-3 (Chinnaiyan et al., 1997; Seshagiri and Miller, 1997; Spector et al., 1997). Molecules bind specific receptors on the cell surface and signal the onset of PCD. EGL-1, for example, binds CED-9 and causes CED-9 to dissociate from CED-4 and CED-3 (Ashkenazi and Dixit, 1998). This dissociation triggers a sequential activation of one caspase by another creating an expanding cascade of proteolytic activity, starting with CED-3 activation and ultimately causing the affected cells to die by apoptosis (Fig. 4.2) (Ashkenazi and Dixit, 1998).

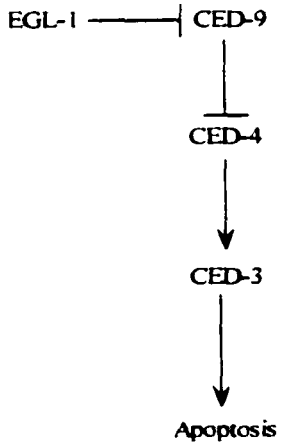

Figure 2.2 Apoptotic pathway in *C. elegans*

2.1.2 Apoptosis Research

Normal metazoan development and health require a sophisticated strategy to control apoptotic cell death. In fact, the onset of apotosis is the result of the ability or tendency of a cell to maintain homeostatis by adjusting its physiological processes. Apoptosis is critical for important biological processes such as morphogenesis, tissue homeostasis, elimination of injured or virally infected cells, and elimination of self-reactive clones from the immune system (Steller, 1995). Although PCD is crucial to the normal development and health of mammalian cells, early or late activation of the death machinery may result in a number of diseases, for example, AIDS, neurogenerative disorders, and ischemic injury (Thompson, 1995). In contrast, unhibited apoptosis may be the precursor of diseases such as cancer, autoimmune disorders, and viral infections (Thompson, 1995).

In his genetic studies involving *C. elegans*, Steller identified mutations in 14 genes that affect apoptosis (Steller, 1995). Two of these genes, CED-9 and CED-3 (cell death defective), were homologous to mammalian genes: the proto-oncogene *bcl*-2 and ICE (interleukin-1-ß-converting enzyme), respectively. Recent work illustrated the important roles of these genes in controlling PCD (Singh et al., 1997). Reed also showed that *bcl*-2 is associated with intracellular membranes of mitochondria, endoplasmic reticulum, and nuclei (Reed, 1994). This protein takes part in the regulation of the redox potential of the cell. Ecotopic expression of *bcl*-2 suppresses cell death triggered by oxidizing agents (Hockenbery et al., 1993). In fact, genetic evidence indicates that CED-9/*bcl*-2 belongs to a family of proteins. These proteins can either suppress apoptosis like *bcl*-2, for example, *bcl*-xL (Boise et al., 1993), while other proteins make cells more susceptible to apoptotic stimuli, for example *bax* and *bcl*-xS (Boise et al., 1993).

A major branch of apoptosis research focuses on the identification of the molecular components of PCD including sensors and triggers as well as different mechanisms to regulate PCD. The tumor suppressor, *p53* is regarded as a sensor of apoptosis (Donehower and Bradley, 1993). *p53* has been identified as a DNA binding protein and transcriptional activator that may be instrumental to DNA repair because it accumulates after the cell's DNA has been damaged (Donehower and Bradley, 1993). Consequently, *p53* may serve as a sensor of DNA damage.

Programmed cell death is carried out by the activity of suicide enzymes called proteases. The role of proteases is to break down proteins. The mediation of PCD is initially conducted by inactive proenzymes. These proenzymes are later activated by proteolytic cleavage. Each activated protease molecule can activate other proenzyme molecules by cutting them up. This process will ultimately activate other proteases leading to PCD. The study of apoptosis can have two distinctly different goals. One is to induce apoptosis so that cells do not grow in an uncontrollable fashion (down regulation), causing cancer. In this context, *bcl*-2 and related cytoplasmic proteins such as *bax* can act as key regulators of apoptosis (Adams and Cory, 1998). The other and opposite goal from an industrial viewpoint, is to prolong cell viability in a cultivation by preventing apoptosis as much as possible (up regulation) so that the recombinant protein of interest can be produced for a longer period, thus giving a higher titer of protein. This will ultimately minimize the down-stream processing cost because of the high concentration of protein in the broth. This research goal is very different from metabolic engineering research to control apoptosis. It is aimed at reducing death in the bioreactor. Since

necrotic cell death is for the most part accidental, the present study focuses on reducing starvation-induced apoptotic cells.

Cell death in bioreactors is indeed a major bottleneck in large-scale production of commercially important biological products such as antibodies and vaccines. The traditional strategies implemented to optimize productivity focused mainly on cell growth since death was considered accidental, passive, and for the most part, uncontrollable. However, as noted by McKenna et al., research in cell death regulation has offered new ways of enhancing cell survival (McKenna et al., 1998). The cells can be genetically engineered to express *bcl-2* or specific survival factors can be added to the medium (Fig 4.3). The death regulator protein, *bcl-2*, blocks apoptosis by interfering with the activation of caspases. In the present study, a novel approach for selection and monitoring of key amino acids that block starvation-induced apoptosis is implemented. This approach is not intended to be a replacement to metabolic manipulation of the cells, it simply offers a different perspective into the control of apoptosis and can be combined with other methodologies to improve the productivity of cellular derived proteins. It is essential to consider the pathway of PCD involving starvation of the cell on certain amino acids before reviewing the literature on control of starvation-induced apoptosis.

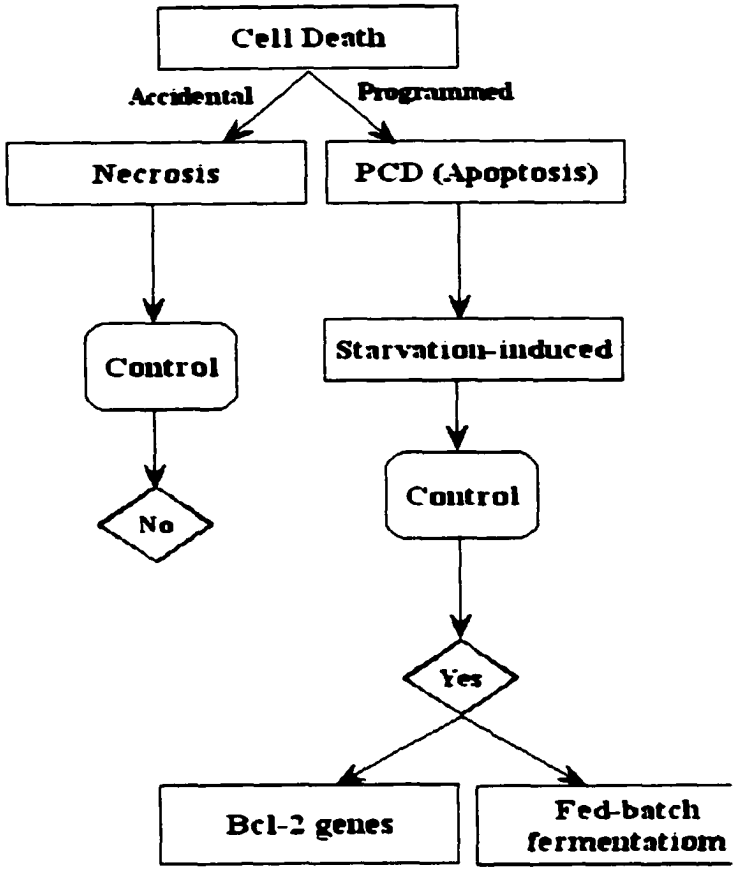

Figure 2.3 Modes of mammalian cell death

2.1.3 Relation between Deprivation of Essential Nutrients and Apoptosis

To understand the relationship between amino acid deprivation and PCD, it is noteworthy to emphasize that the rate of cell growth of cultured mammalian cells is proportional to the rate of protein synthesis minus the rate of protein degradation (Robinson et al., 1976). As mentioned by Stanners et al., the overall rate of protein synthesis depends on the functional amounts of the constituent components of the translational machinery including mRNA, ribosomes, tRNA, initiation factors etc. (Stanners et al., 1978). A change in the concentration of any of these components would

affect the cellular machinery of protein synthesis, and ultimately, cellular proliferation. In translation, all of the elements needed to synthesize a protein, from the mRNA to the amino acids, are brought together on the ribosome by tRNA as the mRNA is read by the ribosome. Specific aminoacyl-tRNA synthetases catalyze the reaction. As the mRNA is read, the specific tRNA is recognized and its amino acid is added to the growing peptide chain. The termination of protein synthesis occurs when a special message is recognized by the mRNA.

Stanners et al. suggested that the decline in the translational machinery could represent the first event to PCD (Stanners et al., 1978). This view was later corroborated by Fukushima et al. who stated, as a result of their work with tsBN269 cells, that a defect in aminoacyl-tRNA synthetase turned on the apoptotic machinery (Fukushima et al., 1996). The link between amino acid deprivation and PCD was given by Stanners et al. who proposed the following mechanism

$$Enzyme\ AA\ (active) \rightleftharpoons Enzyme\ (reversibly\ inactive) \xrightarrow[\text{or mutation}]{-AA + drug} Enzyme\ (permently\ inactive)$$

i.e., in the conformational state corresponding to no bound AA (amino acid), the enzyme (specific aminoacyl-tRNA synthetase) has a high probability of becoming permanently inactive (Stanners et al., 1978). In other words, a reduction in amino acid concentration leads to PCD. Evidences of the active role of amino acyl tRNA syhthetases in the process of apoptosis were also given by Ko et al. in their work using HeLa cells (Ko et al., 2001). They proved that HeLa cells were prone to apoptosis via Fas pathway (McKenna et al.,

1998) as a result of glutamine deprivation. This point is very important since Fas and TNF receptor ligation can induce apoptosis in the absence of RNA or protein synthesis (Yonehara et al., 1989).

Without getting into the details of Fas pathway, it is necessary to understand the way physiological triggers, such as cytokines, work. Cytokines are signaling molecules, with low molecular weight, which attach to high affinity receptors on target cells. They may send signals for cells to survive, proliferate, differentiate, or die (McKenna et al., 1998). Fas ligand (FasL) is a death inducing cytokine that binds the Fas receptor to start the apoptotic death machinery. One suggested pathway is that Fas activates Caspase 8 which activates Caspase 1 which activates Caspase 3 which starts the destructive proteases or endonucleases and leads to apoptosis (McKenna et al., 1998) :

$$Fas \rightarrow Caspase\ 8 \rightarrow Caspase\ 1 \rightarrow Caspase\ 3 \rightarrow Apoptosis$$

It is plausible that the steps involved in starvation-induced apoptosis are: 1) amino acid starvation, 2) inactivation of aminoacyl tRNA synthetase, 3) absence of protein synthesis, 4) Fas pathway is activated, 5) onset of apoptosis.

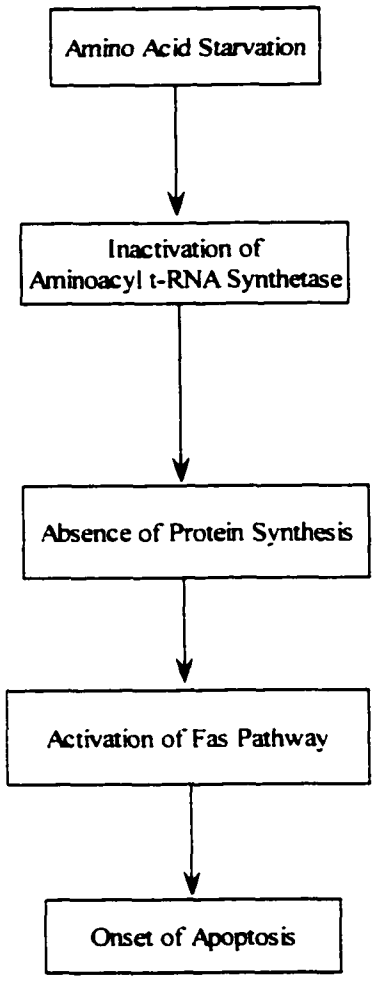

Figure 2.4 Amino acid starvation leads to apoptosis

Their study, however, involved mostly extreme starvation on amino acids. A different model denotes the radioprotectant effect of glutamine for CHO cells (Winters et al., 1994). They found that for a particular dose of radiation, the surviving fraction of CHO cells increases with the concentration of glutamine in the cell culture medium. This indicates that the concentration of apoptotic cells is a monotonous function of level of glutamine in the medium. Distefano and co-workers also proposed a relationship by

which the accumulation of apoptotic cells in the bioreactor is proportional to the concentration of viable cells. In their model, the apoptotic death rate is assumed to be constant (Distefano et al., 1996). To explain why only certain cells in the bioreactor are affected by this mode of death, Franek and Sramkova proposed a negative control of population size theory in which cells die by apoptosis in a starvation induced environment so that each member in the population efficiently utilizes the nutrient available in the environment (Franek and Sramkova, 1996).

2.1.4 Control of Apoptosis by Amino Acid Feed

The lack of available nutrients such as amino acids and glucose has been cited as a potential inducer of apoptosis in cell cultures (Mercille and Massie, 1994). Regardless of the type of bioreactors used, the nutritional demand of mammalian cells often exceeds the available supply (Mercille and Massie, 1994). Nutrient deprivation can also occur in microporous beads (De la Broise et al., 1992) and hollow fibers (Piret and Cooney, 1990). In the human body, nutrient deprivation may cause the cells to die by apoptosis. Ischemia, for instance, has been implicated in many cases as an agent for the onset of PCD (Dragunow et al., 1993). The obstruction of the inflow of arterial blood causes a deficiency of blood in the red blood cells. Heart tissues clinically exposed to ischemic insults and kidney cells during transplantation undergo apoptosis. Nutrient deprivation can also occur in tumors as a result of insufficient blood supply. B-cell hybridomas were also found to be prone to the induction of apoptosis by incubation in methionine-deficient medium (Perreault and Lemieux, 1994). Arginine deprivation induced apoptosis in leukemia L1210 cells (Ormerod et al., 1994). Using human promyelocytic leukemia (*HL-*

60), human oral squamous carcinoma (*HSC-2, HSC-4, NA*), human salivary gland tumour (*HSG*) and rat neuron cells (*PC-12*), Sakagami *et al.* noted that serine depletion accumulated the *G1* arrested cells and a large number of apoptotic cells were produced (Sakagami et al., 1998). Addition of serine to the media prolonged the logarithmic cell growth phase (Sakagami et al., 1998). Sanfeliu and Stephanopoulos found that in the case of CHO cells, the depletion of both glutamine and glutamic acid caused the cells to die by apoptosis (Sanfeliu and Stephanopoulos, 1999). They further observed that the presence of protective factors such as serum in the culture medium, the availability of essential nutrients, and the over-expression of antideath genes can help in preventing apoptosis in cell culture. It should be noted that regulation of antideath genes such as *bcl-2* can also delay the onset of apoptosis (Murray et al., 1996). However, this approach is beyond the scope of this research. Tey et al. (2000) have studied the influence of *bcl-2* expression on the robustness of a CHO cell line (22H11). They have used a CHO cell line transfected with the expression vector pEF*bcl-2* and control vector pEF*neo*.

One of the explanations for apoptosis is the inhibition of mRNA and protein synthesis as in the case of the human promyelocytic leukemia (*HL-60*) (Martin et al., 1990). Also, in D5 hybridoma cells, it has been demonstrated that inhibition of protein synthesis (by addition of cycloheximide) or transcription (by addition of actinomycin D) induced apoptosis (Perreault and Lemieux, 1993). It has also been reported that nutrient deprivation and anoxia arising from inadequate blood supply resulted in a decreased level of high energy phosphate (Tozer and Griffith, 1992). According to Mercille and Massie, the lack of available high-energy phosphates and the consequent decrease in protein synthesis may then be responsible for induction of apoptosis under nutrient-deprived

conditions (Mercille and Massie, 1994). These researchers found that induction of apoptosis following the addition of cycloheximide, actinomycin D, or heat shock was much more rapid than what was found following the removal of glutamine, glucose, or cysteine. Removal of oxygen or nutrients may cause intracellular ATP levels and protein synthesis rates to decrease gradually in all cells. They also contend that to enter apoptosis, hybridoma cells may have to reach a critical state that will result in the inefficient translation of short-lived apoptotic inhibitory proteins. This critical state may vary within a population of cells. However, once this level is reached, the PCD would be activated irreversibly, causing the cells to undergo the morphological changes associated with the action of degenerative enzymes.

In research involving CHO cells, addition of glutamine and asparagine in the bioreactor may be essential for cell survival. Glutamine has been found to protect CHO cells from radiation killing (Winters et al., 1994). Recently, glutamine has also been used in controlling starvation-induced apoptosis (Sanfeliu and Stephanopoulos, 1999). The anti-apoptotic role of asparagine is better known in works on acute lymphoblastic leukaemia (ALL). The effective drug used against ALL is asparaginase since it depletes asparagine in serum and cells (Muller and Boos, 1998). The leukemic T-cells lacking asparagine synthetase ultimately die by apoptosis. By 1978, a group of researchers working with CHO cells, has already established a connection between amino acid starvation and the protein synthetic machinery of CHO cells (Stanners et al., 1978). They suggested that the decline in the translational machinery could represent the first event in the cell's rapid death. They found that starvation for asparagine caused a loss in cell viability (Stanners et al., 1978).

The major drawback in the control approach used to minimize apoptosis so far implemented, is the lack of a systematic method to select the amino acids or nutrients that can potentially delay apoptosis. It is customary to use only one nutrient in controlling apoptosis. Even then, the feeding of this nutrient is not based on an optimal feeding policy. The lessons from penicillin production actually showed us that following an optimum profile can largely increase the productivity. Part of the problem is the lack of adequate models to correlate apoptotic cells to the many factors that may cause apoptosis. Such a model would allow the use of sensitivity analysis for the selection of nutrients with the most impact of PCD. The reduced set can then be monitored and proper control actions can then be taken to manipulate the intensity of these antiapoptotic signals received by the cells.

To link the concentration of apoptotic cells to the level of amino acids, attention should be paid to the pathway identified for the initiation of protein synthesis in mammalian cells. Differences in the affinity of mRNAs for the 40 S subunits and initiation factors may affect the relative efficiencies of mRNA molecules when the activity or concentration of these components is changed (Bergmann and Lodish, 1979). The Sverdberg unit S represents the sedimentation velocity of a component in a centrifuge. It is related to the molecular weight. Ribosomes are composed of small and large subunit RNAs and proteins. According to Bergmann and Lodish (1979), it may take the ribosomes less or more time to translate different mRNA molecules, depending on the concentration of certain species that take part in the translation process. Translation is divided into initiation, elongation, and termination. In initiation, there are at least 3 mRNA binding events: mRNA is bound to one or more initiation factors, the 40 S

ribosomal subunit is bound to the mRNA-factor complex, and the 60 S ribosomal subunit is joined to the 40 S mRNA. In the kinetic model of protein synthesis that they proposed, it was assumed that the formation of 80 S initiation complexes immediately succeeded the formation of 40 S mRNA complexes. The formation of 80 S complexes is equivalent to the rate of joining of an mRNA.factor complex with the activated 40 S ribosomal subunits. This rate is:

$$Q = K_1 . m . R^{**} \qquad (1)$$

where Q is defined as the rate of formation per mRNA of an 80 S initiation complex, K_1 is a proportionality constant that may depend on the mRNA molecule, R^{**} is the concentration of activated 40 S ribosomal units, and m is the fraction of mRNA factor complexes. Due to the fact that an mRNA molecule has to wait for the ribosome to move down the mRNA before attaching to another ribosome, the equation becomes:

$$Q = K_1 . m . P_1 . R^{**} \qquad (2)$$

where P_1, the proportion of available mRNA that depends on both the average time between initiation events and the time it takes a ribosome to leave the initiation factor (Bergmann and Lodish, 1979).

The elongation of the polypeptide chain follows the formation of the 80 S ribosome complex. The local elongation rate at position i along a group of identical

mRNAs is equivalent to the rate of movement of ribosomes from position *i*-1 to position *i* or the rate of formation of nascent chains *i* amino acids in length. :

$$Q_i = K_i X_{i-1} P_i \tag{3}$$

K_i is the elongation rate constant at position *i* along the mRNA. K_i depends on many factors one of which is the availability of a specific tRNA and its synthetase. X_{i-1} is the fraction of mRNAs with ribomomes at position *i*-1, and P_i is the fraction of those mRNAs with a ribosome located at position *i*-1. It is assumed that the progress of that ribosome is not hindered by other ribosomes further along the mRNA.

The terminal event in protein synthesis is expressed as

$$Q_t = K_t X_t \tag{4}$$

Q_t is the termination rate, K_t is the termination rate constant, and X_t is the fraction of polysomes with completed, yet unreleased, chains (Bergmann and Lodish, 1979).

Harley et al. formulated a model for messenger RNA translation during extreme amino acid starvation (Harley et al., 1981). They used Eq. (3) to study the effect of extreme amino acid starvation on the kinetics of protein synthesis. A linear relationship was assumed between error frequency due to codon-anticodon mispairing and the time spent by the ribosome at these codons. Their model applied very well to CHO cells with a temperature-sensitive defect in asparaginyl-tRNA synthetase in which they reported an error frequency for the asparagine codons in actin of 0.7×10^{-4}. Actins are proteins found

in microfilaments. They play a role in muscular contraction, maintenance of the shape of the cell and cellular movement. Further analysis clearly showed that inhibition in protein synthesis during amino acid starvation is related to the step time of the ribosome at hungry codons (Harley et al., 1981). A hungry codon usually codes for a rare tRNA molecule (one which is in limited supply in the cell). The decrease in the rate of protein synthesis would ultimately lead to apoptotic death (Stanners et al., 1978).

Although the models represented by Equations (1), (2), (3), and (4) help to understand the relationship between amino acid starvation and the decrease rate in protein synthesis, the coefficients associated with the models are difficult to estimate. These coefficients depend on the cell line and the environmental conditions. While the equations represent simplified versions of protein synthesis, the proposed mechanism can be used for model identification since it establishes a relationship between amino acid starvation and PCD. A generic nonlinear model such as artificial neural networks (NN) can then be used to relate the concentration of key amino acids to the PCD in bioreactors. This methodology is described in the next sections.

2.2 Experimental Procedure

2.2.1 Cultivation Conditions

The CHO cell line, CHO 1-155500, obtained from ATCC was used in this research. The cells produce recombinant tissue-type plasminogen activator (t-PA) that has clinical applications as a thrombolytic agent. The cells were initially thawed and diluted ten-fold (1 ml of culture and 9 ml of 90% HAMSF-12 and 10% FBS). These were then transferred to a 75 ml T-flask containing 95% selection medium and 5% dialyzed fetal

bovine serum. The flask was placed in an incubator set at 37°C and 8 % carbon dioxide overlay. For subsequent studies, the cells grew in a 3-l bioreactor. The pH was controlled at 7.2 by addition of 1 M NaOH and carbon dioxide. The dissolved oxygen was controlled at a concentration of 40% saturated air. The agitation speed was set at 80 RPM. The temperature was maintained at 37°C.

2.2.2 Sample Analysis

The concentration of total cells was measured using a hemacytometer. The samples were initially diluted to 2,000-20,000 cells per ml. Cell viability was assessed by trypan blue exclusion. Flow cytometry was the methodology employed to detect and quantify apoptotic cells (Darzynkiewicz et al., 1992; Telford et al., 1994). Ammonia was assayed enzymatically. The concentrations of lactate and glucose were determined using a YSI analyzer. The compositions of amino acids were determined by HPLC method. The product, t-PA, was analyzed via ELISA.

2.3 Results

NN based sensitivity analysis was performed to determine which amino acids play a bigger role on preventing apoptosis (See chapter 4 for more details). The goal of the study was to identify a reduced set of amino acids that could potentially delay apoptotic death in the bioreactor. Using NN as a generic mathematical function, the following equation was used. The NN output is the concentration of apoptotic cells. Each data point of an input vector k (a selected amino acid) is then perturbed by adding a random number (standard deviation, σ_k). The remaining input vectors (the remaining amino acids)

are kept at their mean concentrations while the output of the NN is computed. Inputs with relatively low sensitivities are ignored.

The sensitivity for input k is

$$S_k = \frac{\sum_{p=1}^{P}\sum_{i=1}^{O}(y_{ip} - \bar{y}_{ip})^2}{\sigma_k^2} \tag{5}$$

where $\bar{y}_{ip}$ is the i^{th} output of the optimum network for the p^{th} pattern. O stands for the number of network outputs ($O = 1$), P is the number of patterns (number of data generated), and σ_i^2 represents the variance of the input perturbation (Principe et al., 2000). Using this technique, we have found that glutamine and asparagine can prevent apoptosis in CHO cells. We propose to use an equation of the form

$$\frac{d(X_{da}(t))}{dt} = k_{da} X_v(t) \tag{6}$$

to model apoptotic cells. k_{da} is a specific apoptotic death rate depending on the concentration of glutamine and asparagine. One can also use NN to model this equation. Taking into account initial conditions, the following equation is obtained

$$X_{da}(t) - X_{da}(0) = f_{NN}(X_v(t) - X_v(0), Gln(t) - Gln(0), Asn(t) - Asn(0)) \tag{7}$$

where X_{da}, X_v, *Gln*, *Asn* are the concentration of apoptotic cells, viables cells, glutamine, and asparagine, respectively. f_{NN} is a neural network function.

During the last ten years, NNs have emerged as an accepted tool for modeling nonlinear processes. Due to their approximation capabilities as well as their inherent adaptive features, artificial NNs offer an appealing alternative to classical methods of modeling dynamic systems. NN models consist of a set of weights, **W**, a set of basis functions **f(.)**, and a set of parameters θ (biases, centers, etc.). Detailed discussions on NN is given in Chapter 4. The general equation can be written as:

$$\hat{y} = f(\bar{x}, w, \theta) \tag{8}$$

where $\hat{y}$ denotes NN prediction. The parameters **W** and θ are adjusted during a "training" procedure in order to minimize some kind of error measure. The development NNs requires a training set made up of known input and output patterns. In the training phase, examples representative of the problem are fed to the network. The network tries to learn the underlying relationship based on the given set using an iterative error-minimization procedure. It is then exposed in the recall phase to inputs already seen. This stage is very important because one has a chance to improve the performance of the network and test different topologies. The final and crucial step is the testing phase during which the network is fed new data. In the present work, Fig. 4.5 represents the architecture of the network used in this work. W and V are the weights of the network, W_b and V_b are the biases. Including the initial conditions in the model is important since these conditions may vary from batches to batches:

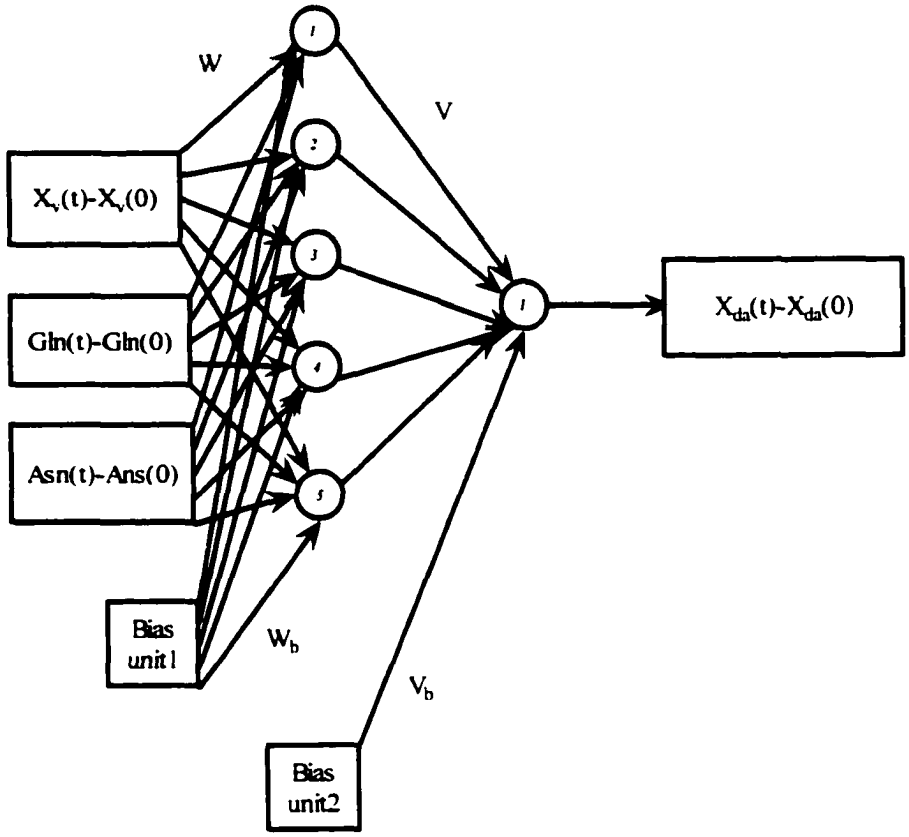

Figure 2.5 Architecture of neural networks

The number of neurons used is 5. The number of epochs used in this work is 40.000. Training of the NN would stop if the MSE reaches a value of 1.0e-7. The learning rate is 0.90. At the end of the 40,000 epochs, the MSE value was 3.38e-5. The network training function updates weights and biases according to a resilient backpropagation algorithm. The complete algorithm can be found in the work of Riedmiller and Braun (Riedmiller and Braun, 1993). The NN predicts very well the concentration of apoptotic cells as indicated

by Fig. 4.6. The line "y=x" is the line of equity. Testing data were used to validate the neural network. Additional data were created to train and test the network. A spline function was used to create the additional data.

Excellent NN prediction of apoptotic cell concentration based on the concentration of amino acids indicates that the mechanism depicted by Equations (1), (2), (3), and (4) may indeed be a valid mechanism to explain amino acid starvation and the onset of apoptosis. Further studies need to be done to find the specific rate constants in the mechanisms applicable to asparagine and glutamine. A good starting point is the rate of mistranslation as a result of low asparagine and glutamine concentration following the work of Harley et al. (Harley et al., 1981). The model would include the increased error frequency during amino acid starvation as a result of asparagine and glutamine limitation. The error rate would be directly related to the delayed time of the ribosome at the hungry codons.

2.4 Conclusions

Apoptosis is a gene-controlled mode of cell death that affects the ability of mammalian cells to produce protein at a maximum. One way to increase productivity is to target the specific growth rate as a way to increase cell productivity. However, because of recent advances in the control and understanding of death, it has become customary to perform metabolic engineering in order to increase the viability of the cells. The final goal is to increase the final titer of protein. The methods used for apoptosis usually consider one amino acid and extreme starvation of the cells on that particular amino acid. Based on the NN model, it is possible to express the concentration of apoptotic cells in terms of two

amino acids. This method can be used for control purposes. This is discussed in Chapter 5.

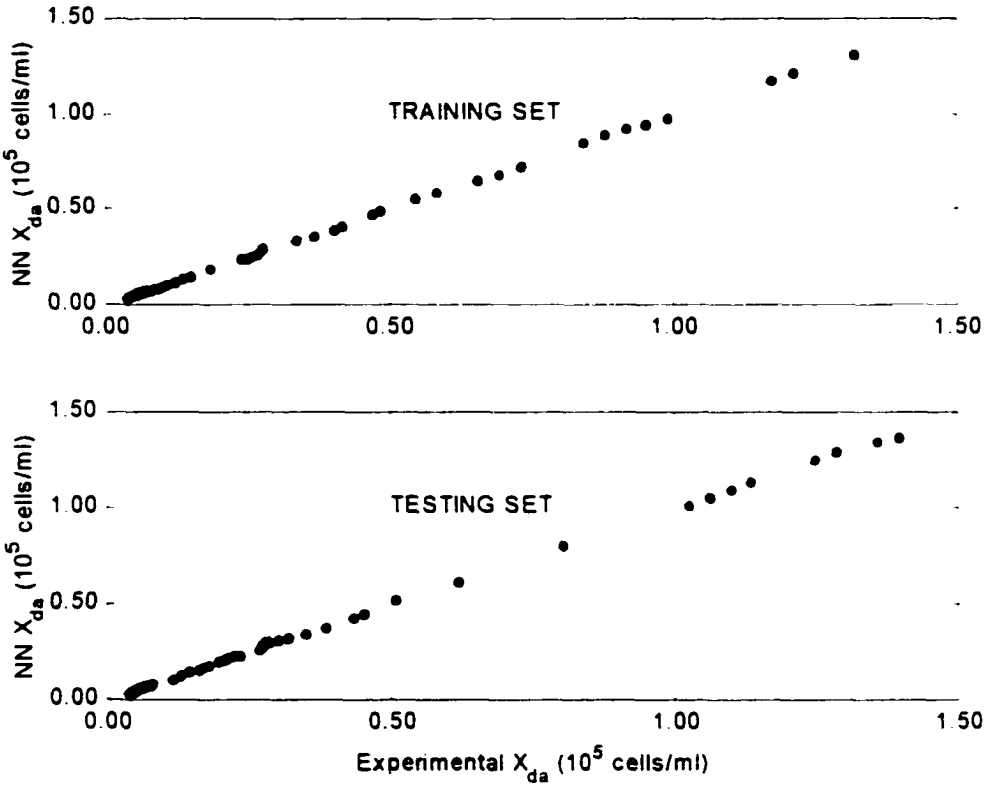

Figure 2.6 Training and testing results

2.5 References

Adams, JM, Cory, S. 1998. The Bcl-2 protein family: arbiter of cell survival. Sci 281:1322-1326.

Ashkenazi, A, Dixit, VM. 1998. Death receptors: Signaling and modulation. Sci 281:1305-1308.

Berges, RS, Furuya, Y, Jacks, T, English, H, Isaacs, J. 1993. Cell proliferation, DNA repair, and p53 function are not required for programmed death of prostatic glandular cells induced by androgen ablation. Proc Natl Acad Sci USA 90:8910-8914.

Bergmann, JE, Lodish, FL. 1979. A kinetic model of protein synthesis: Application to hemoglobin synthesis and translational control. JBC 254:11927-37.

Boise, LH, Gonzalez-Garcia, M, Postema, CE, Ding, L, Lindsten, T, Turka, LA, Mao, X, Nunez, G, Thompson, CB. 1993. *blc* -x, a *blc* -2-related gene that functions as a dominant regulator of apoptotic cell death. Cell 74:1-20.

Chinnaiyan, AM, Chaudhary, D, O'Rourke, K, Koonin, EV, Dixit, VM. 1997. Role of ced-4 in the activation of ced-3. Nature 388:728-729.

Cohen, JJ. 1993. Apoptosis. Immunol Today 14:126-130.

Darzynkiewicz, Z, Bruno, S, Del Bino, G, Gorczyca, W, Hotz, MA. 1992. Features of apoptotic cells measured by flow cytometry. Cytometry 13:795-808.

De la Broise, D, Noiseux, M, Massie, B, Lemieux, R. 1992. Hybridoma perfusion systems: a comparison study. Biotechnol Bioeng 40:25-32.

Deng, G, Podack, ER. 1993. Suppression of apoptosis in a cytotoxic T-cell line by interleukin 2-mediated gene transcription and deregulated expression of the protooncogene bcl-2. Proc Natl Acad Sci USA 90:2189-2193.

Denmeade, SR. Isaacs, JT. 1996. Programmed cell death (apoptosis) and cancer chemotherapy. Cancer Control 3:306-309.

Dickson, AJ. 1998. Apoptosis regulation and its applications to biotechnology. Sci 16:339-342.

Distefano, DJ. Mark, GE. Robinson, DK. 1996. Feeding of nutrients delays apoptosic death in fed-batch cultures of recombinant NSO myeloma cells. Biotechnol Lett 18:1067-1072.

Donehower, LA. Bradley, A. 1993. The tumor suppressor p53. Biochem Biophys Acta 1155:181-205.

Dragunow, M. Young, D. Hughes, P. MacGibbon, G. Lawlor, P. Singleton, K. Sirimanne, E. Beilharz, E. Gluckman, P. 1993. Is c-Jun involved in nerve cell death following status epilepticus and hypoxic- ischaemic brain injury? Brain Res 4:347-352.

Franek, F. Sramkova, K. 1996. Protection of B lymphocite against starvatyion-induced apoptosis: survival-signal role of some amino acids. Immunol Lett 52:139-144.

Franek, F. Vomastek, T, Dolnikova, J. 1992. Fragmented DNA and apoptotic bodies document the programmed way of cell death in hybridoma cultures. Cytotechnol 9:117-123.

Fukushima, K. Motomura, S. Kuraoka, A. Nakano, H. Nishimoto, T. 1996. A single point mutation of hamster aminoacyl-tRNA synthetase causes apoptosis by deprivation of cognate amino acid residue. Genes to cells 1:1087-1099.

Furuya, Y, Isaacs, JT. 1993. Differential gene regulation during programmed death (apoptosis) versus proliferation of proscatic glandular cells induced by androgen manipulation. Endocrinology 133:2660- 2666.

Harley, C B, Pollard, JW, Stanners, CP, Goldstein, S. 1981. Model for messenger RNA translation during amino acid starvation applied to the calculation of protein synthesis error rates. J Biol Chem 256:10786-10794.

Hengartner, MO, Horvitz, HR. 1994. *C. elegans* cell survival gene ced-9 encodes a functional homolog of the mammalian proto-oncogene bcl-2. Cell 76:665-676.

Hockenbery, DM, Oltvai, ZN, Yin, XM, Milliman, CL, Korsmeyer, SJ. 1993. Bcl-2 functions in an antioxidant pathway to prevent apoptosis. Cell 75:241-251.

Hu, WS, Himes, VB 1989. Considerations of mammalian cell metabolism in bioreactors. In: Pages 33-46 Springer-Verlag New York, Inc., New York, NY.

Ko, YG, Kim, EK, Kim, T, Park, H, Park, HS, Choi, EJ, Kim, S. 2001. Glutamine-dependent antiapoptotic interaction of human glutaminyl-tRNA synthatase with apoptosis signal-regulating kinase 1. JBC 276:6030-6036.

Korsmeyer, SJ. 1995. Regulators of cell death. Trends in Genetics 11:101-105.

Lazebnik, YA, Kaufmann, SH, Desnoyers, S, Poirier, GG, Earnshaw, WC. 1994. Cleavage of poly(ADP-ribose) polymerase by a proteinase with properties like ICE. Nature 371:346-347.

Martikainen, P, Kyprianou, N, Isaacs, JT. 1990. Effect of transforming growth factor-beta1on proliferation and death of rat prostatic cells. Endocrinology 127:2963-2968.

Martin, SJ, Lennon, SV, Bonham, AM, Cotter, TG. 1990. Induction of apoptosis (programmed cell death) in leukemic HL-60 cells by inhibition of RNA or protein synthesis. J Immunol 145:1859-1862.

McKenna, SL, McGowan, AJ, Cotter, TG 1998. Molecular mechanisms of programmed cell death. In: Advances in Biochemical Engineering/Biotechnology, Springer, New York.

Mercille, S, Massie, B. 1994. Introduction of apoptosis in nutrient-deprived cultures of hybridoma and myeloma cells. Biotechnol Bioeng 44:1140-1154.

Muller, HJ, Boos, J. 1998. Use of L-asparaginase in Childhood ALL. Critical Reviews in Oncology/Hematology 28:97-113.

Murray, K, Ang, CE, Gull, K, Hickman, JA, Dickson, AJ. 1996. NS0 myeloma cell death: influence of bcl-2 overexpression. Biotechnol Bioeng 51:298-304.

Nunez, G, Clarke, MF. 1994. The Bcl-2 family of proteins: regulators of cell death and survival. Trends Cell Biol 4:399-403.

Oltvai, ZN, Korsmeyer, SJ. 1994. Checkpoints of dueling dimers foil death wishes. Cell 79:189-192.

Ormerod, MG, Orr, RM, Peacock, JH. 1994. The role of apoptosis in cell killing by cisplatin: A flow cytometry study. Br J Cancer 69:93-100.

Perreault, J, Lemieux, R. 1993. Rapid apoptotic cell death of B-cell hybridomas in absence of gene expression. J Cell Physiol 156:286-293.

Perreault, J, Lemieux, R. 1994. Essential role of optimal protein synthesis in preventing the apoptotic death of culture *B* cell hybridomas. Cytotechnol 13:99-105.

Piret, JM, Cooney, CL. 1990. Model of oxygen transport limitations in hollow fiber bioreactors. Biotechnol Bioeng 37:80-92.

Principe, JC, Euliano, NR, Lefebvre, WC 2000. Neural and Adaptive Systems. New York, NY: John Wiley & Sons, Inc..

Reed, JC. 1994. Bcl-2 and the regulation of programmed cell death. Journal of Cell Biology 124:1-6.

Riedmiller, M, Braun, H 1993. A direct adaptive method for faster backpropagation learning: The RPROP algorithm. In: Pages 586-591Proceedings of the IEEE International Conference on Neural Networks, San Francisco.

Robinson, JH, Smith, JA, Dee, LA. 1976. Synthesis and degradation of proteins in cultured, androgen-responsive tumor cells. Exp Cell Res 102:117-126.

Sakagami, H, Satoh, M, Yokote, Y, Takano, H, Takahama, M. 1998. Amino acid utilization during cell growth and apoptosis induction. Anticancer Reseach 18:4303-4306.

Sanfeliu, A, Stephanopoulos, G. 1999. Effect of glutamine limitation of the death of attached Chinese Amster Ovary cells. Biotechnol Bioeng 64:46-53.

Savill, JS, Wyllie, AH, Henson, JE, Walport, MJ, Henson, PM, Hasiett, C. 1989. Macrophage phagocytosis of aging neutrophilis in inflammation. J Clin Invest 83:865-875.

Seshagiri, S, Miller, K. 1997. *Caenorhabditis elegans ced-4* stimulates *ced-3* processing and *ced-3* -induced apoptosis. Curr Biol 7:455-460.

Singh, RP, Al-Rubeai, M, Gregory, CD, Emery, AN. 1994. Cell death in bioreactors: A role for apoptosis. Biotechnol Bioeng 44:720-726.

Singh, RP, Simpson, NH, Perani, A, Goldenzon, C, Al-Rubeai, M. 1997. Essential amino acid deprivation of hybridoma cells results in the induction of high levels of apoptosis, which is suppressed by bcl-2 over-expression. The Genetic Engineer and Biotechnologist 17:121-124.

Smeyne, RJ, Vendrell, M, Hayward, MBSJ, Miao, GG, Schilling, K, Robertson, LM, Curran, T, Morgan, JI. 1993. Continuous c-fos expression precedes programmed cell death in vivo. Nature 363:166-169.

Spector, MS, Desnoyers, S, Hoeppner, DJ, Hengartner, MO. 1997. Interaction between the *C. elegans* cell-death regulators *ced-9* and *ced-4*. Nature 385:653-656.

Stanners, CP, Wightman, TM, Harkins, JL. 1978. Effect of extreme amino acid starvation on the protein synthetic machinery of CHO cells. J Cell Physiol 95:125-138.

Steller, H. 1995. Mechanisms and genes of cellular suicide. Sci 267:1445-1449.

Telford, WG, King, LE, Fraker, PJ. 1994. Rapid quantification of apoptosis in pure and heteregeneous cell population using flow cytometry. Cytometry 172:1-16.

Thompson, CB. 1995. Apoptosis in the pathogenesis and treatment of disease. Sci 267:1456-1462.

Thornberry, NA, Lazebnik, Y. 1998. Caspases: enemis within. Sci 281:1312-1316.

Tey BT, Singh RP, Piredda, L, Piacentini, M, Al-Rubeai, M. Influence of Bcl-2 on cell death during the cultivation of a chinese hamster ovary cell line expressing a chimeric antibody. Biotechnol Bioeng 68:31-43.

Tozer, GM, Griffith, JR. 1992. The contribution made by cell death and oxygenation to 31P MRS observations of tumour energy metabolism. NMR in Biomedicine 5:279-289.

Van Furth, R, Van Zwet, TL. 1988. Immucytochemical detection of 5-bromo-2-deoxyuridine incorporation in individual cells. Journal of Immunological Methods 108:45-51.

Winters, R, Matthews, R, Krishnan, K. 1994. Glutamine protects chinese hamster ovary cells from radiation killing. Life Sci 55:713-720.

Wyllie, AH, Kerr, JFR, Currie, AR. 1980. Cell death: The significance of apoptosis. Int Rev Cytol 68:251-306.

Yonehara, S, Ishiti, A, Yonehara, M. 1989. A cell-killing monoclonal antibody (anti-Fas) to a cell surface antigen codownregulated with the receptor of tumor necrosis factor. J Exp Med 169:1747-1756.

Chapter 3

IDENTIFICATION AND CONTROL OF DISSOLVED OXYGEN IN HYBRIDOMA CELL CULTURE IN A SHEAR SENSITIVE ENVIRONMENT

3.1 Introduction

Biotechnology is often referred to as the use of animal-cell cultures for the production of useful protein products because of the widespread use of animal cells for the development of industrial therapeutics or diagnosis reagents (Dickson, 1998). Recombinant DNA technology has made possible the generation of high-valued proteins with therapeutic potentials (Dickson, 1998). Mammalian cells have been chosen as hosts for protein expression, in particular, monoclonal antibody production (Zhou et al., 1997). Hybridoma cells, recombinant chinese hamster ovary (CHO) and myeloma cells have been used for a number of industrially important therapeutic proteins (Cooney, 1995). Mammalian cells produce a variety of complex proteins such as Hepatitis B virus surface antigen, glycoprotein D of the Herpes Simplex virus, tissue type plasminogen activator (tPA), monoclonal antibodies, and interferon-gamma (Hu and Himes, 1989). Monoclonal antibodies are naturally occurring proteins produced in response to foreign substances in the body (antigens). They prevent and treat disease by eliminating antigens. According to

Dickson, the complex structural nature of these therapeutic proteins and their requirement for post-translational modifications for function make mammalian cells a good host for complete expression of the proteins (Dickson, 1998). However, for scale-up procedures, the oxygen supply rate can severely affect product formation.

The effects of dissolved oxygen on mammalian cells have been studied extensively (Kilburn and Webb, 1968; Self and Kilburn, 1968; Taylor et al., 1971; William et al., 1987). Adequate oxygen supply is often necessary for energy production and formation of cellular constituents such as tyrosine and cholesterol (Blanch, 1996). As noted by several researchers (William et al., 1987; Mizrahi et al., 1972; Reuveney et al, 1986), the optimum DO concentration for antibody concentration may be different from that of cell density. As a result, adaptive control algorithms need to be developed to maintain a desired DO concentration regardless of changes in cell metabolism, medium viscosity, metabolite concentrations, etc.

Control of dissolved oxygen tension in bacterial cell fermentations involves the manipulation of the agitation speed or the gas supply rate in order to optimize the volumetric mass transfer coefficient k_La. This approach gives satisfactory results since the mass transfer coefficient k_L is a function of the power dissipation by impeller per unit volume (De Figueiredo Lopes and Calderbank, 1979). The gas liquid interfacial area, a, also varies with the gas flow rate (Miller, 1974). Since animal cells are more shear sensitive than bacterial cells, the concentration of dissolved oxygen may be controlled by manipulating the partial pressure of oxygen in the liquid phase, and by keeping the gas flow rate and stirring rate constant in the bioreactor (Oeggerli et al., 1995). This control scheme minimizes cell damage since bursting bubbles are greatly reduced at the liquid

surface. Using this technique, various algorithms, including classical (Jung et al., 1992) as well as advanced control methods (Heinzle et al., 1990; Lee et al., 1991; Oeggerli et al., 1995; Sargantanis and Karim, 1999) have been described to improve DO control.

Control of DO in a shear sensitive environment requires tracking of the mass transfer coefficients to ensure adequate oxygen supply to the cells. In the current work, a generalized model predictive controller is employed. Contrary to the black-box input-output model usually implemented in GPC, the present methodology derived the input-output model from a DO balance in the fermentation broth. Based on the outlined procedure, the order of the system can be immediately estimated from the oxygen rate equation. The time-varying nature of the process is observed in real-time in a user-friendly computer environment.

3.2 Generalized Predictive Controller

MPC algorithms use a dynamic model of the process for predicting the controlled variable. MPC methos calculate the sequence of manipulated variable moves $[\Delta\mathbf{u}(k), \Delta\mathbf{u}(k+1), \ldots, \Delta\mathbf{u}(k+Nu-1)]$ that will force the predicted outputs $[\mathbf{y}((k+N_1)|k), \mathbf{y}((k+N_1+1)|k), \ldots, \mathbf{y}((k+N_2)|k)]$ to some desired reference vector $[\mathbf{r}(k+N_1), \mathbf{r}(k+N_1+1), \ldots, \mathbf{r}(k+N_2)]$. The length of the predicted control sequence, Nu, determine the ``control horizon". The range $[N_1, N_2]$ represents the output prediction horizon. Only the first move is implemented, and a new sequence of control inputs is calculated at the next sampling instance. The minimization problem solved on-line by the MPC controller at each sampling point k is

$$\min_{\Delta \mathbf{u}(k),\ldots,\Delta \mathbf{u}(k+N_u-1)} J(k) \tag{1}$$

where

$$J(k) = \sum_{j=1}^{N_2} \| \Gamma [\mathbf{y}(k+j|k) - \mathbf{r}(k+j)] \|^2 + \sum_{j=1}^{N_u} \| \beta [\Delta \mathbf{u}(k+j-1)] \|^2 \tag{2}$$

subject to

$$\mathbf{u}_{min} \leq \mathbf{u}(k) \leq \mathbf{u}_{max} \tag{3}$$

Here, $y(k+j|k)$ represents the j-step ahead predicted output. $\Delta\ \mathbf{u}(k)$ is the control move defined as $\mathbf{u}(k)$-$\mathbf{u}(k-1)$. Γ is a positive definite output error weighting matrix and β is a positive semidefinite input weighting matrix referred to as a move suppression factor. The objective function J is called a quadratic cost function. The formulation of the objective function usually includes an upper u_{max} and a lower bound u_{min} on the input variable $u(k)$, and additional constraints on the allowed control action change between successive sampling intervals. MPC with adaptive model parameters is known as GPC in the literature (Clarke et al., 1987). In this work, the input u and output y are the mole fraction of oxygen through the sparger and the dissolved oxygen concentration, respectively . The input variable is constrained between 0.0 and 0.209. Eq. 2 becomes

$$J(k) = \sum_{j=1}^{N_2} \Gamma[y(k+j|k) - r(k+j)]^2 + \sum_{j=1}^{Nu} \beta[\Delta u(k+j-1)]^2 \qquad (4)$$

subject to

$$0.0 \leq u(k) \leq 0.209 \qquad (5)$$

3.3 Mathematical Model

In a cell-free medium, the oxygen mass balance in the liquid phase is described by the following equation [14]:

$$\frac{dC_{O_2,L}}{dt} = k_L a_B \left(\frac{P}{H} y_{o_2,B} - C_{O_2,L}\right) + k_L a_H \left(\frac{P}{H} y_{o_2,H} - C_{O_2,L}\right) \qquad (6)$$

where B and H refer to the bubble phase and head space, respectively.

Laplace transforms (S-domain) are then used to underline the dynamic relation between a single input variable ($y_{o2,B}$ or $y_{o2,H}$) and the output variable $C_{O2,L}$. The transform of Eq. 6 in the S-domain is

$$C^*_{O_2,L}[S] = \frac{\frac{P}{H}k_L a_B}{S + (k_L a_B + k_L a_H)} y^*_{o_2,B}[S] + \frac{\frac{P}{H}k_L a_H}{S + (k_L a_B + k_L a_H)} y^*_{o_2,H}[S] \qquad (7)$$

where $C^*_{O2,L}[S]$, $y^*_{o2,B}[S]$, and $y^*_{o2,H}[S]$ are, respectively, the Laplace transforms of $C_{O2,L}[t]$, $y_{o2,B}[t]$, and $y_{o2,H}[t]$. The coefficients of the input variables $y^*_{o2,B}[S]$, and $y^*_{o2,H}[S]$ are called transfer functions. Transfer functions relate input variables to output variables. For example, the mole fraction of oxygen in the bubble phase ($y_{o2,B}$) is related to the

concentration of oxygen in the liquid phase ($C_{O2,L}$) by the transfer function $P/ Hk_La_B /S + (k_La_B + k_La_H)$. Eq. 7 was obtained by assuming that the process was initially at steady state. The variables were then expressed in terms of deviations measured from the steady state values (Seborg et al., 1989) ($x^* = x - x_{ss}$). x_{ss} and x^* are defined as the steady state and deviation transform of a variable x, respectively. The concentration of dissolved oxygen was measured with a DO probe calibrated in nitrogen and air-saturated medium at 37°C. DO is defined by the following equation:

$$DO = \left(\frac{100}{C_{O_{2,sat}}}\right) C_{O_{2,L}} \tag{8}$$

where $C_{O2,sat}$ is the equilibrium oxygen concentration. However, in practice, the response of a DO probe exhibits first order response with dead time. The correct form of Eq. 8 is

$$DO[S] = \left(\frac{100}{C_{O_{2,sat}}}\right) \frac{k_p}{\tau_p S + 1} e^{-tdS} C^*_{O_{2,L}} \tag{9}$$

Since the concentration of oxygen in the headspace is held constant and the variables in Eq. 7 are in deviation form, $y^*_{o2,H}[S] = 0$, Eq. 7 then becomes

$$DO[S] = \left(\frac{100}{C_{O_{2,sat}}}\right) \frac{\frac{P}{H} k_L a_B}{S + (k_L a_B + k_L a_H)} \frac{k_p}{\tau_p S + 1} e^{-tdS} y^*_{o2,B}[S] \tag{10}$$

Eq. 10 represents a second order system with time delay *td*. The parameters, k_p and τ_p are, respectively, the steady-state gain and the time constant of the probe. k_p is defined as the

change of the DO probe response for a unit step change in the input variable. The time constant is a measure of the probe dynamics; it is defined as the time taken to reach 63.2% response of the probe output given a step input change. It is a function of probe type, geometry, membrane, and electrolyte property (Jorjani and Ozturk, 1999). Writing K_p as $100/C_{O2\_sat}\,k_p$, Eq. 10 becomes

$$DO[S] = \left[\frac{\frac{P}{H}k_L a_B}{S + (k_L a_B + k_L a_H)}\right] \frac{K_p}{\tau_p S + 1} e^{-t_d S} y^*_{a,B}[S][S] \quad (11)$$

Two variables A and B are introduced such that

$$\begin{cases} A = \frac{P}{H}k_L a_B \\ B = k_L a_B + k_L a_H \end{cases} \quad (12)$$

It can be shown that Eq. 11 can be written in a discrete form (z-transform) as

$$\frac{DO[z]}{y^*_{a,B}[z]} = \frac{a_1 z^{-1-t_d} + a_2 z^{-2-t_d}}{1 + b_1 z^{-1} + b_2 z^{-2}} \quad (13)$$

where

$$a_1 = \frac{-AK_p + A\exp(HT)K_p - AH\left(-1+\exp\left(\frac{T}{\tau_p}\right)\right)K_p\tau_p}{H\exp\left(HT+\frac{T}{\tau_p}\right)(-1+H\tau_p)} \quad (14)$$

$$a_2 = \frac{A\exp\left(\frac{T}{\tau_p}\right)(1-\exp(HT))K_p + AH\exp(HT)\left(-1+\exp\left(\frac{T}{\tau_p}\right)\right)K_p\tau_p}{H\exp\left(HT+\frac{T}{\tau_p}\right)(-1+H\tau_p)} \quad (15)$$

$$b_1 = \frac{-H\exp(HT)(-1+H\tau_p) - H\exp\left(\frac{T}{\tau_p}\right)(-1+H\tau_p)}{H\exp\left(HT+\frac{T}{\tau_p}\right)(-1+H\tau_p)} \quad (16)$$

$$b_2 = \frac{H(-1+H\tau_p)}{H\exp\left(HT+\frac{T}{\tau_p}\right)(-1+H\tau_p)} \quad (17)$$

The model parameters a_i and b_i are usually held constant for time-invariant systems. However, in recursive algorithms, their values are constantly updated to reflect changes in system dynamics. From Eqs 14, 15, 16, and 17, it is evident that the model parameters are functions of the dynamics of the DO probe : t_d, k_p, and τ_p. More importantly, their values also change with the mass transfer coefficients $k_l a_B$ and $k_l a_H$. Normally, the time delay is constant, and k_p, and τ_p are preset by the manufacturer, Eqs 14, 15, 16, and 17 constitute a system of four equations in terms of A and B. The best values of $k_l a_B$ and $k_l a_H$ were calculated by minimizing the sum of the squared residuals of Eqs 14, 15, 16, and 17. The superscipt * is removed in further discussions for simplicity.

3.4 Materials and Methods

3.4.1 Apparatus

The experimental setup is shown in Fig. 3.1 and consists of a 3-L bioreactor. The temperature is controlled at 37°C using a heating tape and a temperature controller (OMEGA, Stamford, CT). As already mentioned, 100% saturation (DO = 100) is

equivalent to the saturation of dissolved oxygen concentration with air at 37°C in a 5% fetal bovine serum medium. A stream of air set at 17.5 vvm enters the top of the bioreactor. During experimental runs, the gas flow rate through the sparger is set at 8.75 vvm. The DO voltage signals are sent to a data acquisition card (NATIONAL INSTRUMENT CORP., Austin, TX) and read by a computer. An algorithm written in CMEX S-function (MATHWORKS, Inc., Natick, MA) uses the information from the DO probe and sends appropriate control signals via a computer card (ADVANTECH, Sunnyvale, CA) to two mass flow controllers (COLE-PARMER, Vernon Hills, Il). The flow rates of oxygen and nitrogen are adjusted by the controllers based on the oxygen mole fraction into the sparger as calculated by the control algorithm. In all cases, the total gas flow rate into the bioreactor remains constant.

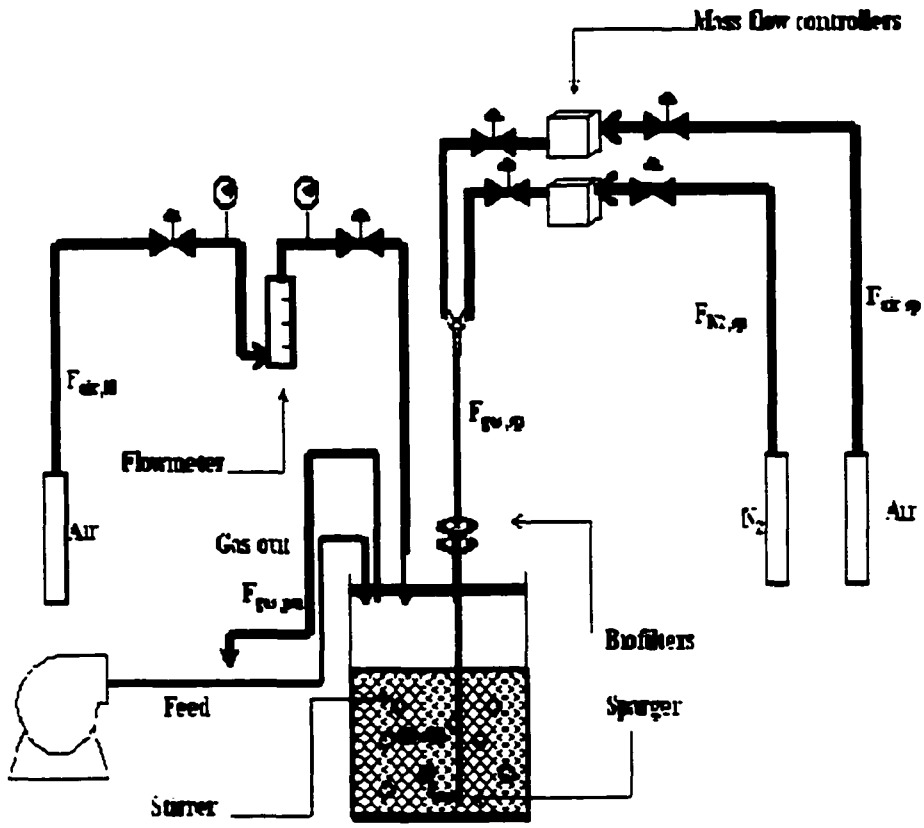

Figure 3.1. Experimental setup for DO control

3.4.2 Sample Analysis

The concentration of total cells were measured using a hemacytometer. The samples were initially diluted to 2,000-20,000 cells per ml. Cell viability was assessed by trypan blue exclusion. Ammonia was assayed enzymatically according to the protocols outlined by Lund (1974). The concentrations of lactate and glucose were determined using an YSI analyzer.

3.4.3 Cell Line and Cultivation Condition

A mouse hybridoma cell producing an antibody against tPA was used. The cell line was obtained from ATCC (Catalog # HB-9156). Tissue-type plasmogen activators are widely used in pharmaceutical research because of their clinical applications as thrombolytic agents. The cells were initially thawed and diluted ten-fold. They were then transferred to a 75-ml T-flask containing 95% selection medium and 5% dialyzed fetal bovine serum. The flask was then placed in a incubator set at 37°C and 8% carbon dioxide overlay. The cells were subsequently transferred to a spinner flask containing 200 ml of selection medium at a concentration of 2.5×10^5 cells/ml and finally to a 1-liter flask seeded at 2.3×10^5 cells/ml. The hydridoma cells grew in this medium and were transferred to a 3-liter bioreactor at a concentration of 3.92×10^5 cells/ml.

3.4.4 Determination of k_p, τ_p and t_d

The dynamic response of the DO probe was investigated by initially placing the probe in liquid water saturated with nitrogen. The probe reading was monitored against time until a steady state is reached. The probe was then placed in liquid water saturated with air. After fitting the model to a ``first-order plus time delay" system, the parameters calculated were $k_p = 1/(8.23\text{-}0.00) = 0.122$ (8.23 $mole/m^3$ is the density of ogygen in air at 37°C), $\tau_p = 13.2$ s and $t_d = 2.3$ s. When switched from saturated air to saturated nitrogen environment, the probe constants were $k_p = 0.122$, $\tau_p = 27.3$ s and $t_d = 0.01$ s. Average values were used in Eq. 10.

Since the response of a discrete-time system is influenced by the sampling time, it is important to calculate an optimum sampling time to reduce the errors in the calculation

of k_La_B and k_La_H. Approximate values of k_La_B ($7.49 \times 10^{-4}\ s^{-1}$) and k_La_H ($5.57 \times 10^{-5}\ s^{-1}$) were estimated at the operating conditions in the 5% fetal bovine serum medium using a dynamic method. Eqs 12, 14, 15, 16, and 17 were used to calculate a sampling time of 37 *s*. The values of a_1, a_2, b_1, and b_2 were computed using a technique outlined in the next section.

3.5 Experiments and Results

In order to estimate the parameters of the z-transform (Eq. 13), the bioreactor containing the selection medium (DMEM) was run using a stirring rate of 80 RPM and a temperature of 37°C. During the experiment the total flow rate through the sparger was kept at 8.75 vvm. The flow rate corresponds to the minimum gas velocity to create very fine bubbles through the sparger. The DO signals were recorded every second. The oxygen mole fraction in the sparger varied randomly from 0.0 to 0.209. The constraints in the composition of oxygen were used in order to maintain a constant gas flow rate of 8.75 vvm. The upper limit, 0.209, corresponds to the composition of oxygen in the air stream fed through the sparger.

To calculate the overall time delay, System Identification Toolbox from MATHWORKS was used after converting the process to an ARX model of the form:

$$DO(k) = \sum_{j=1}^{p} a_j DO(k-j) + \sum_{j=0}^{q} b_j y_{2,b}(k - nk - j) + e(k) \quad (18)$$

or

$$DO = \Phi^T \theta + e \quad (19)$$

where

$$\Phi^T \equiv [-DO(k-1) \quad -DO(k-2)\cdots -DO(k-p) \quad y_{os}(k-nk) \quad y_{os}(k-nk-1)\cdots y_{os}(k-nk-q+1)] \tag{20}$$

and

$$\theta^T \equiv [a_1 \quad a_2 \cdots a_p \quad b_1 \quad b_2 \cdots b_q] \tag{21}$$

After minimizing the sum of squared error, the estimate θ is

$$\theta = [\Phi^T \Phi]^{-1} \Phi^T y \tag{22}$$

A dead time of 4 *s* was obtained after applying Akaike's Information Criterion (Akaike, 1987). The Akaike's Information Criterion was also used to obtain the order of the ARX model ($p = 2$ and $q = 2$). The system order was also verified using Lipschitz quotients (He and Asada, 1993). A nonrecursive least squares (LS) method was then used to estimate the model parameter (Strejc, 1980). The best fit parameters were $a_1 = 1.197$, $a_2 = 0.118$; $b_0 = 1.000$, $b_1 = 0.927$, $b_2 = 0.0734$. The results for one step-ahead prediction are shown in Fig. 3.2. The resulting model was tested on four new sets of y_{os} data which differ in magnitude and frequency. Only one data set is shown (Fig. 3.3). Similar results were obtained for the remaining testing sets. The normal probability plots (Figs 3.2 and 3.3) show that the noise sequence $e(k)$ is white. However, the noise sequence is autocorrelated, which implies correlation with Φ. In this case, the expected value of θ is

$$\varepsilon[\hat{\theta}] = \varepsilon[\theta] + \varepsilon\left[\left[\Phi^T\Phi\right]^{-1}\Phi^T\right]\varepsilon[e] \neq \varepsilon[\theta] \tag{23}$$

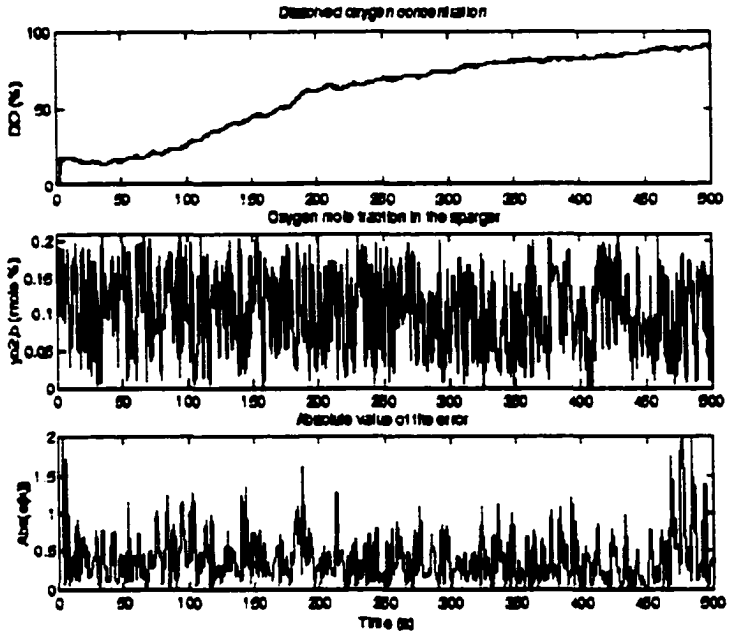

Figure 3.2 One-step ahead prediction for training set

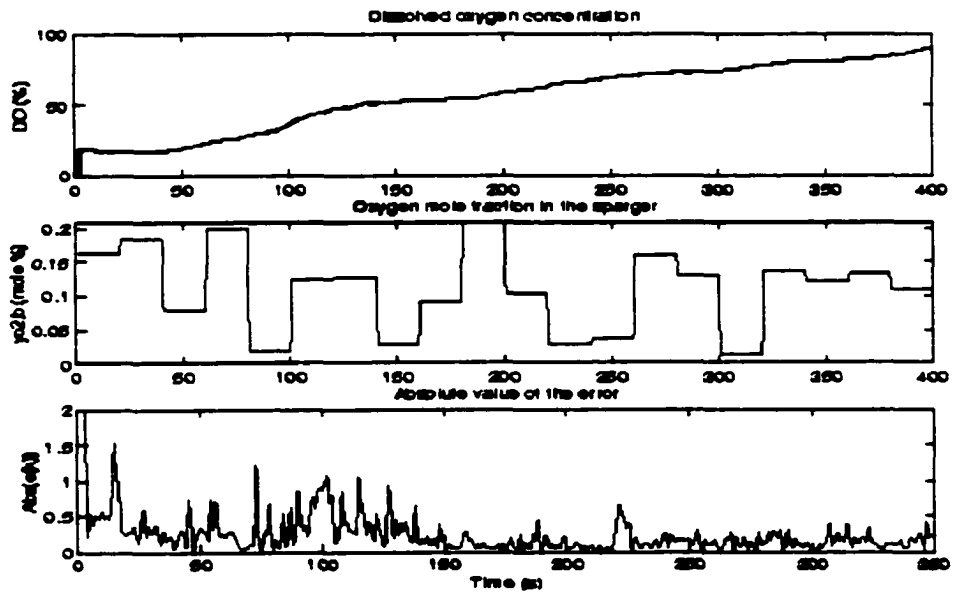

Figure 3.3 One-step ahead prediction for testing set 1

To remove the bias, an AutoRegressive Moving Average model with eXogeneous inputs (ARMAX) were used in real-time in the case of the MPC with invariant model parameters to avoid bias in the parameters. In the case of the GPC, a recursive ARMAX model (RARMAX) was implemented.

3.6 GPC, MPC and PID Control of the Simulated DO Process

Process simulations and real-time implementation are equally important in biotechnology. Initial computer-based simulations help in process identification and control by estimating model structures and tuning parameters such as control and prediction horizons, sampling time, and weights on manipulated variable changes. Simulink (MATHWORKS, Inc., Natick, MA) provides the simulated environment for this work. Stability of GPC is usually insured by proper choices of prediction, control horizons and weighting matrices in the objective function (Sistu and Bequette, 1996). The GPC problem solved in this work also constrains the oxygen mole fraction into the sparger between 0.0 and 0.209. A control horizon of 4 and a prediction horizon of 10 were used. These values were chosen based on the speed of the response and the stability of the controller. The weights on manipulated variable changes that improved system performance and stability were 100, 75.0, 50.0, 25.0. The model parameters were calculated recursively. To simulate the process, the true plant is approximated by the solution to Eq. 13 at discrete time intervals using the parameters computed from Matlab. It should be mentioned that instead of this trial and error approach, one could use the Nonlinear Control Design Blockset (MATHWORKS, Inc., Natick, MA) to optimize the

parameters. The results are shown in Fig. 3.4. The range of manipulated variable is [-0.209, 0.209]. The mole fraction of oxygen through the sparger is actually limited to [0.0, 0.209]. However, since the controller output is in the deviation form, negative values for $yo_{2,k}$ are observed. The current and delayed outputs of the plant were fed to the GPC algorithm. The controller computed four manipulated variable moves after updating the model parameters. The first move was fed-back to the DO process. The setpoints were scheduled to change at regular time intervals.

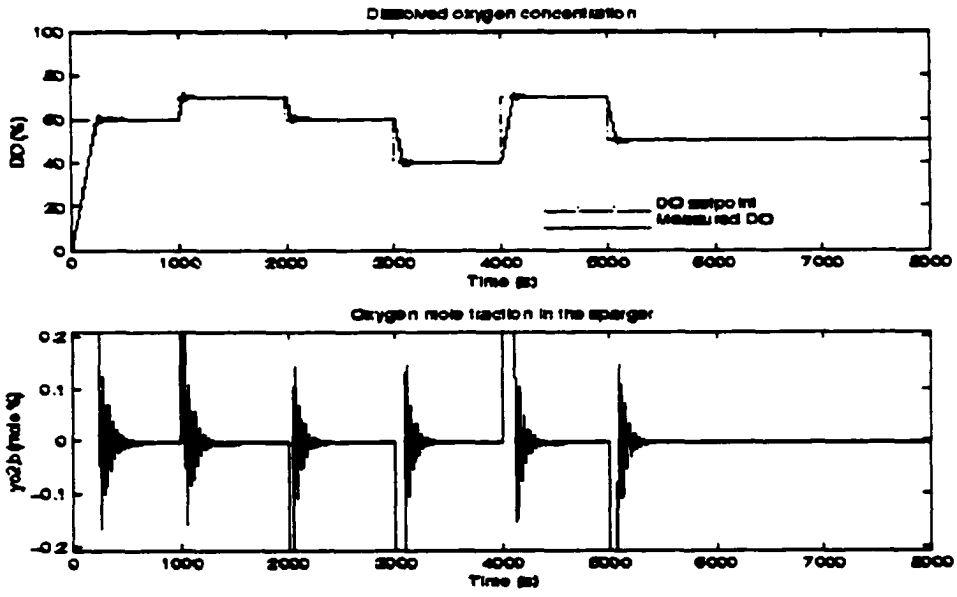

Figure 3.4 Simulation of GPC control results of the DO process

The GPC controller was compared to PID and MPC controllers for the simulated case. In order to tune the PID controller, the model was built using Simulink (MATHWORKS, Inc., Natick, MA). The velocity form of the PID controller was used and stored in a file. The tuning parameters used: $T_d = 0.01$, $T_i = 1.0 \times 10^8$, $K = 1.0 \times 10^{-4}$ represent the derivative time, the integral time and the gain, respectively. These parameters were obtained by trial and error and gave satisfactory results (Fig. 3.5). Tuning of the PID controller was difficult because of the constraints imposed on the manipulated variable. The controller acted like an ON-OFF controller taking on values of -0.209 and 0.209 to follow the setpoint changes. The ON-OFF behavior of the manipulated variable $y_{o2,B}$ is shown with only 500 data points in Fig. 3.5. Other tuning parameters have been used with no improvement in the manipulated variable profile.

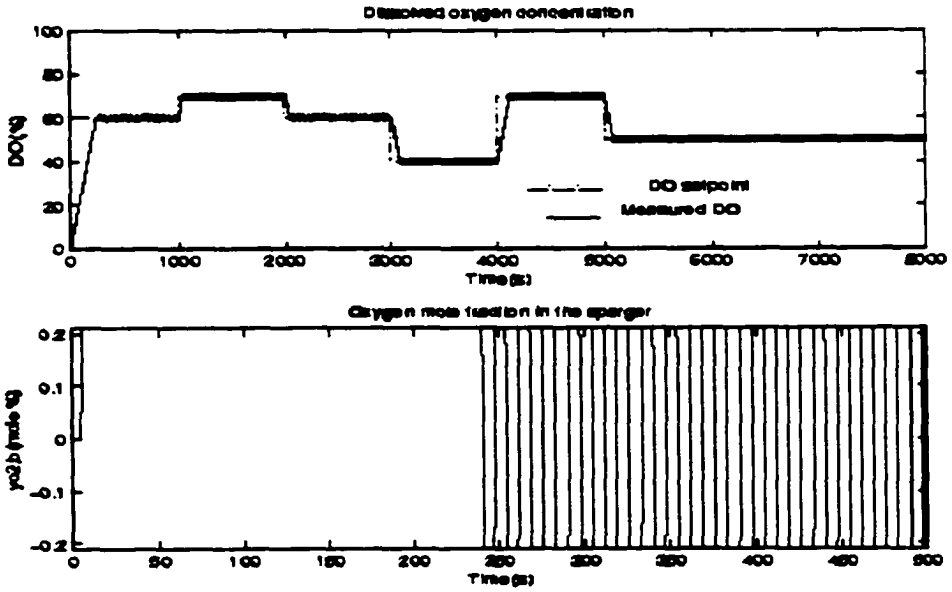

Figure 3.5 Simulation of PID control of the DO process

The MPC controller was implemented using the model parameters obtained in the system identification. The same tuning parameters were used as in the GPC case with the exception that the model parameters did not change during the simulated run. A constrained MPC was implemented. The results are shown in Fig. 3.6. The results are very identical to the GPC case.

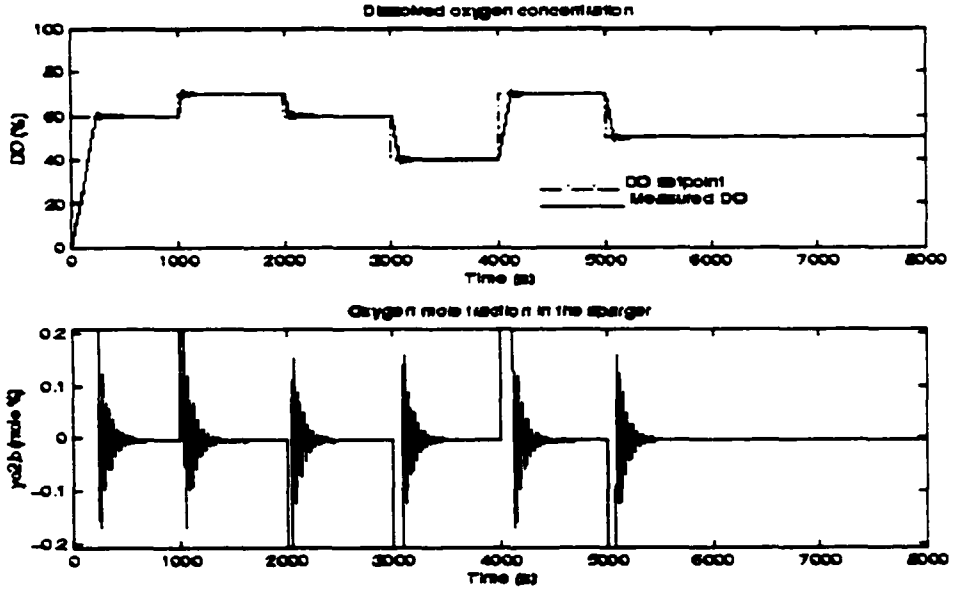

Figure 3.6 Simulation of MPC control of the DO process

3.7 Experimental Results Using Cell-free Medium

The controllers were first tested in a cell-free medium. The tuning parameters used in the simulation runs were maintained for all three controllers. The setpoints were

scheduled to change between 40% and 70% DO. The total flow rate of the inlet gas remained constant during the fermentation. In order to implement the GPC controller, Real Time Window Target (MATHWORKS, Inc., Natick, MA) was used. The software works in conjunction with Matlab and Simulink (MATHWORKS, Inc., Natick, MA). The velocity form of the PID controller was used. The state variables, the controller input and output signals and the model parameters were plotted in real-time, and could be monitored on the computer screen, which facilitated process monitoring and control. The results are shown in Fig. 7 for a two-hour run.

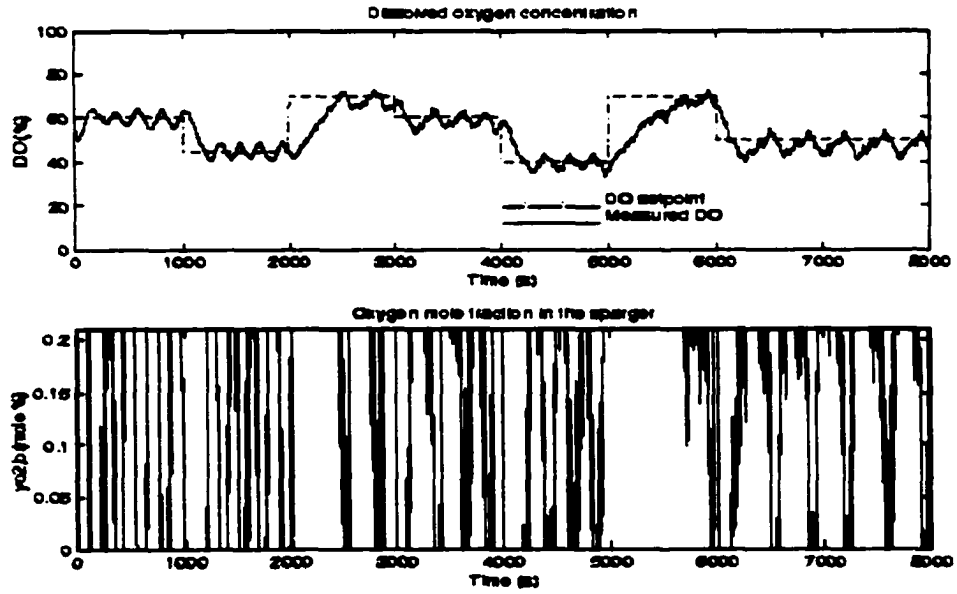

Figure 3.7 Experimental results of GPC control of the DO process in a cell-free medium

The PID controller was implemented using the tuning parameters already computed. The ON-OFF behavior of the output signal was again noticed (Fig. 8).

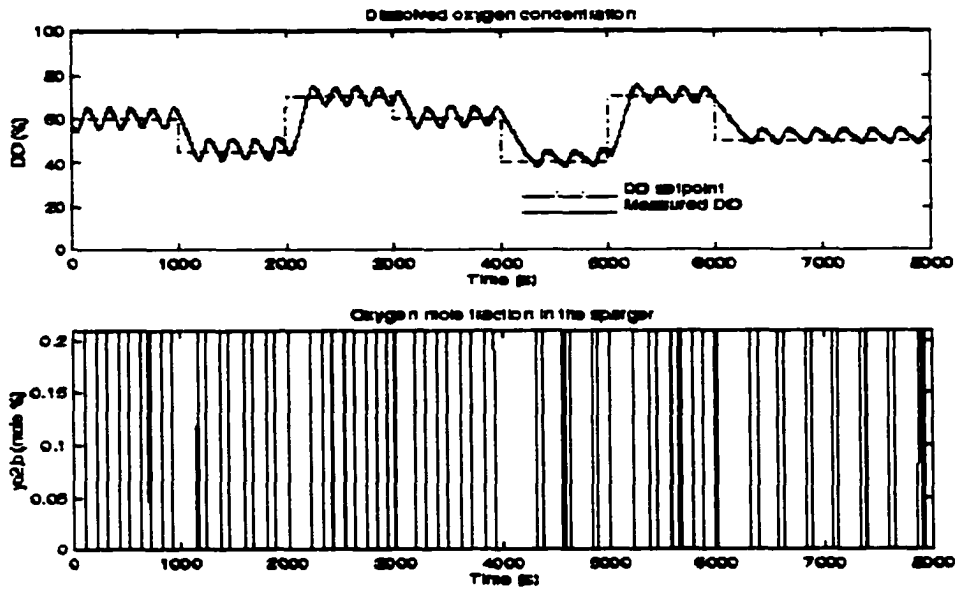

Figure 3.8 Experimental results of PID control of the DO process in a cell-free medium

However, in terms of speed of response, the PID performed better than the GPC controller and showed less overshoot especially when the DO was set at 50%. A similar dynamic response was observed for the MPC (Fig. 3.9). Contrary to the results obtained in the simulation case, the MPC exhibited an ON-OFF behavior. However, a satisfactory setpoint tracking was maintained.

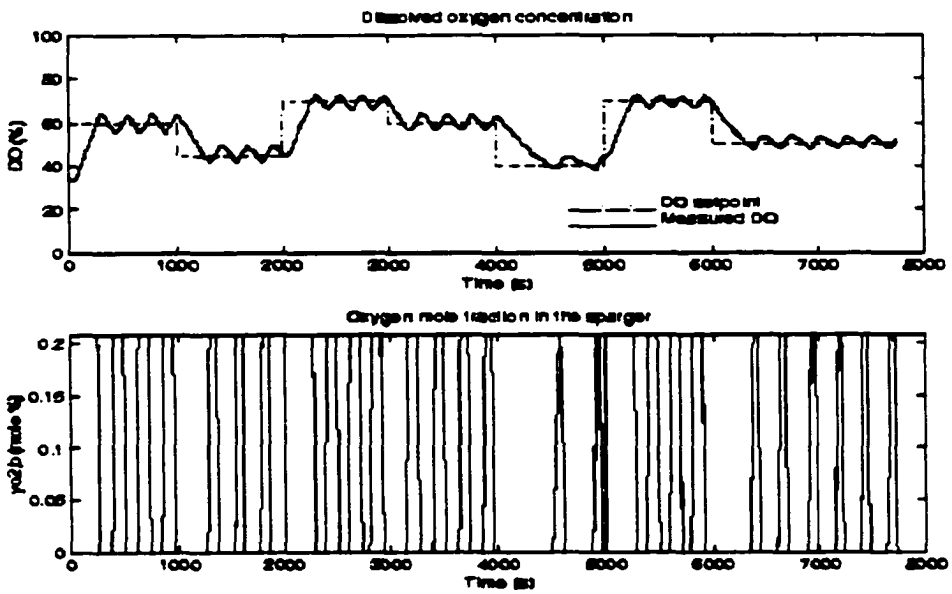

Figure 3.9 Experimental results of MPC control of the DO process in a cell-free medium

3.8 Experimental Results Using Hybridoma Cells

The controllers were applied to the cultivation of hybridoma cells for 30 hours. For the first 5 hours, the viable cells concentration increased from 3.92 to 5.50 × 10^5 cells/ml during application of the GPC controller. The glucose concentration decreased from 2.90 to 2.70 *g/l*. The depletion of glucose in the medium, one of the primary energy sources for mammalian cell cultures (Zhou and Hu, 1994) is indicative of cellular metabolic activity. Lactic acid and ammonia concentrations also increased in the biorector. From a control standpoint, these bioreactions introduce a disturbance to the process (Eq. 6), namely the oxygen uptake rate (OUR). The resulting process is therefore more difficult to control than the dissolved oxygen in a cell-free fermentation broth. The controller may need to

adapt to the time-variant nature of the process.

After implementation of the controllers. it appears that the GPC outperformed the PID and MPC controllers. The concentration of the dissolved oxygen is shown in Fig. 3.10, 3.11, and 3.12 for the PID, MPC, and GPC cases, respectively. The setpoint of DO was kept at 45%. The norm of the errors between the setpoint and the controller output signals was used as a performance index. The results are tabulated (Table 3.1). The model parameters (Eq. 18) as well as the air and nitrogen flow rate are plotted in Fig. 3.13.

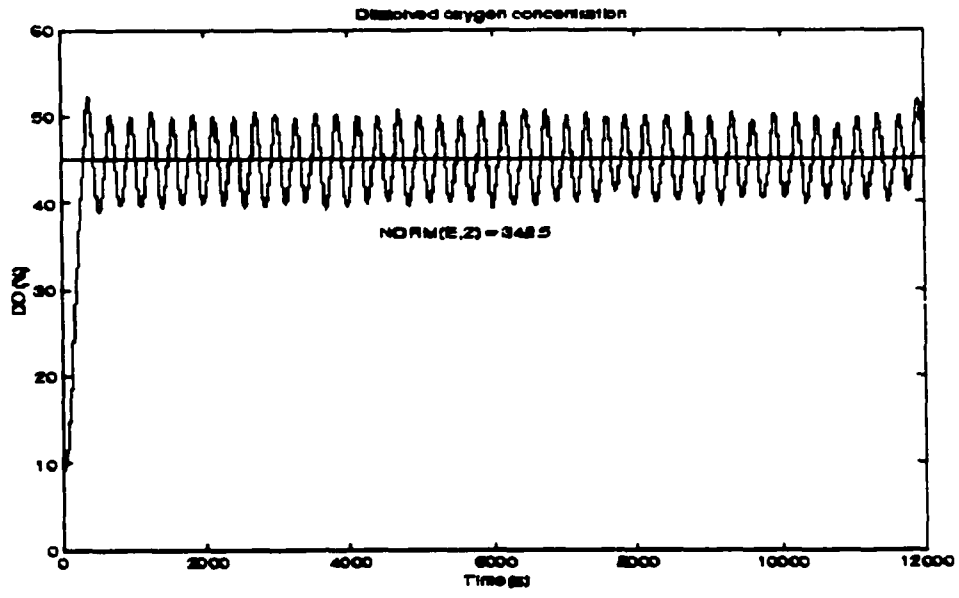

Figure 3.10 PID control of DO in hybridoma cell culture

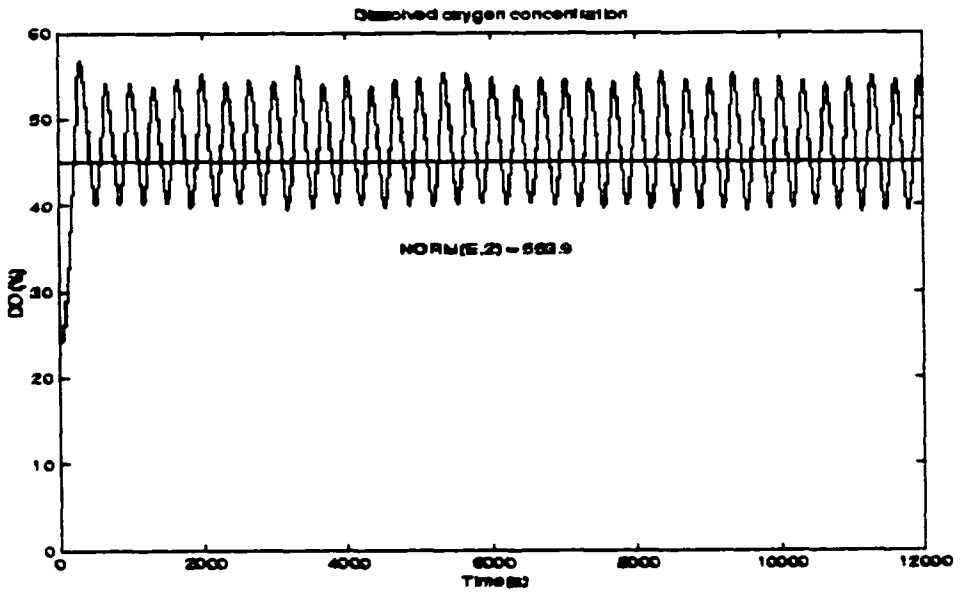

Figure 3.11 MPC control of DO in hybridoma cell culture

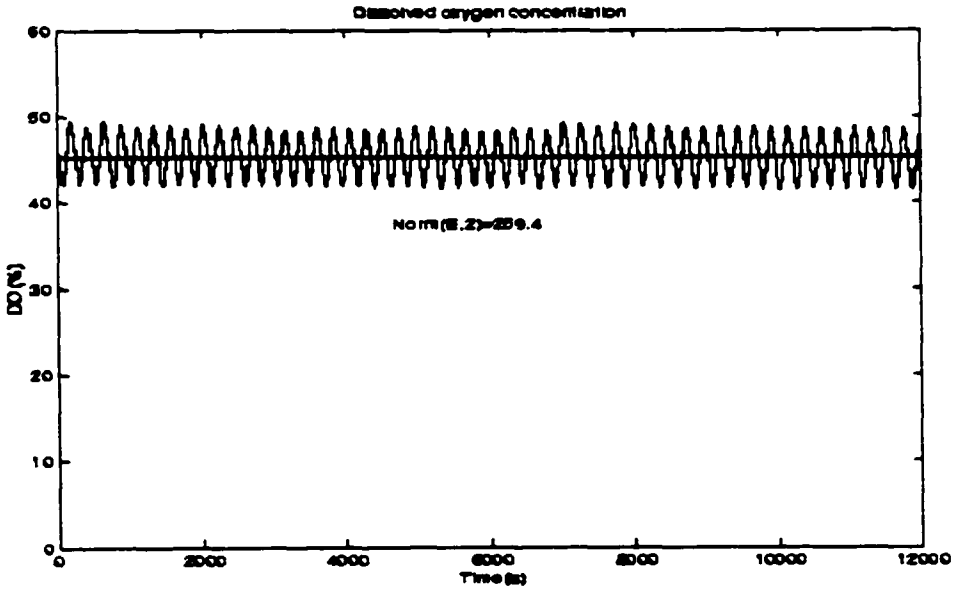

Figure 3.12 GPC control of DO in hybridoma cell culture

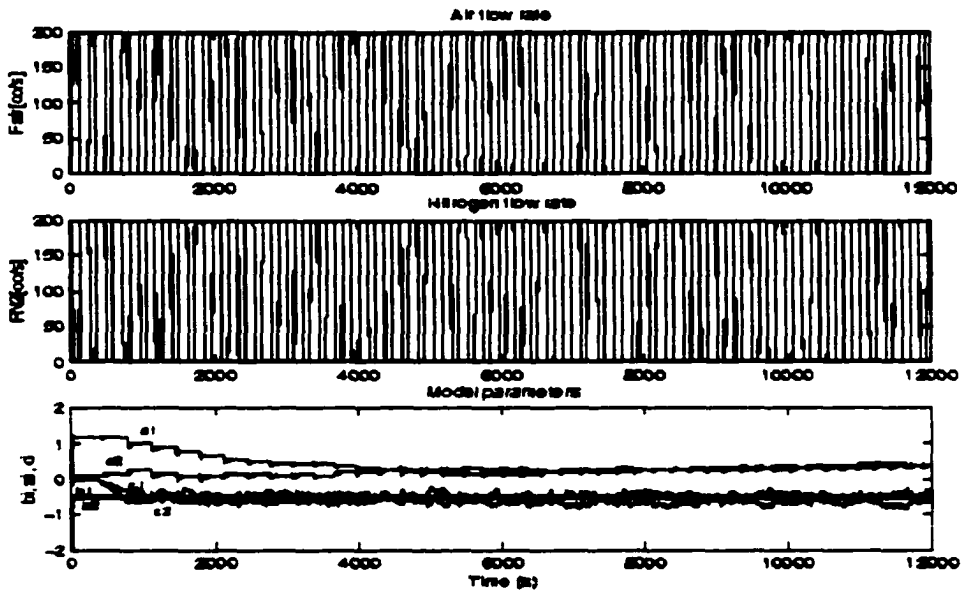

Figure 3.13 Gas flow rates and model parameters (Eq. 18)

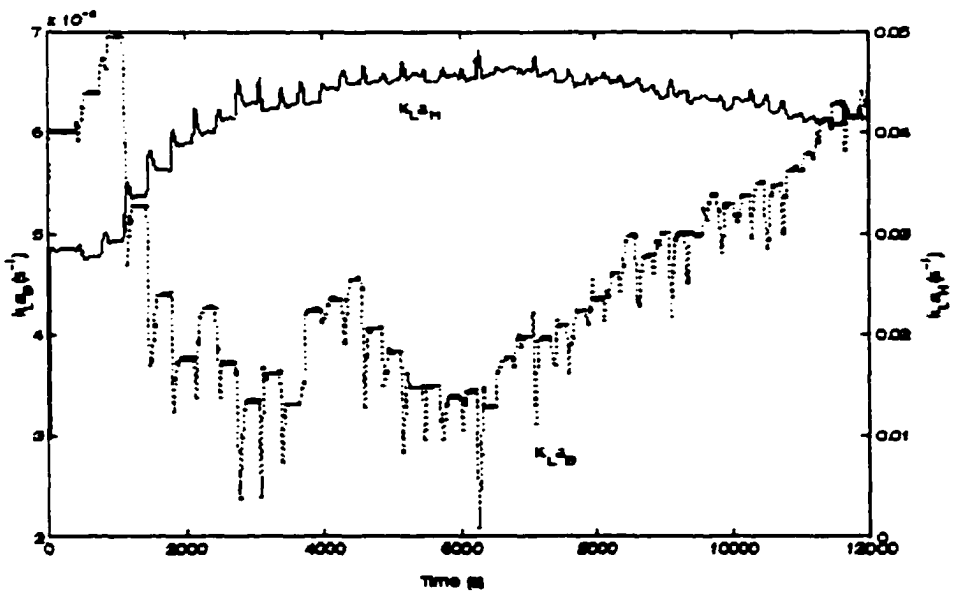

Figure 3.14 Mass transfer coefficients k_La_B and k_La_H

Controller	GPC	PID	MPC
Error Norm	259.4	348.5	553.9

Table 3.1 Controller performance in hybridoma cell

3.9 Discussions

Computer-aided simulations were used to help in the analysis of the DO process as well as the design of the GPC, MPC and PID controllers. One novel approach was to reconcile the parameters of the input-output model of the DO process with the overall mass transfer coefficients (Eqs 14, 15, 16, and 17). This approach simplifies process identification and reduces the chances of over-parameterization. The order of the system was verified using Akaike's Information Theoretic Criterion (Akaike, 1987) and Lipschitz quotients (He and Asada, 1993). The approach presented here allows the use of input-output (black box) type of model to determine physiologically important parameters such as $k_L a_B$ and $k_L a_H$.

Although simulations aid in the design of controllers, the results may vary significantly with the experimental results. Based on the simulated results shown in Figs 4, 5, and 6, the output "chattering" observed in real-time application for all three controllers would be hard to predict. The chattering can be caused by the ON-OFF behavior of the control signals. In process control literature, controller chattering is the result of variable structure system and control designs have been proposed to alleviate the high frequency oscillations (Chang et al., 1992; Munoz and Sbarbaro, 2000). In the present case, the

chattering is attributed to the constraints on the inputs of the controllers. A first-order filter is recommended as an initial step in alleviating the chattering. Fig. 14 shows that the model parameters vary during the course of the experiment. The k_La_B values are of the same order of magnitude as the one computed in the cell-free environment. The k_La_H values vary significantly. The head space mass transfer coefficient is expected to be less than k_La_B because of the sparger located near the bottom of the vessel. The discrepancy in k_La_H values needs to be investigated further. Errors in the overall mass coefficient are also introduced by the presence of the moving average term in the ARMAX model.

The controllers were tested on a bioreactor containing hybridoma cells. The resulting process poses a more difficult challenge than DO control in cell-free medium because of the introduction of disturbances in the process. The run lasted 30 hours. For the first 5 hours, the viable cells concentration increased from 3.92 to 5.50 × 10^5 cells/ml and decreased thereafter. This may be due to the fact that the cells were near the stationary phase in the 1-liter spinner flask prior to the transfer. Only 0.5 liter of fresh medium was added. This approach was taken in order to test the controllers in a high cell density environment. Table 3.1 shows that the GPC outperformed the other controllers. This is due to the ability of the GPC to adapt to changes in DO dynamics caused by changes in cell metabolism. The MPC did not perform as well as the PID, which was unexpected.

The experimental work was done using 3-liter bioreactor. In the context of this investigation, the objective of a scale-up strategy is to maintain a constant dissolved oxygen concentration in a large scale fermenter using the methodology outlined above. It should be noted that the performance criterion of a successful biochemical process

generally depends on optimum temperature, pressure, pH, and substrate concentration. These laboratory scale fermenter conditions are maintained during scale-up by taking into account factors such as heat transfer surface-to-volume ratio, oxygen transfer rate, quality of mixing, superficial air velocity, age and stability of culture (Humphrey, 1998).

Oxygen transfer rate is an important variable in the design of large scale fermentation system. Because mammalian cells are shear-sensitive, an optimal balance between mixing requirements, oxygen transfer and shear rate must be achieved in the bioreactor in order to maintain a low-shear environment. One of the strategies suggested by Hubbard focus on maintaining mass transfer coefficients constant in scaling up processes involving aeration (Hubbard, 1987). The approach is based on the fact that most fermentations are oxygen limited. It is then important to provide equal oxygen transfer at various scales of operation. By using the same superficial velocity, and mass transfer coefficient per unit volume, for instance, new values for total gas flow rate and impeller speed can be calculated for large scale bioreactors (Hubbard, 1987). The GPC controller will use these updated values for adequate oxygen transfer. Furthermore, the present methodology can be used to validate the upscaling procedure since it provides a soft(software-based) sensor for mass transfer coefficients. The reader is encouraged to review the work of Humphrey for scale-up of bioreactors (Humphrey, 1998).

3.10 Conclusion

A method of controlling dissolved oxygen in a shear sensitive environment was developed using the oxygen mole fraction as manipulated variable. In the case of the generalized predictive controller, the state variables including the model parameters were observed in real-time in a Simulink environment using Real Time Windows Target. An input-output model of dissolved oxygen was used to estimate the overall mass transfer coefficients: k_La_B and k_La_H. The order of the system was found to be 2, which agreed very well with the rate equations describing the DO process. After testing the PID, the MPC and GPC controller on a cell free medium, it was found that the GPC performed slightly better than the MPC. A cycling effect was observed in all three cases, which may be due to constraints on the input variable. The GPC performed better when tested on a culture of hybridoma cells.

3.11 Notation

u	manipulated variable vector
y	controlled variable vector
r	reference variable vector
y	mole fraction (%)
u_{min}	lower bound of manipulated variable vector
u_{max}	upper bound of manipulated variable vector
Γ	weighting matrix on output error
β	weighting matrix on control moves

k	sampling time (s)
j	step ahead prediction index
N_2	maximum prediction horizon (s)
Nu	maximum control horizon (s)
nk	delay in manipulated variable u (s)
C	concentration ($mol\ L^{-1}$)
P	total pressure (bar)
H	Henry coefficient ($bar\ L\ mol^{-1}$)
k_La	mass transfer coefficient (s^{-1})
S	Laplace variable
y	mole fraction in the gas phase
A	model parameter defined by Eq. 12
B	model parameter defined by Eq. 12
a	coefficients of ARX model (Eq. 14 and 15)
b	coefficients of ARX model (Eq. 16 and 17)
k_p	steady state gain of DO probe
τ_p	time constant of DO probe (s)
t_d	time delay of DO probe (s)
K_p	parameter defined in Eq. 11
e	modelling error (Eq. 18)
p	maximum lag in the output variable
q	maximum lag in the input variable

DO dissolved oxygen concentration (% of air saturation)

Greek letters

Φ regressor matrix

θ parameter vector

θ estimated paramater vector

Δ denotes the difference operator

ε expected value

Subscrpits

O_2 refers to oxygen

sat refers to saturation

B refers to bubble

H refers to headspace

L refers to liquid phase

sp refers to sparger

pu refers to purge

Superscripts

* refers to deviation variables

3.12 Acknowledgment

The presented work was supported by the National Science Foundation (BES-9622526), the UNCF-Merck Graduate Science Research Dissertation Fellowship, and the Colorado State Experiment Station.

3.13 References

Akaike, H. Factor analysis and AIC. *Psychometrika*, 1987, *52*, 317-332.

Blanch, H.W.; Clark, D.S. *Biochemical Engineering*. Marcel Dekker, Inc., New York, N.Y., 1996.

Chang, F.J.; Twu, S.H.; Chang, S. Tracking control of DC motors via an improved chattering alleviation control. *IEEE Trans. Ind. Electron.*, 1992, *39*, 25-29.

Clarke, D.W.; Mohtad, C.; Tuffs, P.S. Genelarized predictive control - Part I. The basic algorithm. *Automatica*, 1987, *23*, 137-148.

Cooney, C.L. Are we prepared for animal cell technology in the 21st century. *Cytotechnol.*, 1995, *18*, 3-8.

De Figueiredo Lopes, M.M.; Calderbank, P.H. The scale-up of aerated mixing vessels for specified oxygen dissolution rates. *Chem. Eng. Sci.*, 1979, *34*, 1333-1338.

Dickson, A.J. Apoptosis regulation and its applications to biotechnology. *Sci.*, 1998, *16*, 339-342.

He, X.; Asada, H. in *Proc. of the Am. Contr. Conf.* San Francisco, CA, 1993.

Heinzle, E.; Oeggerli, A.; Dettwiler, B. On-line fermentation gas analysis: Error analysis and application of mass spectrometry. *Anal. Chim. Acta*, 1990, *238*, 101-115.

Hu, W.S.; Himes, V.B. in *Bioproducts and Bioprocesses*, Flechter; Okada; Tanner, Eds., pp 33-46. Springer-Verlag New York, Incorporated, 1989.

Hubbard, D.W. in *Biotechnology Processes Scale-up and Mixing*, Ho, C.S.; Oldshue, J.Y., Eds., pp 168-184. American Institute of Chemical Engineers, New York, 1987.

Humphrey, A. Shake flask to fermentor: what have we learned? *Biotechnol. prog.*, 1998, pp 3-7.

Jorjani, P.; Ozturk, S.S. Effects of cell density and temperature on oxygen consumption rate for different mammalian cell lines. *Biotechnol. Bioeng.*, 1999, pp 349-356.

Jung, H.C.; Oh, D.K.; Jung, H.K. Control of dissolved oxygen concentration in mammalian cell culture using a computer-coupled mass flow controller. *Biotechnol. Technol.*, 1992, *6*, 405-408.

Kilburn, D.G.; Webb, F.C. The cultivation of animal cells at controlled dissolved oxygen partial pressure. *Biotechnol. Bioeng.*, 1968, *10*, 801-814.

Lee, S.C.; Hwang, Y.B.; Chang, H.N.; Chang, Y.K. Adaptive control of dissolved oxygen concentration in a bioreator. *Biotechnol. Bioeng.*, 1991, *37*, 597-607.

Lund, P. in *Methods of enzymatic analysis*, Bergmeyer, H.U., Ed., volume 4, pp 1719-1722. Verlag Chemie Weinheim, Academic press, New York, 2nd edition, 1974.

Miller, D.N. Scale-up of agitated vessels gas-liquid mass transfer. *Mathematical Programming*, 1974, *20*, 442--453.

Mizrahi, A.; Vosseller, G.V.; Yagi, Y.; Moore, G.E. The effect of dissolved oxygen partial pressure on growth, metabolism and immunoglobulin production in a permanent human lymphocyte cell line culture (36092). *Proc. Soc. Exp. Biol. Med.*, 1972, *139*, 118-122.

Munoz, D.; Sbarbaro, D. A adaptive sliding-mode controller for discrete nonlinear systems. *IEEE Trans. Ind. Electron.*, 2000, *47*, 574-581.

Oeggerli, A.; Eyer, K.; Heinzle, E. On-line gas analysis in animal cell cultivation: I. Control of dissolved oxygen and pH. *Biotechnol. Bioeng.*, 1995, *45*, 42-53.

Reuveney, S.; Velez, D.; Macmillan, J.D.; Miller, L. Factors affecting cell growth and monoclonal antibody production in stirred reactors. *J. Immunol. Methods*, 1986, *86*, 53-59.

Sargantanis, I.G.; Karim, M.N. Variable structure NARX models: Application to dissolved-oxygen bioprocess. *AIChE J.*, 1999, *45*, 2034-2045.

Seborg, D.E.; Edgar, T.F.; Mellichamp, D.A. *Process dynamics and control*. John Wiley and Sons, Cambridge, MA, 1989.

Self, D.A.; Kilburn, D.G.; Lilly, M.D. The influence of dissolved oxygen partial pressure on the level of various enzymes in mouse LS cells. *Biotechnol. Bioeng.*, 1968, *10*, 815-828.

Sistu, P.B.; Bequette, B.W. Nonlinear model-predictive control: Closed-loop stability analysis. *AIChe J.*, 1996, *42*, 3388-3402.

Strejc, V. Least squares parameter estimation. *Automatica*, 1980, *16*, 535-550.

Taylor, G.W.; Kondig, J.P.; Nagle, S.C. Jr.; Higuchi, K. Growth and metabolism of L-cells in a chemically defined environment culture systems 1. effects of o_2 tension on L-cell cultures. *Appl. Microbiol.*, 1971, *21*, 928-933.

Zhou, W.; Hu, W.S. On-line characterization of a hybridoma cell culture process. *Biotechnol. Bioeng.*, 1994, *44*, 170-177.

Zhou, W.C.; Chen, C.C.; Buckland, B.; Aunins, J. Fed-batch culture of recombinant NS0 myeloma cells with high monoclonal antibody production. *Biotechnol. Bioeng.*, 1997, *55*, 783-792.

William, M.M.; Charles, R.W.; Harvey, W.B. Effects of dissolved oxygen concentration on hybridoma growth and metabolism in continuous culture. *J. Cell Physiol.*, 1987, *132*, 524-530.

This chapter has been published in Biotechnology Progress:

Simon, L, and Karim MN. 2001. Identification and control of dissolved oxygen in hybridoma cell culture in a shear sensitive environment," *Biotechnol Progress* 17: 634-642.

Chapter 4

DATA-BASED ANALYSIS OF BIOPROCESSES

4.1 Introduction

Bioprocesses are the results of complex metabolic reactions occurring within a cell. The formation of genetically engineered product depends on several factors. Among these, the origin of the cell line, compositions of the complex medium, and biochemical pathways are noteworthy (Bardford et al., 1992). Mathematical descriptions of these biochemical reactions are usually nonlinear and time-varying. Unstructured models assume balanced growth of microorganism, i.e., a doubling of cell number is followed by a doubling in the composition of major cellular components, such as enzymes, DNA, and RNA. These models are inadequate for transient regimes since they assume no time delay following a change in the compositions of the growth medium (Patarinska et al., 2000). One such model was studied by Glacken (1987) to explain hybridoma culture kinetics. Several structured models, which account for intracellular metabolism, have also been proposed in the literature to explain growth of microorganisms and product formation (Patarinska et al., 2000; Farza et al., 2000; Lee, 1992). The derived equations are nonetheless simplified versions of biochemical transformations taking place within the cell

and fail to provide a complete description of the factors that regulate the complex of physical and chemical processes.

There are various reasons to use black box (input-output) models instead of structured or unstructured approaches to describe biotechnological processes (Saucedo and Karim, 1997). Depending upon the state equations describing the dynamic behavior of the fermentation, the cellular specific growth rate, μ, for instance, may be a complex function of state variables, which are difficult to measure on-line. Farza et al. (2000) noticed that the choice of a model for μ is often onerous. They devised nonlinear observers for on-line estimation of this parameter instead of assuming an specific equation for μ. The identification of the dynamics of microbial systems, although fundamental to a better understanding and prediction of biotransformations, gives rise to intractable problems, impractical for control purposes.

Another reason to employ input-output models is the lack of accurate kinetic models. The development of growth kinetics is central for the design and optimization of fermentation systems. However, most classical models only provide macromeasures of an array of enzymatic reactions occurring within the cells. The biological cell system is, in fact, affected by perturbations in the compositions of the growth medium including changes in pH, temperature, dissolved oxygen (DO), and substrate concentrations. The dependence of cell growth on certain environmental factors is poorly understood. As a result, assumptions concerning the cells and the number of components limiting the reaction rate are made in order to formulate useful kinetic equations (Lee, 1992). Black box models are not based on material balance equations. They do not require the knowledge of specific state equations and can be extended to incorporate new process

information. Examples of these models are autoregressive exogenous (ARX) (Ljung, 1987) models, nonlinear autoregressive exogenous (NARX) models (Sargantanis and Karim, 1999), and artificial NN models (Eikens, 1996). This contribution explores the implementation of black box models to two biological processes. The first case study analyzes the dependence of apoptotic cells on viable cells, asparagine and glutamine; the second involves the applications of NNs to an industrial fermentation process. These processes are very difficult to model using a first principle model approach. The dependence of apoptotic cells on viable cells, asparagine and glutamine has not been described mathematically. The high number of state variables of the industrial fermentation process would give rise to complex models. As a result, a black box model seems appropriate in both cases.

4.2 Case Studies

4.2.1 Model of Starvation-induced Apoptosis on Two Amino Acids

Recombinant mammalian cells produce important biological proteins such as Hepatitis B virus surface antigen, glycoprotein D of the Herpes Simplex virus, tissue type plasminogen activator, monoclonal antibodies and interferon-gamma. However, as noted by Murray et al. (1996), the productivity of recombinant mammalian cell lines in batch culture is limited by the rate at which cells die right after reaching a maximum cell density. Maintaining cell viability in mammalian cells is a challenge because of apoptosis – programmed cell death (PCD). For hybridoma, myeloma, and CHO cells, PCD is a way of life and can be induced in response to several stress conditions, including starvation-

induced, during the declining phase of batch culture (Singh et al., 1994; Franek et al., 1992; Mercille and Massie, 1994).

The two mechanisms of cell death reported in the literature are necrosis and apoptosis (Wyllie et al., 1980). Necrosis, also called accidental cell death or pathological cell death, is a passive process that occurs when the cells are exposed to extreme environmental or physiologic stresses. The cells undergoing necrosis play a passive role in initiating the process of death. In PCD, on the contrary, the cells participate actively in the death mechanism (Wyllie et al., 1980). Models of starvation-induced apoptosis, based on relevant amino acids, are important to facilitate control of PCD. Since classical descriptions of the dynamics of mammalian cells do not take into account the dependence of the apoptotic specific death rate on amino acid concentrations, the control of PCD is difficult in the current framework. It should be noted that Cowger et al. (1999) proposed a kinetic model that accounted for both apoptosis and necrosis in insect-cell cultivation. However, the apoptotic death rate was held constant in their mathematical description. In this study, the concentration of apoptotic cells was predicted using an input/output ARX model. The system incorporated the concentrations of asparagine, glutamine, viable and apoptotic cells at previous time steps.

4.2.2 Cultivation Conditions

The CHO cell line, CHO 1-155500, obtained from ATCC (American Type Culture Collection, Manassas, VA) was used in this research. The cells produce recombinant tissue-type plasminogen activator (t-PA) that has clinical applications as a thrombolytic agent. The cells were initially thawed and diluted ten-fold (1 ml of culture and 9 ml of

90% HAM'S/F-12 medium and 10% fetal bovine serum). These were then transferred to a 75 ml T-flask containing 95% selection medium (Dulbecco's Modified Eagle Medium) and 5% dialyzed fetal bovine serum. The flask was placed in an incubator (VWR Scientific Products, model 2325, West Chester, PA) set at 37°C and 8 % carbon dioxide overlay. For subsequent studies, the cells grew in a 3-l bioreactor (New Brunswick, Scientific, CO., Inc., Edison, NJ). The pH (Cole-Parmer Instrument Company, Vernon Hills, Illinois) was controlled at 7.2 by addition of 1 M NaOH and carbon dioxide. The dissolved oxygen (Cole-Parmer Instrument Company, Vernon Hills, Illinois) was controlled at a concentration of 40% saturated air. The agitation speed was set at 80 RPM. The temperature was maintained at 37°C.

4.2.3 Sample Analysis

The concentration of total cells was measured using a hemacytometer. The samples were initially diluted to 2,000-20,000 cells per ml. Cell viability was assessed by trypan blue Trypan blue exclusion (Phillips, 1973). Flow cytometry (Coulter EPICS V, Beckman Coulter Inc., Miami, FL) was the methodology employed to detect and quantify apoptotic cells (Darzynkiewicz et al., 1992; Telford et al., 1994; Darzynkiewicz et al., 1997). Sub G1 peak by propidium iodide staining was used to quantify apoptotic cells. The DNA of apoptotic cells usually breaks up and small molecular weight fragments are left free in the nucleus. Following alcohol fixation, these fragments were eluted by washing in PBS buffer. After staining by propidium iodide, these cells are quantified since they show a reduced fluorescence and a Sub-G1 peak. The compositions of amino acids

were determined by a HPLC (Waters, Milford, Massachusetts), method (Reid et al., 1987). The product, t-PA, was analyzed via ELISA (Hermann, 1986).

4.2.4 Apoptosis Model

The first objective was to model the concentration of apoptotic cells using the concentrations of viable cells, glutamine and asparagine. Previous work done in our laboratory has shown that, for the CHO cell line used, glutamine and asparagine can protect the cells against death by apoptosis. However, in previous approaches, it was assumed that the concentration of apoptotic cells at time t only depends on the concentrations of viable cells, glutamine and asparagine at the same time. Although this assumption is valid when one takes into account the time constant for cell cultures, a complete description of starvation induced apoptosis on key amino acids should include the dependence of PCD at time t on the concentration of viable cells, glutamine, asparagine, and apoptotic cells at time t-i, i is the lag of the system and may vary for each input and output variable.

Process data were generated by running two different batch fermentations. In system identification, the optimal number of parameters had to be determined to minimize the variance contribution to the modeling error. Several methodologies for structure selection have been proposed in the literature including Akaike Information Criterion (AIC) (Akaike, 1987). These methods usually assume an explicit form of the model describing the actual plant. Since feedforward NNs with one hidden layer have been proven to be sufficient to approximate any arbitrary continuous function (Hornik et al.,

1989), they can provide a nonlinear expansion of lagged input and outputs. The optimal system order can then be determined by constructing different combinations of input and output lags. The performance of each network model is evaluated using a loss function such as the mean squared error (MSE). The lag number, which corresponds to the network architecture with the lowest MSE, determines the order of the system. The problem with the outlined approach lies in the calculation of the optimal NN weights, which is equivalent to solving a global optimization problem. There is no guarantee of reaching a global minimum since the minimum MSE depends on the initial values of the weights. Although this problem can be circumvented by randomization of the initial weight matrix, network growing (Fahlman and Lebiere, 1990), or network pruning techniques (Reed, 1993), these methodologies are time consuming and computationally expensive. They can, however, be used to improve the network performance once the order of the system is identified.

In the present work, an ARX description was used to represent the system. The ARX function was chosen because of its simplicity and ease of parameter convergence. The model with the minimum MSE (or norm) is selected. A similar approach is implemented in Matlab^{R} with the function "ARXSTRUC", although restricted to single input-single output (SISO) systems. An algorithm was written that uses different combinations of input and output lag for multiple input, single output (MISO) systems. The maximum lags in the input and output were allowed to vary from 1 to 3 hours. The parameter of the model was identified using input-output data from a batch fermentation run, and the structure corresponding to the minimum loss function was selected. To

measure the performance of the optimum model, different prediction horizons (1, 2, and 5) were tested using data from a different batch fermentation run. An equation of the form

$$x_{ap}(k) = a_1 x_{ap}(k-1) + b_1 x_v(k-1) + b_2 x_v(k-2) + b_3 Gln(k-1) + b_4 Asn(k-1) + e(k) \quad (1)$$

was obtained. The variables x_{ap}, x_v, Gln, and Asn represent the concentrations of apoptotic, viable cells, glutamine and asparagine, respectively. The respective values of the parameters a_1, b_1, b_2, b_3, and b_4 are -0.9935, 0.0622, -0.0651, -0.1688×10^{-4} and -0.0892×10^{-3}. A total of 81 ARX models was generated for one, two and five-step ahead prediction. Fig. 4.1 shows the norm of the ARX models. The best representation corresponds to ARX model 10 in the figure. As can be observed from Fig 4.1, ARX model 10 describes the data more accurately since the error norm reaches a minimum for one, two, and five-step ahead prediction corresponds to ARX model 10. E is the residual of the model, T is the transpose, and $dim(E)$ is the number of the data (116 data points) used in each model. Since each fermentation run lasted about 5 days, additional data points were generated using a spline function. The experimental and predicted data are plotted in Figures 4.2 and 4.3. These graphs also show that it is not necessary to incorporate nonlinear terms in the ARX model to describe PCD. Indeed, a neural network model did not improve the prediction of experimental data (Fig. 4.4).

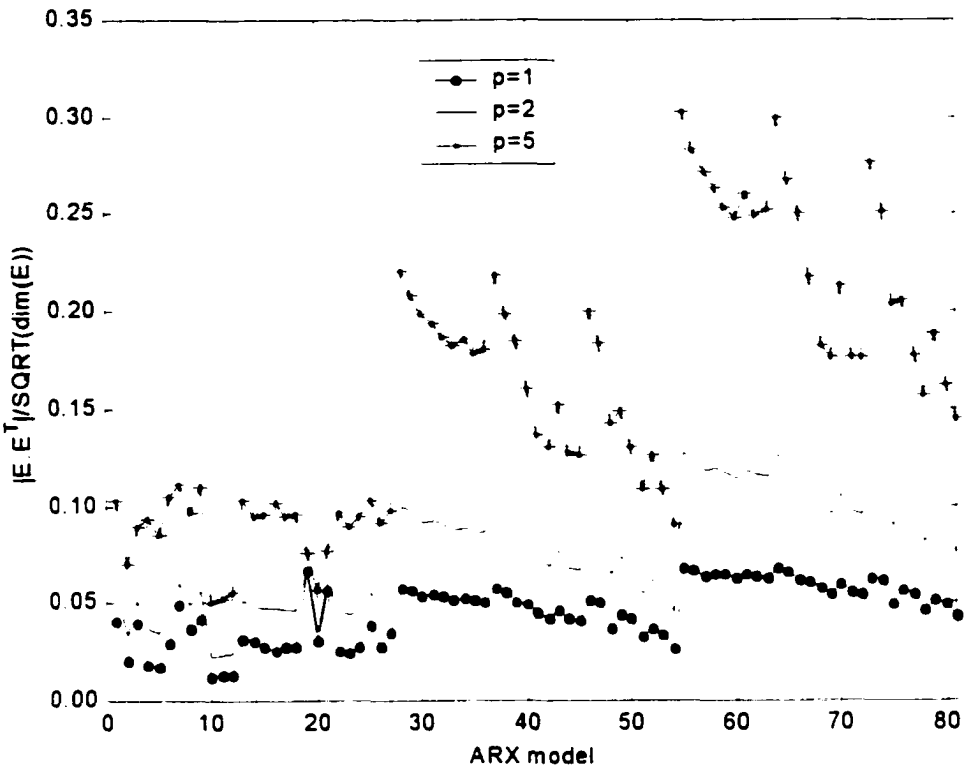

Figure 4.1 Performance (MSE) of the ARX models for 1, 2, and 5-step ahead prediction.

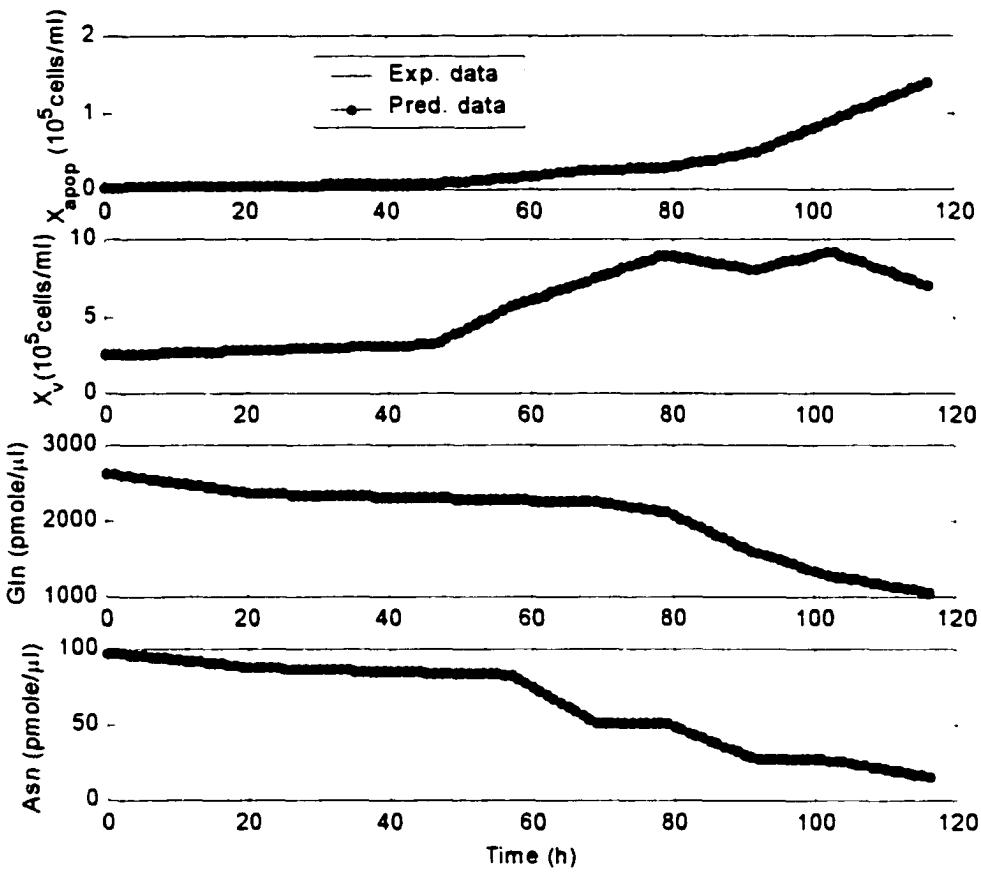

Figure 4.2 Experimental and predicted data for ARX model

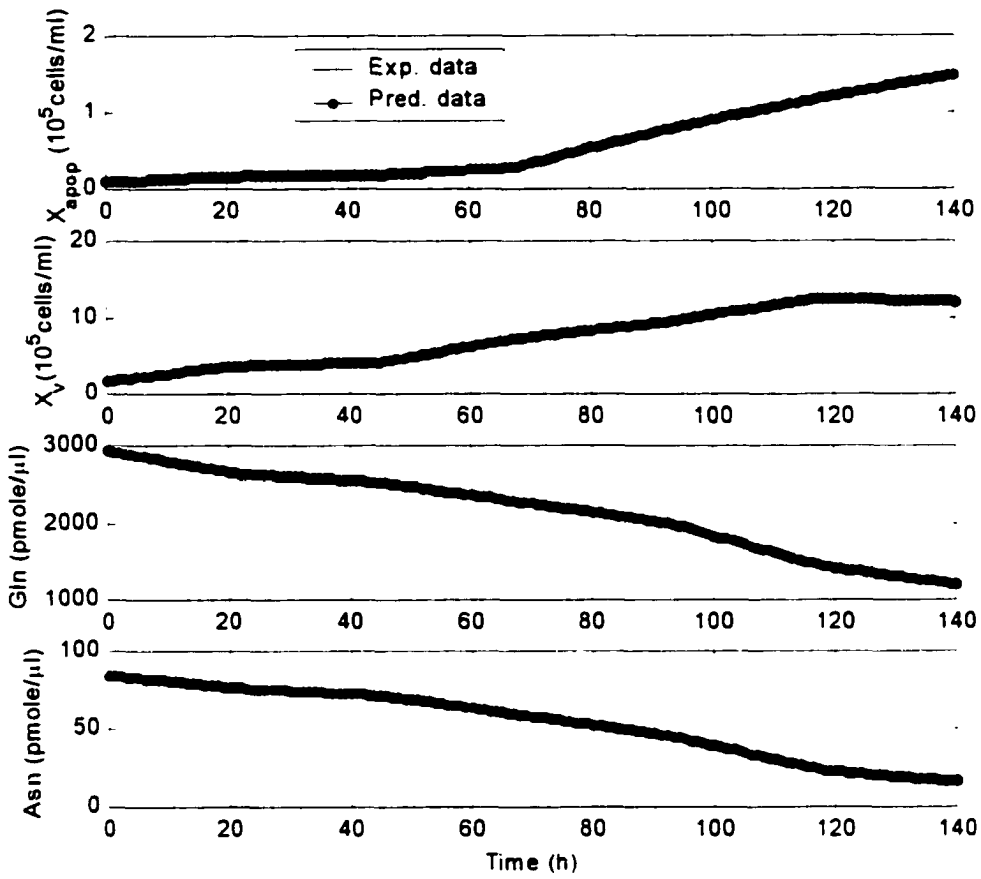

Figure 4.3 Predicted data for ARX model

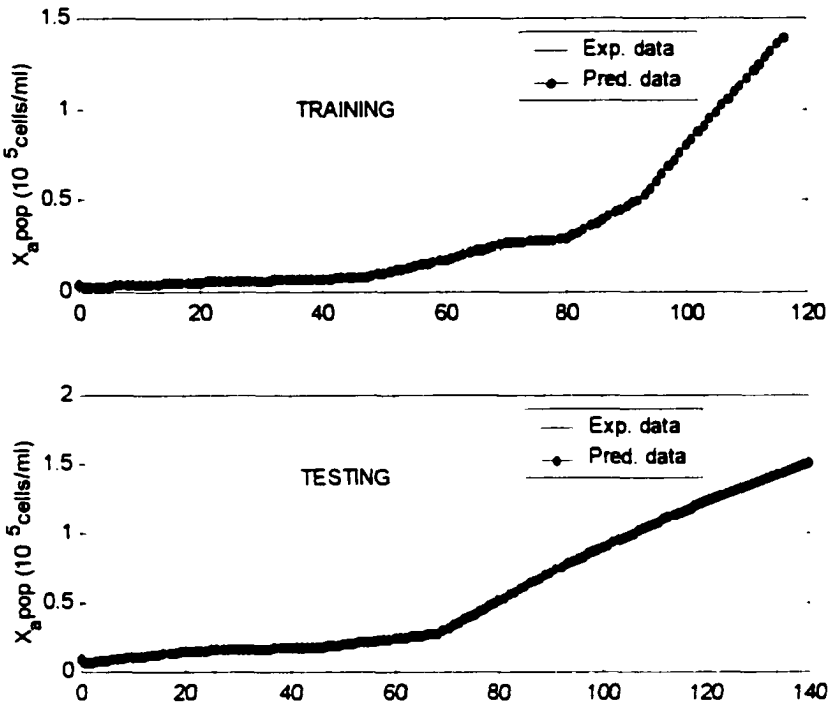

Figure 4.4 Training and testing of apoptotic cell concentration data for NN model

4.3 Analysis of Fermentation Using Neural Networks

This study investigated the applications of NN to the modeling of fermentation data. The input variables of the model are the optical density of the cell culture (OD), specific growth rate (U), pH (PH), temperature (T), stirring rate (RPM), dissolved oxygen concentration (DO), fermentor volume (FV), volume of base added (VB), concentration of glucose (GLC), and the conductance of the cultivation sample (COND). The output variable is the yield of protein in the bioreactor. The primary objective of the study was to reduce the dimensionality of the input set using various preprocessing methods such as correlation, partial correlation, and sensitivity analysis. The secondary objective was to

compare the performance of a NN based on the full set of input variables with that of a NN built using the reduced set of input variables.

The choice of methodology depends on the nature of the biological process. In the first experimental study, apoptosis was modeled using an ARX model. PCD is a response of the cells to changes in environmental conditions such as the concentrations of certain amino acids. The observed density of apoptotic cells in the bioreactor was the result of changes initiated in the medium at different instants in the past. In that case, an ARX model was appropriate since it captured the transient regime. The second case study assumed that the protein yield could be calculated based on the current fermentation states. A static NN model was implemented as a soft-sensor to approximate the protein yield in the bioreactor.

4.3.1 Neural Networks

During the last ten years, NNs have emerged as an accepted tool for modeling nonlinear processes (Baughman and Liu, 1995; Bharath and Drosen, 1994; Eikens and Karim, 1999; Simon et al., 1998; Simon and Karim, 2000). They are modeled after the structure of the brain. The learning ability of a neural network is based on its architecture and the algorithmic method chosen for training. Two main training methods are used. An unsupervised learning, in which no sample outputs are provided to the network, and a supervised leaning, in which a target output vector is supplied by the user. The four major learning laws are the Hebb's rule, the Hopfield law, the delta rule, and the Kohonen's learning law.

Due to their approximation capabilities, as well as their inherent adaptive features, artificial NNs offer an appealing alternative to classical methods of modeling nonlinear dynamic systems. NN models consist of a set of weights, **w**, a set of basis functions, $f(.)$, and a set of parameters, **p** (biases, centers, etc.). The general equation can be written as:

$$\hat{y} = f(\mathbf{xi}, \mathbf{w}, \mathbf{p}) \tag{2}$$

where $\hat{y}$ denotes the NN estimation and **xi** is the input vector. Parameters **w** and **p** are adjusted during a "training" procedure in order to minimize some kind of error measure. Different architectures of neural networks have been implemented in the literature (Eikens and Karim, 1999; Karim et al., 1997; Karim and Rivera, 1992; Simon et al., 1998; Simon and Karim, 2000). The development of a NN requires a training set made up of known input and output patterns. In the training phase, examples representative of the problem are propagated to the network. The weights are adjusted to minimize a performance criterion such as the squared error between the experimental or measured output and the output predicted by the network. The network learns the underlying relationship based on the given set using an iterative error-minimization procedure. On-line or off-line learning is used for training. In on-line training, the input-output data pairs (also called exemplars) presented to the network are stored and can be accessed repeatedly. In off-line training, the weights are updated after each exemplar is fed to the network. The exemplar is then discarded. Off-line learning offers several advantages over on-line learning. The former allows the networker to monitor the objective function for a particular set of weights. Different techniques, such as multiple random initializations or genetic algorithms (GAs), can then be tested to improve the performance of the network. Freeman (1994) presented a brief introduction to the use of GAs in the optimization of NN weights.

A validation set is either used to refine the topology (also called architecture or structure) of the network or to serve as a stopping criterion. Parameters such as the number of units in a hidden layer or the number of hidden layers determine the structure of the network. In the first methodology, the NN designer assesses the performance of different trained networks by evaluating an objective function using the validation set. The network with the smallest error is selected. In the second approach, training and validating take place concurrently. The network stops learning once the sum of residuals, based on the validation set, starts to increase beyond a user-specified number of iterations. A testing set is later used to avoid overfitting. A common practice among networkers is to use training and testing sets, especially when the number of experimental data is limited.

The performance of the network also depends on the numerical condition of the system being studied. Willis et al. (1992) suggested the use of scaled input data in order to obtain a well-conditioned problem. One can also preprocess the data to eliminate irrelevant inputs, and to avoid the "curse of dimensionality" (Bellman, 1961). Since the network has to map from a high-dimension input space to an output space, it is conceivable that, during training, the network adjusts its weights based on the extraneous portion of the input space. This would considerably affect the convergence speed of the optimization scheme. It should be noted, however, that the removal of redundant or irrelevant inputs is not a simple task, especially for complex, time-varying, nonlinear biological systems. Therefore, in practical applications, it is customary to use a network to learn the underlying relationship between the input and output data. Sensitivity analysis methods are then implemented to sort out the relevant input variables. In this contribution, a similar approach was taken. However, due to the fact that NNs are prone

to the "curse of dimensionality", several other techniques were used to identify the relevant portion of the input space.

4.3.2 Sensitivity Analysis

NNs based sensitivity analysis is used to measure the causal importance of individual input variables. To perform input-sensitivity analysis, a network is initially trained until the optimum weights are computed. In this application, the purpose of the network is to model protein yield based on the available measured fermentation states. A sensitivity analysis about the mean is implemented to extract the significant states contributing to the formation of protein. The methodology consists of varying individually an input variable (i) while fixing the remaining inputs at their mean values. The ratio of the deviations of the output and input i from their mean values are recorded. This technique is equivalent to taking the partial derivative of a function. The relative sensitivity is calculated by dividing the result by the ratio of the process output to input i; both, set at their average values. Inputs with relatively low sensitivities are discarded. Measures of importance for linear systems are described in the work of Darlington (1968).

The steps involved in the analysis are: 1) function approximation/mapping using a network, 2) calculation of the means and standard deviations for each input variable, 3) estimation of the NN response based on the mean values of the input variables, 4) estimation of the NN output based on values of the input variable taken above and below the mean, 5) determination of the sensitivity of the yield to step changes in the state variable.

4.3.3 Partial Correlation Analysis

Partial correlation analysis (PCA) is used to measure the relationship between two variables controlling the contribution of other variables. With this type of analysis the correlation that remains between two variables after removing the linear effects of other independent variables can be easily measured. Spurious correlations can be easily dealt by controlling extraneous variables to reveal the true relationship between two variables. Jehle et al. (1998) used PCA to evaluate the net contribution of circulating insulin like growth hormone (IGF) system components to the bone mineral density (BMD) of hip in Type 1 and Type 2 diabetes mellitus patients, controlling for age, diabetes duration, height, weight, and bone mass index (BMI). The partial correlation of X (input vector) and Y (process performance), with the effects of Z (input vector) removed, is given by

$$r_{XY.Z} = \frac{r_{XY} - (r_{XZ})(r_{YZ})}{\left(1 - r_{XZ}^2\right)^{1/2}\left(1 - r_{YZ}^2\right)^{1/2}} \tag{3}$$

where r_{XY} is the correlation coefficient between X an Y, r_{XZ} is the correlation coefficient between X and Z, and r_{YZ} is the correlation coefficient between Y and Z.

4.4 Results

4.4.1 Neural Networks

4.4.1.1 Experimental procedure

A bacterium producing a certain protein was grown in a fermentor. The type of bacterium and the protein are not revealed to protect the privacy of the company. The measured variables of a typical fermentation run were the optical density of the sample

cultivation (OD), specific growth rate (U), pH (PH), temperature (T), stirring rate (RPM), dissolved oxygen concentration (DO), fermentor working volume (V), volume of base added (VB), concentration of glucose (GLC), and the conductance of the cultivation sample (COND). The process performance was measured in terms of yield of protein in the bioreactor. Normalized culture fermentation data from a typical run are shown in Figures 4.4 and 4.5

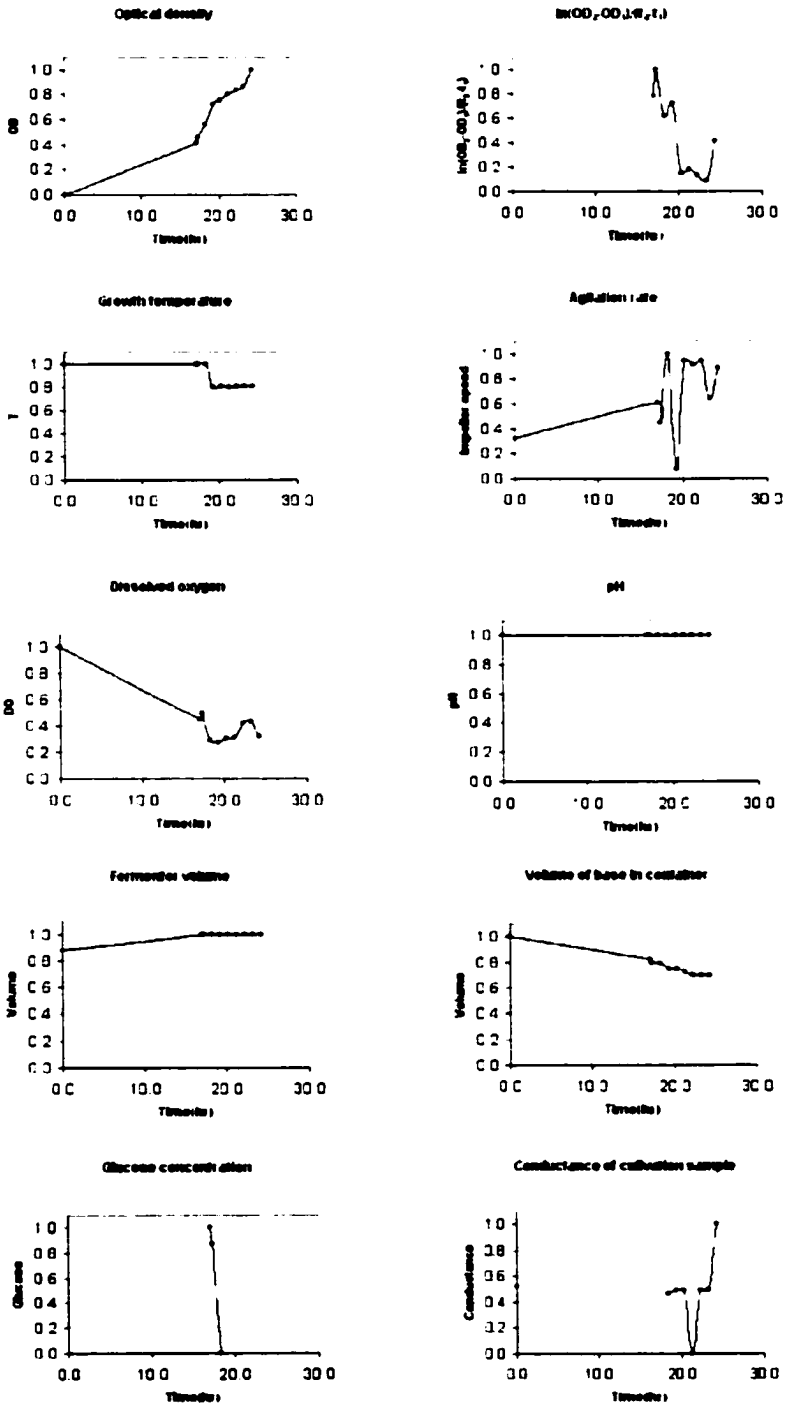

Figure 4.5 Typical normalized fermentation state variables

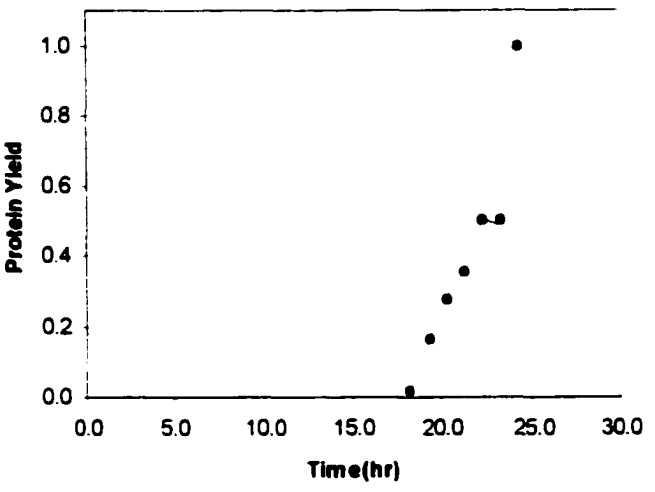

Figure 4.6 Typical normalized protein yield

Prior to NN training, the fermentation data had to be preprocessed to approximate missing values. Linear interpolation was used to estimate missing data points. The structure of the network with original input vector dimension is shown in Figure 4.6.

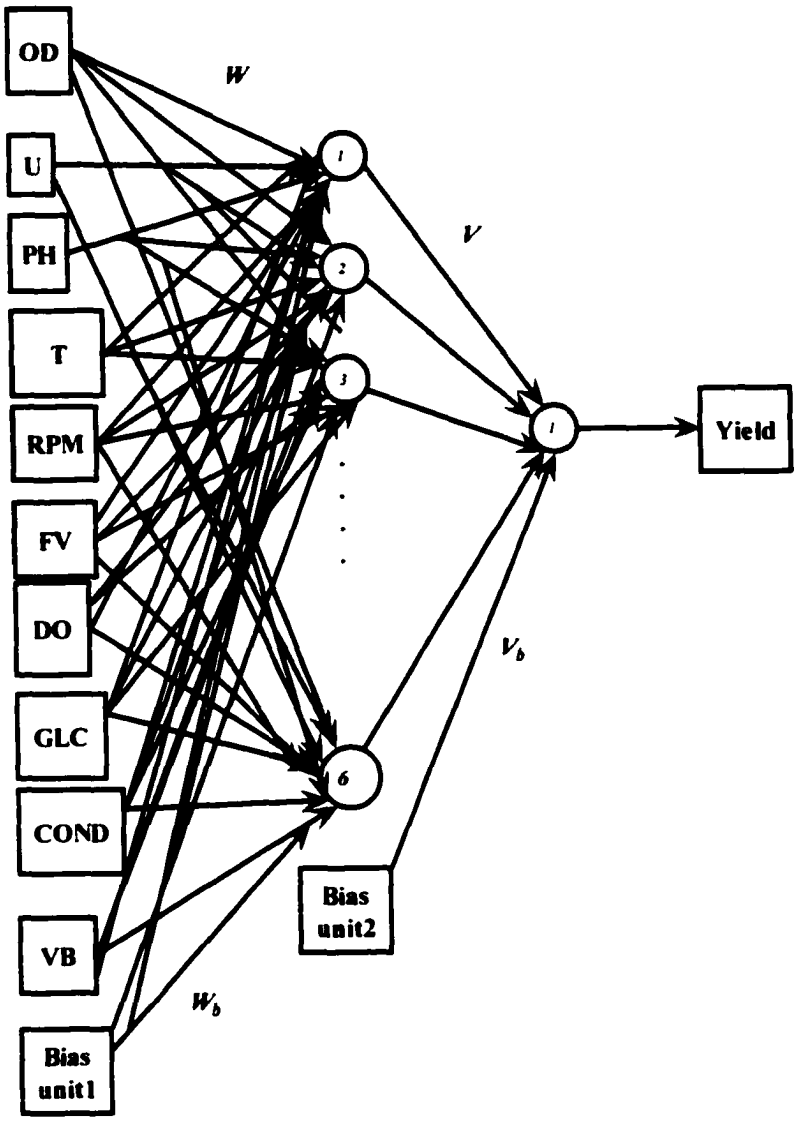

Figure 4.7 Network topology

The pH was not used since it remains constant in the course of the fermentation. The components of the input vector were OD, U, T, RPM, DO, FV, VB, GLC, and COND. The order of the experiments was randomized, but the order of the data in an experiment did not change. One hidden layer with six neurons was used. Six runs were selected for training purposes and two for testing purposes. The Levenverg-Marquart

backpropagation method was used for training. The results of the training and testing phase are shown in Figures 4.8 and 4.9.

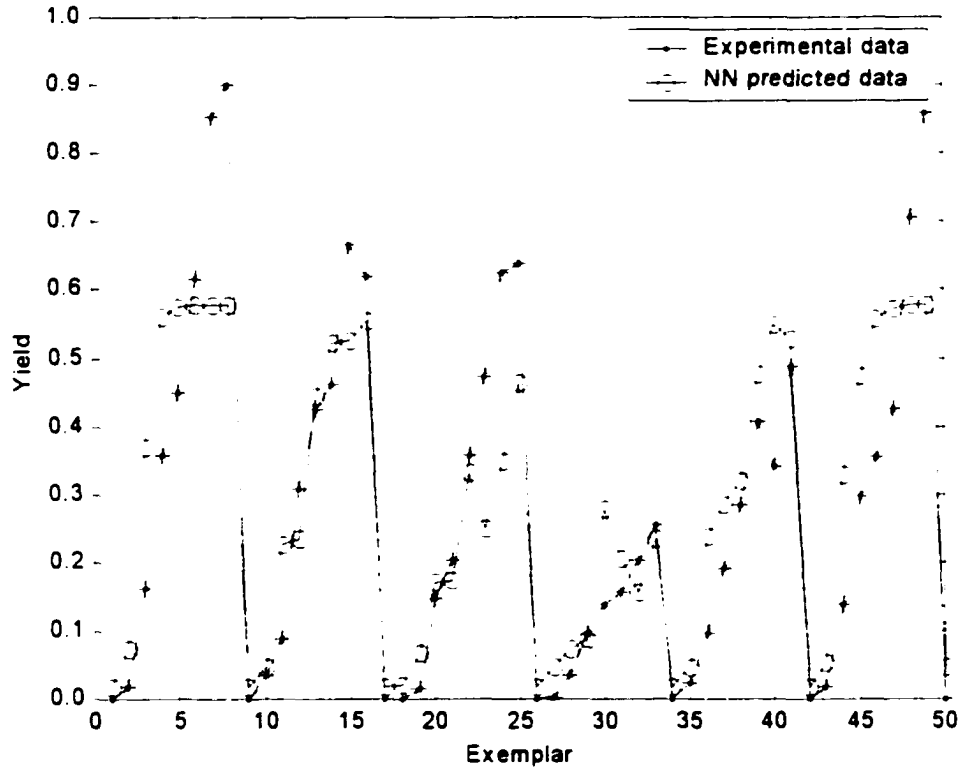

Figure 4.8 NN training results with nine inputs [OD U T RPM DO FV FB GLC COND], one hidden layer and six neurons. Six runs selected at random were used for training.

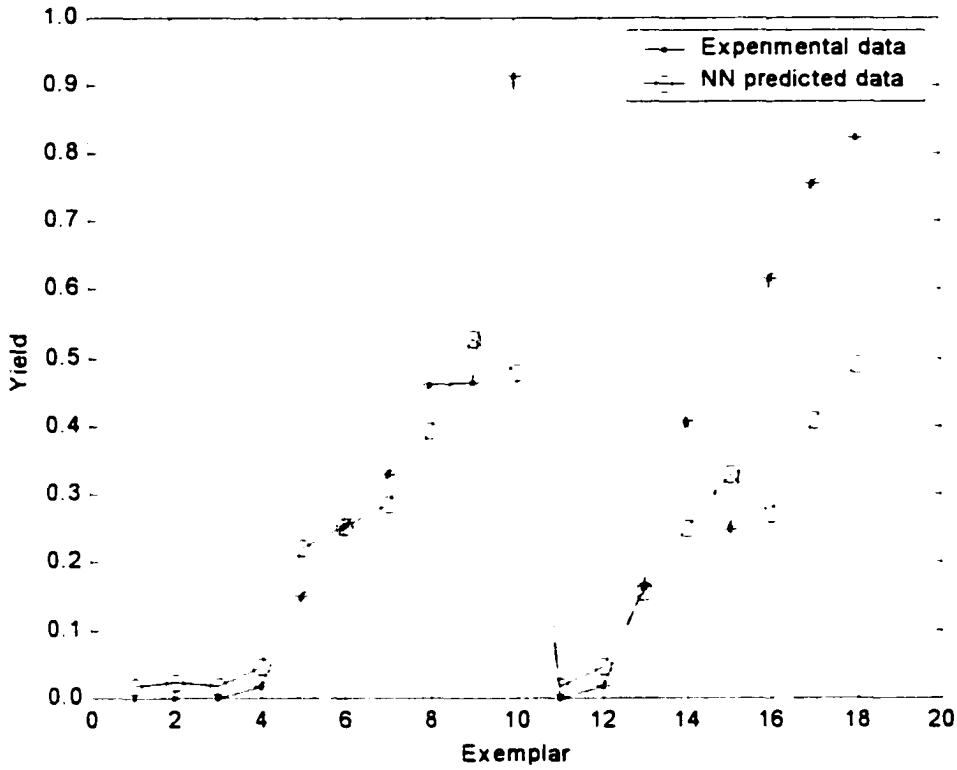

Figure 4.9 NN testing results with nine inputs [OD U T RPM DO FV FB GLC COND], one hidden layer, and six neurons. Two runs were used for testing.

An increase in the hidden layer nodes did not improve the performance of the network on the testing set. The results are shown in Figures 4.10 and 4.11.

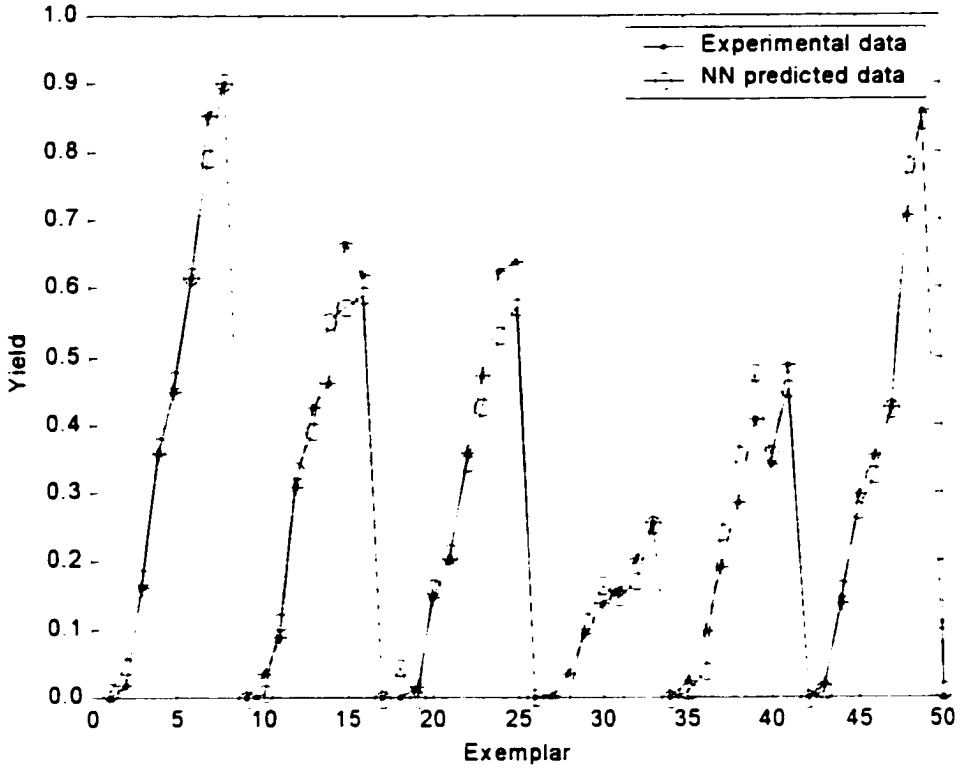

Figure 4.10 NN training results with nine inputs [OD U T RPM DO FV FB GLC COND], one hidden layer, and 15 neurons. Six runs selected at random were used for training.

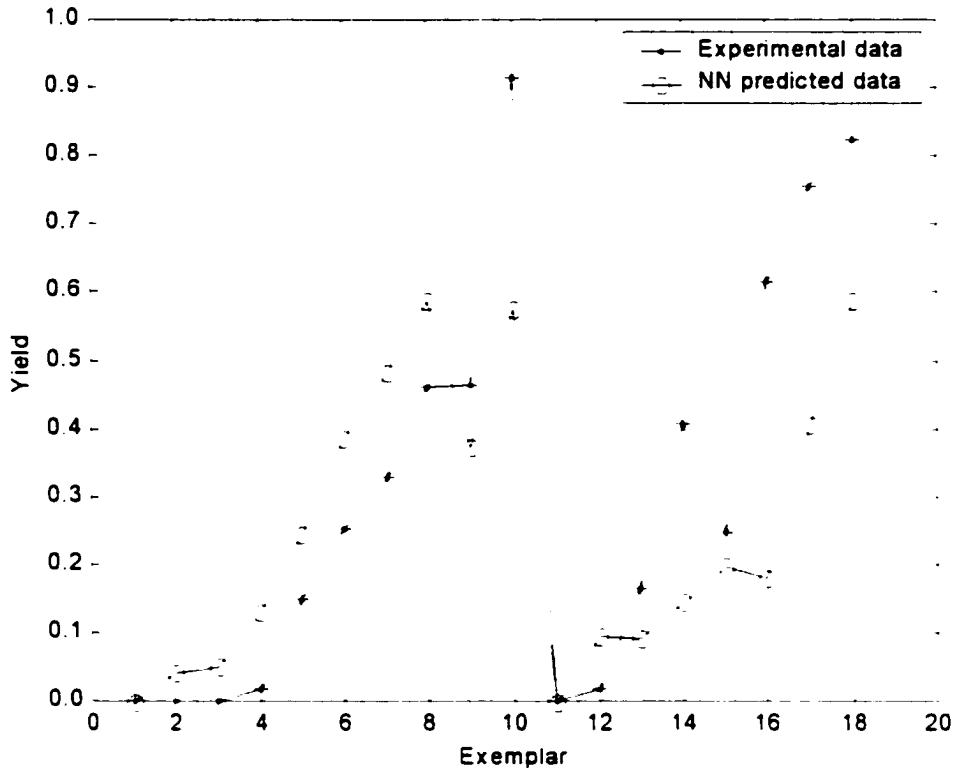

Figure 4.11 NN testing results with nine inputs [OD U T RPM DO FV FB GLC COND], one hidden layer, and 15 neurons. Two runs were used for testing.

The dimension of the input vector was reduced using sensitivity analysis (results shown in next section). The set of inputs to be used for NN training were: RPM, T, FV, OD, COND, U, and GLC. The resulting NN estimations are shown in Figures 4.12 and 4.13.

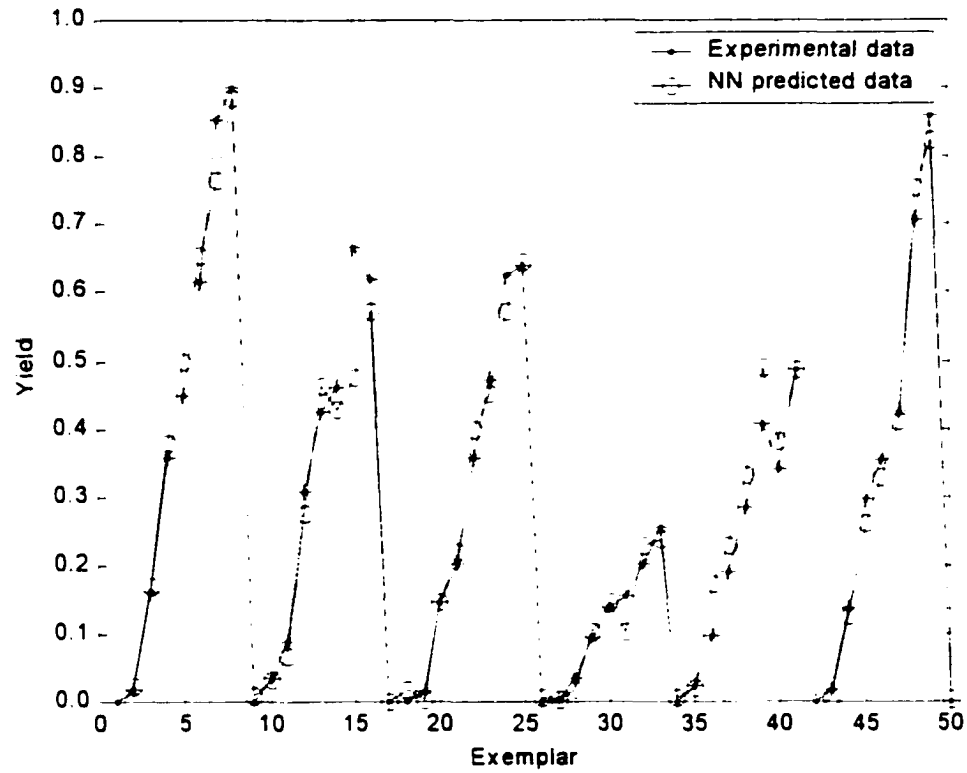

Figure 4.12 NN training results with seven inputs [OD U T RPM FV COND GLC], one hidden layer, and 15 neurons. Six runs selected at random were used for training.

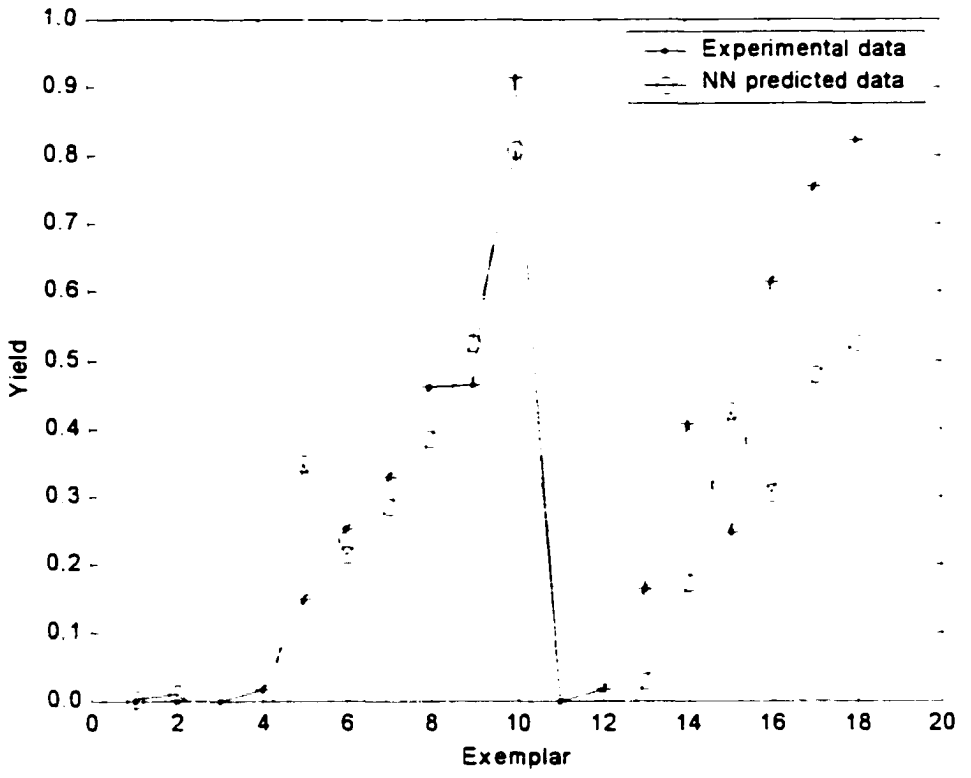

Figure 4.13 NN testing results with seven inputs [OD U T RPM FV COND GLC], one hidden layer, and 15 neurons. Two runs selected at random were used for testing.

When we compare the performance (MSE) of the network with 9 input variables (Figures 4.8 and 4.9) with the network with the reduced set (Figures 4.12 and 4.13), the following results are obtained (Table 4.1):

	MSE	
	Training set	***Testing set***
9-input NN	1.01×10^{4}	1.62×10^{4}
7-input NN	756.48	1.26×10^{4}

Table 4.1 Performances of 9-input and 7-input NNs.

4.4.1.2 Neural Network Sensitivity Analysis

NN sensitivity analysis was used to reduce the dimension of the input space. Performing sensitivity analysis on a trained network often eliminates irrelevant inputs. The removal of insignificant variables diminishes data collection cost and can sometimes improve a network's performance. Furthermore, sensitivity analysis helps understand the underlying relationships between state variables and process outputs by outlining the meaningful portion of the input space. The relative sensitivity of the optical density (OD) for one standard deviation above the mean, for instance, can be calculated as follows. The input vector V_{OD} to the network is:

$$V_{OD} = [OD_{ave} + std(OD) \quad U_{ave} \quad T_{ave} \quad RPM_{ave} \quad DO_{ave} \quad FV_{ave} \quad BV_{ave} \quad GLC_{ave} \quad COND_{ave}] \qquad (4)$$

where *ave* is the arithmetic average and *std*, the standard deviation. The network output is evaluated by

$$Y_{OD} = F(V_{OD}) \tag{5}$$

where F is the NN mapping. In this case, the sensitivity of the protein yield to a positive step change in the optical density is given by

$$S_{OD} = \left| \frac{\frac{(Y_{+} - Y_{ave})}{Y_{ave}}}{\frac{std(OD)}{OD_{ave}}} \right| \tag{6}$$

Y_{ave} is

$$Y_{ave} = F(V_{ave}) \tag{7}$$

where

$$V_{ave} = [OD_{ave} \quad U_{ave} \quad T_{ave} \quad RPM_{ave} \quad DO_{ave} \quad FV_{ave} \quad BV_{ave} \quad GLC_{ave} \quad COND_{ave}] \tag{8}$$

This calculation is repeated for three points above the mean. The results are averaged and reported as S_{OD+}. S_{OD-} is the relative sensitivity below the mean. The indices are given in Table 4.1.

4.4.2 Partial Correlation Analysis

A detailed treatment of partial correlation analysis can be found in the work of Takeuchi et al. (1982). Partial correlation analysis is used to study the relationship between two variables removing the contributions of extraneous independent variables. It was used in this work to study the effect of a state fermentation variable on the protein yield while controlling other variables. The results are given in Table 4.2

Input variable	S_+	S_-	Partial correlation
COND	0.15	0.14	-0.10
GLC	0.30	2.83	0.03
U	0.34	0.79	-0.20
BV	1.35	4.91	-0.02
FV	1.53	1.16	-0.13
RPM	2.66	2.83	-0.12
T	2.75	6.18	-0.07
DO	3.70	1.00	0.50
OD	5.03	0.96	0.65

Table 4.2 Sensitivity analysis and partial correlation table

From relative sensitivity analysis above the mean and an index above 1.0, the yield is sensitive to changes in RPM, T, DO, FV, BV, and OD. Relative sensitivity analysis below the mean and an index above 1.0 shows that the relevant input variables are RPM, T, DO, FV, BV, and GLC. After performing partial correlation analysis, and selecting correlation coefficient with absolute values of 0.10 and above, the following significant variables are obtained: COND, RPM, FV, U, DO, OD. The variables chosen from these analyses are RPM, T, DO, FB, BV, OD, GLC, COND, and U. In summary, the complete input set contributes to the protein yield. These results are conservative since each methodology is

prone to errors. Further analysis such as a correlation matrix can help eliminate redundant variables.

4.4.3 Correlation results

A correlation matrix computes the strength and direction of the linear relationship between two variables. Depending on the direction, the correlation coefficient (R) can be either positive or negative. The strength is indicated by the magnitude of the correlation coefficient. A direct perfect relationship has an R of +1 while the R-value for an inverse relationship is –1. The function "CORRMAP," from PLS toolbox 2.0 from Matlab^{R}, produces a pseudocolor map which shows the amount of correlation of between variables in a data set (Wise and Gallagher, 1998). The color-coded correlation map shown in Fig. 4.13 shows the correlation between all pairs of variables in the data set.

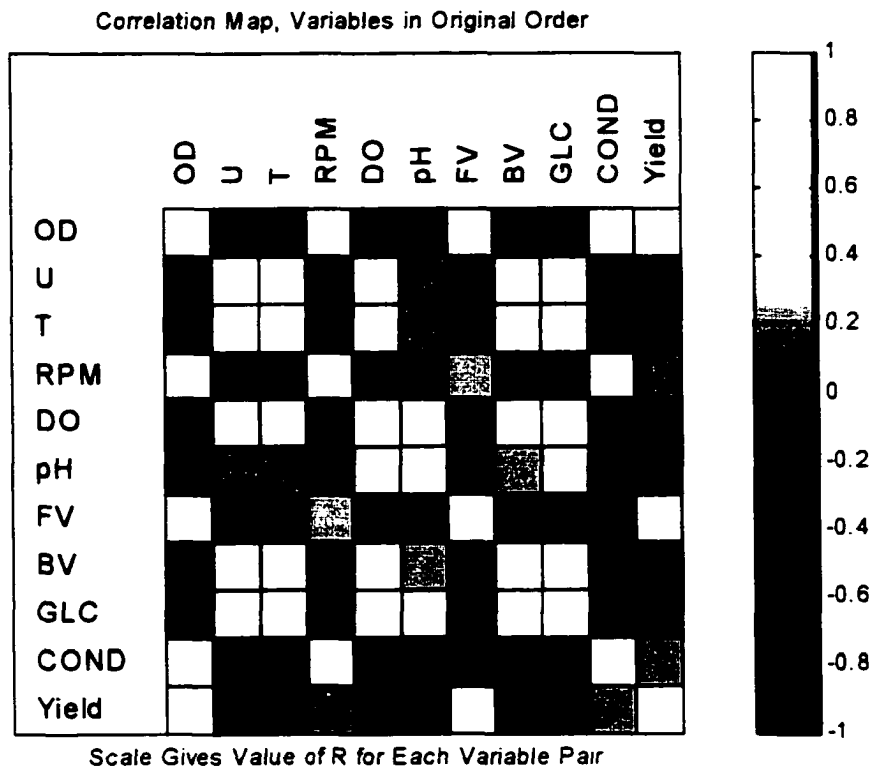

Figure 4.14 Correlation map

Using the correlation map analysis, the correlated variables are (OD, BV) with an r-value of -0.8678, (DO, OD) with an r-value of -0.8348, (GLC, DO) with an r-value of 0.8309, and (GLC, BV) with an r-value of 0.8309. Variables are correlated if the absolute value of the correlation coefficient between the variables are at least 0.8. DO and OD are also correlated to the yield (partial correlation analysis). From the sensitivity analysis and the correlation map, the significant inputs are OD, U, T, RPM, FV, COND, and GLC.

4.5 Conclusions

An ARX model was used to model apoptotic cells as a function of the concentration of viable cells, glutamine and asparagine. In the present work, an ARX description was used to represent the system because of its simplicity and ease of parameter convergence. To select the model structure, the criterion used was the minimum of the mean squared error. An algorithm was written that uses different combinations of input and output lag for multiple input, single output (MISO) systems. The optimum linear model captures the dynamics of the process accurately. Similar results were obtained with a neural network.

A second case study involved the use of a network to model fermentation data. By combining correlation map, partial correlation, and NN based sensitivity analyses, the dimension of the input vector was reduced with satisfactory NN predictions. The protein yield was more sensitive to a change in the optical density, specific growth rate, temperature, stirring rate, fermentor working volume, conductance, and the glucose concentration. A better network performance was achieved for the reduced set than the complete set network.

4.6 References

Akaike, H. 1987. Factor analysis and AIC. Psychometrika 52:317-332.

Bardford, JP, Phillips, PJ, Harbour, C. 1992. Simulation of animal cell metabolism. Cytotechnol 10:63-74.

Baughman, DR, Liu, YA 1995. Neural Networks in Bioprocessing and Chemical Engineering. San Diego, CA: Academic Press.

Bellman, R 1961. Adaptive Control Processes: A Guided Tour. Princeton, NJ: Princeton University Press.

Bharath, R, Drosen, J 1994. Neural Network Computing. New York, NY: McGraw-Hill.

Cowger, NL, O'Connor, KC, Hammond, TG, Lacks, DJ, Navar, GL. 1999. Characterization of bimodal cell death of insect cells in a rotating-wall vessel and shaker flask. Biotechnol Bioeng 64:14-26.

Darlington, RB. 1968. Multiple regression in psychological research and practice. Psychological Bulletin 69:161-182.

Darzynkiewicz, Z, Bruno, S, Del Bino, G, Gorczyca, W, Hotz, MA. 1992. Features of apoptotic cells measured by flow cytometry. Cytometry 13:795-808.

Eikens, B, Karim, MN. 1999. Process identification with multiple neural network models. Int J Control 72:576-590.

Eikens, B. 1996. Neural Network Modeling and Control: Case Studies in Chemical Engineering. Ph.D. Dissertation. Colorado State University, Ft Collins, CO.

Fahlman, SE, Lebiere, C. 1990. The cascade-correlation learning architecture. Advances in Neural Information Processing Systems 2:524-532.

Farza, M, Nadri, M, Hammouri, H. 2000. Nonlinear observation of specific growth rate in aerobic fermentation processes. Bioprocess Eng 23:359-366.

Franek, F, Vomastek, T, Dolnikova, J. 1992. Fragmented DNA and apoptotic bodies document the programmed way of cell death in hybridoma cultures. Cytotechnol 9:117-123.

Freeman, JA 1994. Simulating neural networks with Mathematica. New York: Addison-Wesley Publishing Company.

Glacken, MW. 1987. Development of mathematical descriptions of mammalian cell culture kinetics for the optimization of fed-batch bioreactors. Ph.D. Dissertation. Massachusetts Institute of Technology, Cambridge, MA.

Hermann, JE. 1986. Enzyme-linked immunoassays for the detection of microbial antigens and their antibodies. Adv Appl Microbiol 31:271-289.

Hornik, K, Stinchcombe, M, White, H. 1989. Multilayer feedfoward neural networks are universal approximators. Neural Networks 2:359-366.

Jehle, PM, Jehle, DR, Mohan, S, Böhm, BO. 1998. Serum levels of insulin-like growth factor system components and relationship to bone metabolism in Type 1 and Type 2 diabetes mellitus patients. Journal of Endocrinology 159:297-306.

Karim, MN, Rivera, S. 1992. Artificial neural networks in bioprocess state estimation. Adv Bioechem Eng Biotechnol 46:2-33.

Karim, MN, Yoshida, T, Rivera, SL, Saucedo, VM, Eikens, B, Oh, GS. 1997. Global and local neural network models in Biotechnology. J Ferment Bioeng 83:1-11.

Lee, JM 1992. Biochemical Engineering. Englewood Cliffs: Prentice Hall.

Ljung, L 1987. System identification. Theory for the user. New Jersey: Prentice-Hall.

Mercille, S, Massie, B. 1994. Introduction of apoptosis in nutrient-deprived cultures of hybridoma and myeloma cells. Biotechnol Bioeng 44:1140-1154.

Murray, K, Ang, CE, Gull, K, Hickman, JA, Dickson, AJ. 1996. NS0 myeloma cell death: influence of bcl-2 overexpression. Biotechnol Bioeng 51:298-304.

Patarinska, T, Dochain, D, Agathos, SN, Ganovski, L. 2000. Modelling of continuous microbial cultivation taking into account the memory effects. Bioprocess Eng 22:517-527.

Reed, R. 1993. Pruning algorithms - A survey. IEEE transactions on neural networks 4:740-747.

Reid, S., Randerson, DH, Greenfield, PF. 1987. Amino acid dtermination in mammalian cell culture supernatants. J Biotechnol 1:68-72.

Sargantanis, IG, Karim, MN. 1999. Variable structure NARX models: Application to dissolved-oxygen bioprocess. AIChE J 45:2034-2045.

Saucedo, VM, Karim, MN. 1997. Analysis and Comparison of Input Output Models in a Recombinant Fed-Batch Fermentation. J Ferm Bioeng 83: 70-78.

Simon, L, Karim, MN, Schreiweis, A. 1998. Prediction and classification of different phases in a fermentation using neural networks. Biotechnol Tech 12:301-304.

Simon, L, Karim, MN. 2000. Probabilistic neural networks using Bayesian decision strategies and a modified Gompertz model for growth phase classification. Biochem Eng J 7:41-48.

Singh, RP, Al-Rubeai, M, Gregory, CD, Emery, AN. 1994. Cell death in bioreactors: A role for apoptosis. Biotechnol Bioeng 44:720-726.

Takeuchi, K, Yanai, H, Mukherjee, BN 1982. The foundations of multivariate analysis : a unified approach by means of projection onto The foundations of multivariate analysis : a unified approach by means of projection onto linear subspaces. New York: Wiley.

Telford, WG, King, LE, Fraker, PJ. 1994. Rapid quantification of apoptosis in pure and heteregeneous cell pupulation using flow cytometry. Cytometry 172:1-16.

Willis, MJ, Montague, GA, Di Massimo, C, Tham, MT, Morris, AJ. 1992. Artificial neural networks in process estimation and control. Automatica 28:1181-1187.

Wise, BM, Gallagher, NB 1998. PLS Toolbox for use with Matlab. Manson, WA: Eigenvector Research, Inc.

Wyllie, AH, Kerr, JFR, Currie, AR. 1980. Cell death: The significance of apoptosis. Int Rev Cytol 68:251-306.

Chapter 5

CONTROL OF STARVATION-INDUCED APOPTOSIS IN CHO CELL CULTURES

5.1 Introduction

The two mechanisms of cell death reported in the literature are necrosis and apoptosis (Wyllie et al., 1980). Necrosis is a passive process that occurs when the cells are exposed to extreme environmental or physiologic stresses. Apoptotic cells are induced to commit suicide under normal physiological conditions. Apoptosis or programmed cell death (PCD) is crucial to the normal development and homeostatis of multicellular organisms. It can be used in multicellular organisms to kill virus-infected cells and cancer cells (Reed, 1994; Oltvai and Korsmeyer, 1994; Nunez and Clarke, 1994; Korsmeyer, 1995).

Starvation-induced apoptosis is very common in mammalian cells. According to Franek and Sramkova, a group of amino acids helps the suppression of apoptosis in hybridoma cells (Franek, 1995; Franek and Sramkova, 1995; Franek and Sramkova, 1996). The activation of PCD in B lymphocite hybridoma allowed the cells to survive in a nutrient-limited medium (Franek and Sramkova, 1996). The identified amino acids play a survival-signal role because they do not promote cell division, but stop or delay

apoptotic death. By 1978, a group of researchers, working with CHO cells had already established a connection between amino acid starvation and the protein synthetic machinery of CHO cells (Stanners et al., 1978). They suggested that the decline in the translational machinery could represent the first event in the cell's rapid death (Stanners et al., 1978). The extent of apoptotic death depends largely on the mammalian cell line and the concentration of amino acids in the medium. Sakagami et al. (1998) showed that amino acid requirements vary depending on the cell line. Statistical analysis may need to be conducted in order to identify a set of apoptosis-suppressing amino acids. The regulation of all 20 amino acids would be both difficult, from a control standpoint, and not economically viable.

The study of apoptosis can have two distinctly different goals: one is to induce apoptosis so that cells do not grow in an uncontrollable fashion (down regulation) to prevent spread of cancer. In this context, Bcl-2 and related cytoplasmic proteins such as Bax can act as key regulators of apoptosis to determine the fate of the cells (Adams and Cory, 1998). The other and opposite goal, from an industrial point of view, is to prolong viability of the cells in a cultivation. By preventing apoptosis as much as possible (up regulation), the recombinant protein of interest can be produced for a longer period, thus giving a higher titer of protein. This will ultimately minimize the down-stream processing cost.

Classical descriptions of the dynamics of mammalian cells rarely include death by necrosis and apoptosis. Controlling PCD is therefore difficult in the current framework. It should be noted that Cowger et al. (1999) proposed a kinetic model that accounted for both apoptosis and necrosis in insect-cell cultivation. However, the apoptotic death rate

was held constant in their model. To explicitly account for the role of amino acids on PCD, a first principle model is appropriate. Because of the nonlinearity exhibited by cell growth cycle and amino acid consumption, the Unscented Kalman Filter (UKF) is a promising tool to estimate the state variables for real-time control (Julier et al., 1995). The manipulated variable vector is composed of the flow rates of glucose and two amino acids that participate in the suppression of apoptosis. The control variable is the concentration of apoptotic cells in the bioreactor. Since the depletion of amino acids can irreversibly compromise the ability of the cells to synthesize proteins, a predictive model to estimate the concentration of apoptotic cells N-sample intervals ahead is suitable. Corrective control actions can then be taken at the current time to minimize apoptotic death in the bioreactor.

This chapter is structured as follows: (1) Cultivation conditions and methods of sample analysis are outlined. (2) Sensitivity analysis and neural networks are then introduced. (3) A set of governing equations is written for batch growth assuming a well-mixed bioreactor. (4) An oxygen mass balance in the liquid phase is derived to provide the output equation for the filter. (5) The UKF for state estimation is discussed as well as the use of a model predictive controller (MPC). In the last section, the results are presented and discussed.

5.2 Cultivation Conditions and Sample Analysis

5.2.1 Cultivation Conditions

The CHO cell line, CHO 1-155500, obtained from ATCC (American Type Culture Collection, Manassas, VA) was used in this research. The cells produce recombinant

tissue-type plasminogen activator (t-PA) that has clinical applications as a thrombolytic agent. The cells were initially thawed and diluted ten-fold (1 ml of culture and 9 ml of 90% HAM'S/F-12 medium and 10% fetal bovine serum). These were then transferred to a 75 ml T-flask containing 95% selection medium (Dulbecco's Modified Eagle Medium) and 5% dialyzed fetal bovine serum. The flask was placed in an incubator (VWR Scientific Products, model 2325, West Chester, PA) set at 37°C and 8 % carbon dioxide overlay. For subsequent studies, the cells grew in a 3-l bioreactor (New Brunswick, Scientific. CO., Inc., Edison, NJ). The pH (Cole-Parmer Instrument Company, Vernon Hills, Illinois) was controlled at 7.2 by addition of 1 M NaOH and carbon dioxide. The dissolved oxygen (Cole-Parmer Instrument Company, Vernon Hills, Illinois) was controlled at a concentration of 40% saturated air. The agitation speed was set at 80 RPM. The temperature was maintained at 37°C.

5.2.2 Sample Analysis

The concentration of total cells was measured using a hemacytometer. The samples were initially diluted to 2,000-20,000 cells per ml. Cell viability was assessed by trypan blue Trypan blue exclusion (Phillips, 1973). Flow cytometry (Coulter EPICS V, Beckman Coulter Inc., Miami, FL) was the methodology employed to detect and quantify apoptotic cells (Darzynkiewicz et al., 1992; Telford et al., 1994; Darzynkiewicz et al., 1997). Sub G1 peak by propidium iodide staining was used to quantify apoptotic cells. The DNA of apoptotic cells usually breaks up and small molecular weight fragments are left free in the nucleus. Following alcohol fixation, these fragments were eluted by washing in PBS buffer. After staining by propidium iodide, these cells are quantified since

they show a reduced fluorescence and a Sub-G1 peak.

Ammonia was assayed enzymatically with glutamate dehydrogenase (Lund, 1977). The concentrations of lactate and glucose were determined using a YSI analyzer (YSI 2000, YSI Incorporated, Yellow Springs, Ohio). The compositions of amino acids were determined by HPLC (Waters, Milford, Massachusetts), method (Reid et al., 1987). The product, t-PA, was analyzed via ELISA (Hermann, 1986).

5.3 Sensitivity Analysis

Neural network (NN) based sensitivity analysis was implemented to study the survival-signal role of the amino acids. The purpose of the analysis was to determine the most sensitive set of apoptosis-preventing amino acids. Neural network was used as a generalized function that mapped the concentration of amino acids onto the concentration of apoptotic CHO cells. The elimination of irrelevant input variables (variables that do not affect the outcome of a process) reduces data collection and gives insights into the underlying relationships between input and output variables. The goal of the study was to identify a reduced set of amino acids that could potentially delay apoptotic death in the bioreactor. It should be noted that Principal Component Analysis (PCA) (Jackson, 1991) could also be used to reduce the dimension of the input space.

To perform input-sensitivity analysis, a NN is trained until the optimum weights are computed and stored. The inputs to the NN are the essential and non-essential amino acids. The NN output is the concentration of apoptotic cells. Each data point of an input vector k (a selected amino acid) is then perturbed by adding a random number (standard deviation, σ_k). The remaining input vectors (the remaining amino acids) are kept at their

mean concentrations while the output of the NN is computed. Inputs with relatively low sensitivities are ignored.

The sensitivity for input k is

$$S_k = \frac{\sum_{p=1}^{P}\sum_{i=1}^{O}(y_{ip} - \bar{y}_{ip})^2}{\sigma_k^2} \qquad (1)$$

where $\bar{y}_{ip}$ is the i^{th} output of the optimum network for the p^{th} pattern. O stands for the number of network outputs ($O = 1$), P is the number of patterns (number of data generated), and σ_k^2 represents the variance of the input perturbation (Principe et al., 2000). Three commonly-applied methods using neural network sensitivity analysis for input variable reduction have been reported in the literature (Caldwell, 1995; Caldwell, 1996).

5.4 Neural networks

Neural networks had two applications in this study. The first use of neural networks was to approximate the complex nonlinear relationships between the concentrations of amino acids in the bioreactor and the concentration of apoptotic cells. The resulting nonlinear mapping facilitates the sensitivity analysis as outlined in the previous section. The second use of neural networks was to estimate the concentration of apoptotic CHO cells based on the concentration of viable cells and the reduced amino acid set.

During the last ten years, neural networks (NN) have emerged as an accepted tool for modeling nonlinear processes. Due to their approximation capabilities as well as their

inherent adaptive features, artificial NNs offer an appealing alternative to classical methods of modeling dynamic systems. Neural network models consist of a set of weights, **w**, a set of basis functions *f(.)*, and a set of parameters **p** (biases, centers, etc.). The general equation can be written as:

$$\hat{y} = f(\mathbf{xi}, \mathbf{w}, \mathbf{p}) \tag{2}$$

where $\hat{y}$ denotes the neural network estimation and **xi** is the input vector. Parameters **w** and **p** are adjusted during a "training" procedure in order to minimize some an error function. Different architectures of neural networks have been implemented in the literature (Karim and Rivera, 1992; Bharath and Drosen, 1994; Baughman and Liu 1995; (Karim et al., 1997; Simon et al., 1998; Eikens and Karim, 1999; Simon and Karim 2000a). The development of a neural network requires a training set made up of known input and output patterns. In the training phase, examples representative of the problem are fed to the network. The network tries to learn the underlying relationship based on the given set using an iterative error-minimization procedure. In the recall phase, the exemplars used in the training phase are fed to the NN. This stage is very important because one has a chance to improve the performance of the network and test different topologies. The final and crucial step is the testing and validation phases during which the network is fed new data.

5.5 Kinetic Model of CHO Cultivation

The state equations in the Unscented Kalman Filter are based on a mathematical representation of a dynamical system. For this purpose, the following governing equations were derived for the cultivation of CHO cells in the bioreactor:

$$X_T(t) = X_v(t) + X_{da}(t) + X_{dn}(t) \tag{3}$$

$$\frac{d(X_v(t))}{dt} = (\mu - k_d)X_v(t) \tag{4}$$

$$\frac{d(X_{da}(t))}{dt} = k_{da}X_v(t) \tag{5}$$

$$\frac{d(X_{dn}(t))}{dt} = k_{dn}X_v(t) \tag{6}$$

$$\mu = \frac{\mu_{max}Glc(t)Gln(t)}{(k_{Glc} + Glc(t))(k_{Gln} + Gln(t))K_{inh}} \tag{7}$$

$$K_{inh} = \left(\frac{Glc(t)}{k_{Glc}} + 1\right)\left(\frac{Lac(t)}{k_{Lac}} + 1\right)\left(\frac{Am(t)}{k_{Am}} + 1\right) \tag{8}$$

$$k_d = k_{dn} + k_{da} \tag{9}$$

$$k_{dn} = const \tag{10}$$

$$k_{da} = f_{NN}(Gln, Ans) \tag{11}$$

$$\frac{d(Gln(t))}{dt} = -k_{deg}Gln(t) - q_{Gln}X_v(t) \tag{12}$$

$$\frac{d(Am(t))}{dt} = k_{deg}Gln(t) + q_{Am}X_v(t) \tag{13}$$

$$\frac{d(Lac(t))}{dt} = \frac{1}{Y_{\frac{Lac}{Lv}}}\frac{d(X_v(t))}{dt} \tag{14}$$

$$\frac{d(Glc(t))}{dt} = -\frac{1}{Y_{\frac{Lac}{Glc}}}\frac{d(X_v(t))}{dt} \tag{15}$$

$$\frac{d(Asn(t))}{dt} = -\frac{1}{Y_{\frac{Lac}{Asn}}}\frac{d(X_v(t))}{dt} \tag{16}$$

$$\frac{d(P(t))}{dt} = \alpha\frac{d(X_v(t))}{dt} + \beta X_v(t) \tag{17}$$

The definitions of the variables and the parameter values are listed in Table 5.1. The relative sensitivities of the model parameters were also computed (Table 5.1). The sensitivity values were calculated based on a 5% change in the process parameters at a fermentation time of 100 hours. The equations are valid for the lag , exponential and the stationary phase of the growth cycle. Eqs. (3) and (4) were used by Glacken et al. (1989) in their mathematical model of hybridoma cells. Eq. (5) was used by Distefano et al. in their investigation of a feeding policy to delay the onset of apoptosis (Distefano et al., 1996). However, their methodology neglected death by necrosis, assuming that apoptosis was the major mode of cell death. The specific apoptotic death rate (k_{da}) remained constant in their analysis. The forms of Equations (7) and (8) were based on previously published models of mammalian cells. In Eq. (9) the specific death rate k_d is defined as the sum of a specific death by necrosis (k_{dn}) and apoptotic death (k_{da}).

Variable and Parameter	Definition	Numerical value	Unit	Relative Sensitivity
X_T	Total cell concentration	—	10^5 cells/ml	—
Xv	Viable cell concentration	—	10^5 cells/ml	—
X_{da}	Apoptotic cell concentration	—	10^5 cells/ml	—
X_{dn}	Necrotic cell concentration	—	10^5 cells/ml	—
Glc	Glucose concentration	—	g/l	—
Asn	Asparagine concentration	—	pmole/ml	—
Gln	Glutamine concentration	—	pmole/ml	—
Lac	Lactate concentration	—	g/l	—
Am	Ammonium concentration	—	µg/ml	—
P	tPA concentration	—	µg/ml	—
μ_{max}	Maximum specific growth rate	0.18	h^{-1}	$(\Delta X_T/X_T)/(\Delta\mu_{max}/\mu_{max}) = 9.18\times10^{-1}$
k_{dn}	specific necrotic death rate	3.00×10^{-3}	h^{-1}	$(\Delta X_{dn}/X_{dn})/(\Delta k_{dn}/k_{dn}) = 3.81\times10^{-1}$
k_{da}	specific apoptotic death rate	—	h^{-1}	—
k_{Glc}	Glucose Monod constant	2.09	g/l	$(\Delta X_T/X_T)/(\Delta k_{Glc}/k_{Glc}) = -1.41\times10^{-1}$
k_{Gln}	Glutamine Monod constant	2.79×10^{4}	pmole/ml	$(\Delta X_T/X_T)/(\Delta k_{Gln}/k_{Gln}) = -8.15\times10^{-1}$
ki_{Lac}	Lactate inhibition constant	1.07×10^{4}	g/l	$(\Delta X_T/X_T)/(\Delta ki_{Lac}/ki_{Lac}) = -3.46\times10^{-2}$
ki_{Glc}	Glucose inhibition constant	2.04[1]	g/l	$(\Delta X_T/X_T)/(\Delta ki_{Glc}/ki_{Glc}) = 7.43\times10^{-1}$
ki_{Am}	Ammonium inhibition constant	16.45	µg/ml	$(\Delta X_T/X_T)/(\Delta ki_{Am}/ki_{Am}) = 3.24\times10^{-1}$
k_{deg}	Glutamine decomposition constant	4.32×10^{-3}	h^{-1}	$(\Delta Gln/Gln)/(\Delta k_{deg}/k_{deg}) = 2.43\times10^{-1}$
q_{Gln}	Specific glutamine uptake rate	4.81	pmole/(10^5 cells.h)	$(\Delta Gln/Gln)/(\Delta q_{gln}/q_{gln}) = 1.51\times10^{-1}$

q_{Am}	Specific ammonium uptake rate	5.43×10^{-2}	$\mu g/(10^5$ cells.h)	$(\Delta Am/Am)/(\Delta q_{Am}/q_{Am}) = 7.72 \times 10^{-1}$
$Y_{Xv/Glc}$	Glucose yield coefficient	4.90	$(10^5$ cells)/g	$(\Delta Glc/Glc)/(\Delta Y_{Xv/Glc}/Y_{Xv/Glc}) = 2.18 \times 10^{-1}$
$Y_{Xv/Lac}$	Lactate yield coefficient	4.70	$(10^5$ cells)/g	$(\Delta Lac/Lac)/(\Delta Y_{Xv/Lac}/Y_{Xv/Lac}) = -7.39 \times 10^{-1}$
$Y_{Xv/Asn}$	Asparagine yield concentration	4.69×10^{-2}	$(10^5$ cells)/pmole	$(\Delta Asn/Asn)/(\Delta Y_{Xv/Asn}/Y_{Xv/Asn}) = 5.72 \times 10^{-1}$
α	Growth associated coefficient	4.34×10^{-1}	$\mu g/(10^5$ cells.h)	$(\Delta P/P)/(\Delta \alpha/\alpha) = 2.64 \times 10^{-1}$
β	Non-growth associated coefficient	5.58×10^{-2}	$\mu g/h$	$(\Delta P/P)/(\Delta \beta/\beta) = 7.17 \times 10^{-1}$

Table 5.1. Nomenclature and parameter values for solving the model equations

Eq. (10) assumes a constant specific necrotic rate. This is a simplification which does not take into account the dependence of necrotic death on the accumulation of ammonia and unknown factors in the bioreactor. However. the unscented Kalman filtering technique used in this work accounts for model uncertainties. Eq. (11) is a departure from classical growth models. The apoptotic specific kinetic death rate is expressed as a function of the concentration of glutamine and asparagine in the bioreator. This assumption is validated by input sensitivity analysis on the data. There are evidently other factors responsible for programmed cell death. However, this approach is consistent with starvation-induced PCD based solely on amino acid consumption. Model uncertainty is also taken into consideration in the proposed methodology. Eqs (5) and (11) are combined into one equation

$$X_{da} = f_{NN}(X_v(t), Gln(t), Asn(t)) \tag{18}$$

where f_{NN} is a NN mapping. Glutamine and ammonia kinetics were approximated via first-order decomposition of glutamine to ammonia, the cell's uptake of glutamine, and release of ammonia in the bioreactor as shown by Eqs. (12) and (13). The glutamine decomposition constant, k_{deg}, from Eq. (13) is multiplied by a conversion factor during simulation since Am is in unit of μg/ml. The yields reported in Eqs. (14), (15), and (16) are average values. Their values may change in the course of the fermentation. Eq. (17) shows that t-PA is a growth and non-growth associated product. This model was selected after comparing a growth-associated model with the proposed model. The parameters of the model were obtained by fitting the batch data to Eqs. (3), (4), (6), (12), (13), (14), (15), (16), and (17). These model equations were later used in the filter.

5.6 Modeling of Oxygen in the Bioreactor

The unscented Kalman filter uses measurements that are corrupted by noise in order to approximate the individual state variables of a dynamical sytem. These measurements are usually functions of one or more state variables. In this work, the observed variable is the oxygen uptake rate. The output equation is derived from the following liquid phase oxygen balance:

$$\frac{dC_{O_2}}{dt} = K_L a_B \left(C^*_{O_2,B} - C_{O_2}\right) + K_L a_H \left(C^*_{O_2,H} - C_{O_2}\right) - OUR \tag{19}$$

where C_{O_2} is the concentration of dissolved oxygen in the liquid phase. $C^*_{O_2,H}$ and $C^*_{O_2,B}$ represent the liquid phase concentration of oxygen in equilibrium with the headspace

and bubble phase, respectively, values for which can be obtained by applying Henry's law (Ducommun et al., 2000). K_La_B and K_La_H are the overall mass transfer coefficients in the bubble phase and headspace, respectively. The concentration of dissolved oxygen C_{o_2} was measured with a dissolved oxygen (DO) probe, calibrated between 0 % and 100 %. The methodology assumes that the dissolved oxygen concentration is being controlled such that

$$\frac{dC_{o_2}}{dt} = 0 \tag{20}$$

The oxygen uptake rate obtained from (19) and (20) is then used in the following equation:

$$OUR = \left(q_{o_2,s} + q_{o_2,m}\right).X_v \tag{21}$$

where $q_{o_2,m}$ and $q_{o_2,s}$ are the specific uptake rates for the growth maintenance and requirement, respectively. An average value of 2.85×10^{-13} (mol\cell.h) was used for $q_{o_2,s} + q_{o_2,m}$ (Ducommun et al., 2000). Eq. (21) represents the output equation for the filters which can be used to calculate X_v. Shimizu and Takamatsu used the Extended Kalman Filter for the on-line estimation of the specific growth rate of baker's yeast cells in a fed-batch fermentation (Shimizu and Takamatsu, 1989). They used the condition number of a coefficient matrix derived from stoichiometric equations to select the most appropriate set of observed variables (e.g., oxygen uptake rate, carbon dioxide production rate, ethanol production rate, or ammonia uptake rate). Their approach is suitable for systems with two or more output equations. In this work, we assume one measured variable.

5.7 Filtering Technique for State Estimations

This paper uses the unscented Kalman Filter (UKF) proposed by Julier et al. (1995) to estimate the system state variables, because of its simplicity and the nonlinear nature of the state equations. The Extended Kalman Filter (EKF) is a standard technique used for state estimation of nonlinear systems (Wu and Bellgardt, 1998). However, the performance of the EKF is compromised by linearization of the system dynamics and the computational overhead due to the derivation of the Jacobian matrices. In the EKF, the state distribution is approximated by a Gaussian random variable. This variable is then propagated using a first-order linearization of the nonlinear system. For highly nonlinear systems, this propagation can introduce large errors and even divergence of the filter. To reduce the error, the Iterative Extended Kalman Filter (IEKF) is sometimes used (Sargantanis and Karim, 1994). However, for systems with a linear output equation, it can be shown that the IEKF is equivalent to an EKF. In the UKF algorithm, the state distribution is propagated through the true nonlinear system by using a minimum set of points. The posterior mean and covariance are accurate to the 3rd order in a Taylor series expansion.

The Kalman filter gives the minimum mean-squared error (MMSE) linear estimate of a state vector $\mathbf{x}(k)$. The prior estimate $\hat{\mathbf{x}}(k-1)$ and the current observation $\mathbf{z}(k)$ are assumed to be Gaussian random variables. For discrete-time non-linear systems, the state and output equations are:

$$\dot{\mathbf{x}}(t) = \mathbf{f}\left[\mathbf{x}(t), \mathbf{u}(t)\right] + \mathbf{v}(t) \qquad (22)$$

$$\mathbf{z}(t_k) = \mathbf{h}\left[\mathbf{x}(t_k), \mathbf{u}(t_{k-1})\right] + \mathbf{w}(k) \tag{23}$$

where $\mathbf{x}(t)$ is the state vector (9×1) of the system at time t obtained from Eqs. (3), (4), (6), (12), (13), (14), (15), (16), and (17) after adding a white noise $\mathbf{v}(t)$. The manipulated variable vector $\mathbf{u}(t_{k-1})$ is **0** for the batch fermentation case. $\mathbf{f}(\mathbf{x}(t), \mathbf{u}(t))$ is the 9×1 state function vector model. $\mathbf{z}(t_k)$ is the output observation scalor at time step k given by Eq. (21), and $\mathbf{h}(\mathbf{x}(t_k), \mathbf{u}(t_{k-1}))$ is the observer equation. The measurement white noise (1×1) is given $\mathbf{w}(k)$. The components of $\mathbf{x}(t)$ are $X_T(t)$, $X_v(t)$, $X_{dn}(t)$, Gln(t), Am(t), Lac(t), Glc(t), Asn(t), and P(t). $z(t_k)$ is given by OUR.

In general, recursive linear estimators are used to obtain the minimum mean squared error (MMSE) estimates of the state variables. The update equations are:

- Linear state update equation:

$$\hat{\mathbf{x}}(k+1 \mid k+1) = \hat{\mathbf{x}}(k+1 \mid k) + \mathbf{K}(k).(\mathbf{z}(k+1) - \hat{\mathbf{z}}(k+1 \mid k)) \tag{24}$$

- Linear covariance update equation:

$$\mathbf{P}(k+1 \mid k+1) = \mathbf{P}(k+1 \mid k) - \mathbf{K}(k+1)\mathbf{P}_{vv}(k+1 \mid k)\mathbf{K}^T(k+1) \tag{25}$$

where $\mathbf{P}_{vv}$ ($k+1|k$) is the covariance of the innovation error $\mathbf{z}(k+1) - \hat{\mathbf{z}}(k+1 \mid k)$ and $\mathbf{K}$(k) is the Kalman gain.

To write the predicted equations, the EKF assumes that the errors in the state estimates are small.

$$\begin{aligned} \mathbf{x}(k+1 \mid k) &= E\left[\mathbf{f}\left[\mathbf{x}(k), \mathbf{u}(k+1)\right] \mid \mathbf{z}^k\right] \\ &\approx \mathbf{f}\left[E\left[\mathbf{x}(k) \mid \mathbf{z}^k\right], \mathbf{u}(k+1)\right] \\ &= \mathbf{f}\left[\hat{\mathbf{x}}(k \mid k), \mathbf{u}(k+1)\right] \end{aligned} \tag{26}$$

Julier et al. (1995) point out that the predicted mean obtained from Kalman filter estimation does not take into account the effect of the distribution of the errors on the

state prediction. The EKF also assumes that the state errors propagate through a separate linearized equation, which is rarely true. They proposed the UKF algorithms which can be summarized as follows:

- A set of $2n$ points made up of standard deviations $\sigma_i(k|k)$ selected from the columns of the matrices $\pm(n\mathbf{P}(k|k)^{1/2}$ is computed. n is the dimension of the state vector $\mathbf{x}(k)$ and $\mathbf{P}(k|k)$ is the covariance. The mean of the set is zero. Each point of the set is translated as $\mathbf{X}_i(k|k) = \sigma_i(k|k) + \hat{\mathbf{x}}(k|k)$. The new set has the same covariance $\mathbf{P}(k|k)$ with mean $\hat{\mathbf{x}}(k|k)$.
- Each point is transformed through the state equations as $\mathbf{X}_i(k+1|k) = \mathbf{f}\left[\mathbf{X}_i(k|k), \mathbf{u}(k+1)\right]$.
- The mean and covariance of the $2n$ points in the set $\mathbf{X}_i(k+1|k)$ are calculated and represented by $\hat{\mathbf{x}}(k+1|k)$ and $\mathbf{P}(k+1|k)$ respectively.

5.8 Model Predictive Control

Estimation of the state variables is necessary to control the concentration of apoptotic cells in the bioreactor. It should be noted that apoptosis is very sensitive to the concentrations of the significant amino acids. Depletion of any of those amino acids can irreversibly compromise the ability of the cells to produce t-PA. The MPC algorithm is very suitable for this process since it allows the prediction, N-sample intervals ahead, of the concentration of apoptotic cells. Appropriate corrective control actions can then be taken at the current time to minimize apoptotic death in the bioreactor.

MPC offers several advantages to control cell culture processes. MPC is well suited for adaptive control of processes with variable parameters such as specific growth rates (Clarke et al., 1987). Mammalian cell culture processes are also nonlinear, which poses a challenge to classical controllers. MPC techniques, although initially based on linear models, can be extended to systems with nonlinear dynamics.

Model predictive control is based on a model of a process to evaluate how control strategies will impact the future behavior of the process. The control strategy of the MPC is to calculate $\Delta\mathbf{u(k)}$, $\Delta\mathbf{u(k+1)}$, ... $\Delta\mathbf{u(k+Nu-1)}$, the sequence of control signal increments that will force the predicted outputs $\mathbf{y((k+N_1)|k)}$, $\mathbf{y((k+N_1+1)|k)}$,...., $\mathbf{y((k+N_2)|k)}$ to some desired reference vector $\mathbf{r((k+N_1)|k)}$, $\mathbf{r((k+N_1+1)|k)}$,..., $\mathbf{r((k+N_2)|k)}$. The length of the predicted control sequence, from *0* to *Nu*, determines the control horizon. N_1 to N_2 represents the output prediction horizon. Only the first move is implemented, and a new sequence of control inputs is calculated at the next sampling instance. In conventional MPC, process uncertainties and disturbances are accounted for in the control trajectory evaluated at each sample time (Yu et al., 1992). The minimization problem is:

$$\min_{u(k),\ldots,u(k+Nu-1)} J = \sum_{j=1}^{N_2} \|y(k+j\,|\,k) - r(k+j)\|_{\Gamma} + \sum_{l=1}^{Nu} \|\Delta u(k+l-1\|\beta \qquad (27)$$

r(k) is the desired output reference vector, *y(k+j|k)* represents the *j*-step ahead predicted output, $\Delta\mathbf{u(k)}$ is the control move defined as $\mathbf{u(k)-u(k-1)}$. $\|\Delta\mathbf{u(k)}\|$ is defined as $(\mathbf{u(k)-u(k-1)})^2$ in Eq. (27). Γ is a positive definite output error weighting matrix, and β is a positive semidefinite input weighting matrix referred to as a move suppression factor. The objective function *J* is called a quadratic cost function. The formulation of the objective cost function usually includes upper and lower bounds on the output and input variables,

and additional constraints on the allowed control action change between successive sampling intervals in the manipulated input horizon. The manipulated variable $\mathbf{u}(k)$ is represented by the flow rates of glucose, glutamine and asparagine (obtained from sensitivity analysis). The control variable $y(k)$ is the concentration of apoptotic cells.

5.9 Results and Discussion

5.9.1 Sensitivity Analysis

Batch experiments were conducted to show the role of certain amino acids in suppressing starvation-induced apoptotis. The neural network based sensitivity analysis screened for two amino acids that were involved in PCD. Such a small set of apoptosis-preventing amino acids was necessary in order to devise a simplified feeding strategy. The 3-liter bioreactor was run for about 6 days. A sampling time of 1 hour was used. The neural network was trained using 11 amino acids (Asn, Gln, Arg, Pro, Tyr, Val, Met, Cys, Ile, Leu, Phe) since preliminary analysis in spinner flasks identified this set. It should be noted that the cultivations conditions in the spinner and the bioreactors were slightly different. For instance, the pH in the spinner varies while a constant pH value of 7.2 was kept in the bioreactor. The topology of the NN is sketched in Fig. 5.1. Prior to training the NN, the data were passed to a cubic spline to create additional data for the training and testing phases. The data were normalized between 0 and 1. One hundred nineteen exemplars were used during the training phase; 24 exemplars were used for testing purposes. The structure of the neural network was: 11 input nodes in the input layer (n =11), 20 nodes in the hidden layer (m = 20), and one node in the output layer (v= 11x20, w=20x1). The training and testing results are shown in Fig. 5.2. The experimental

apoptotic cells were plotted on the x-axis and the NN predictions on the y-axis. The NN predictions were accurate as can be shown by the points falling on the line "y=x". It should be noted that more nodes in the input layer were used with no significant improvement in the NN predictions. The number of nodes in the hidden layer was chosen by trial and error after testing networks with fewer nodes. A feed-forward NN was used for training. The MSE obtained after 3000 epochs was 4.4×10^{-4} upon which training was stopped. More training time did not improve the prediction of the testing set. The weights were stored for sensitivity analysis.

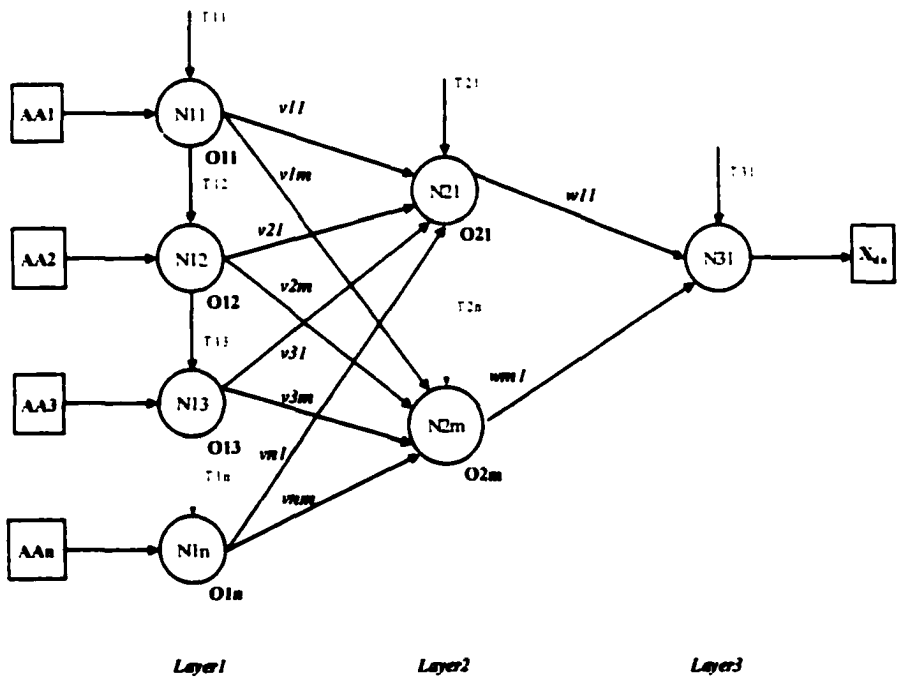

Figure 5.1. Topology of the NN used in the sensitivity analysis to predict the concentration of apoptotic cells (X_{da}) based on the concentrations of eleven amino acids (AA).

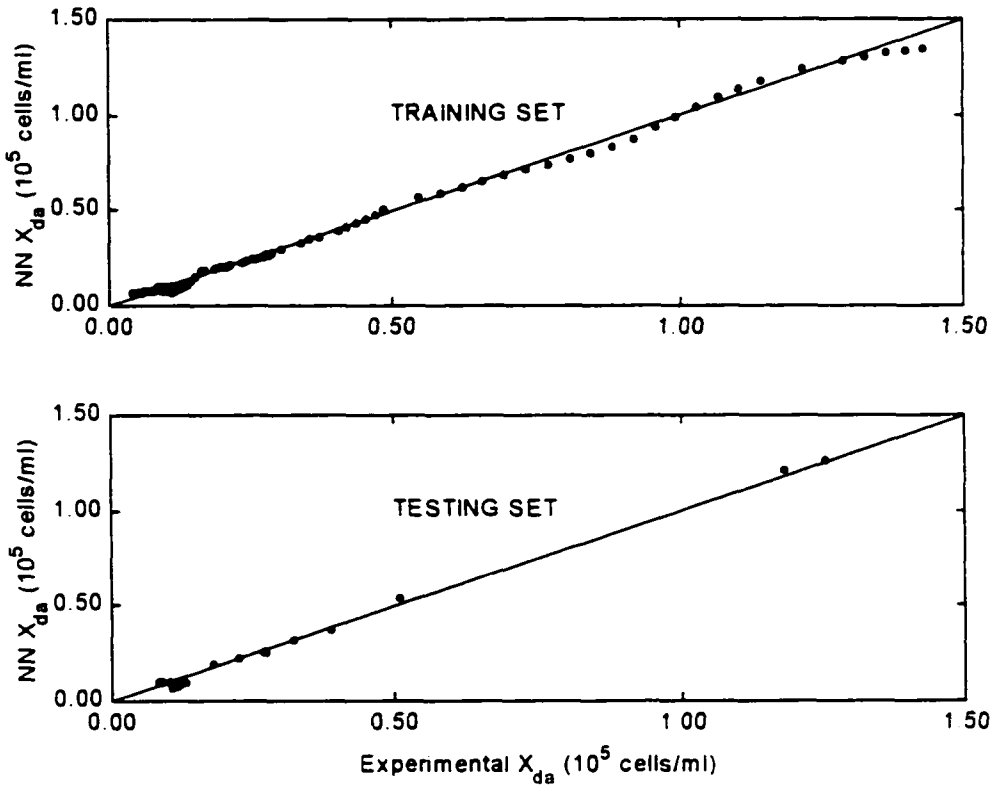

Figure 5.2 Sensitivity analysis to select significant amino acids.

Sensitivity analysis around the means was then used with the optimum network weights (Principe et al., 2000). The results are shown in Fig. 5.3. The onset of apoptosis is more sensitive to the concentrations of glutamine and asparagine in the medium. Preliminary experiments carried out in spinner flasks also identified glutamine as a specific signal molecule in PCD. The choice of a second amino acid with apoptosis-suppressing potential was difficult because 7 more amino acids were selected including asparagine. It should be noted that spinner flask experiments took place in an incubator, in which pH and oxygen concentration were not controlled. Furthermore, glutamine and asparagine have

been cited for the role in preventing apoptosis. Glutamine has been found to protect CHO cells from radiation killing (Winters et al., 1994). Recently, glutamine has also been used in controlling starvation-induced apoptosis (Sanfeliu and Stephanopoulos, 1999). The anti-apoptotic role of asparagine is better known in research on acute lymphoblastic leukaemia (ALL). The effective drug used against ALL is Asparaginase since it depletes asparagine in serum and cells (Muller and Boos, 1998). The leukemic T-cells lacking asparagine synthetase ultimately die by apoptosis.

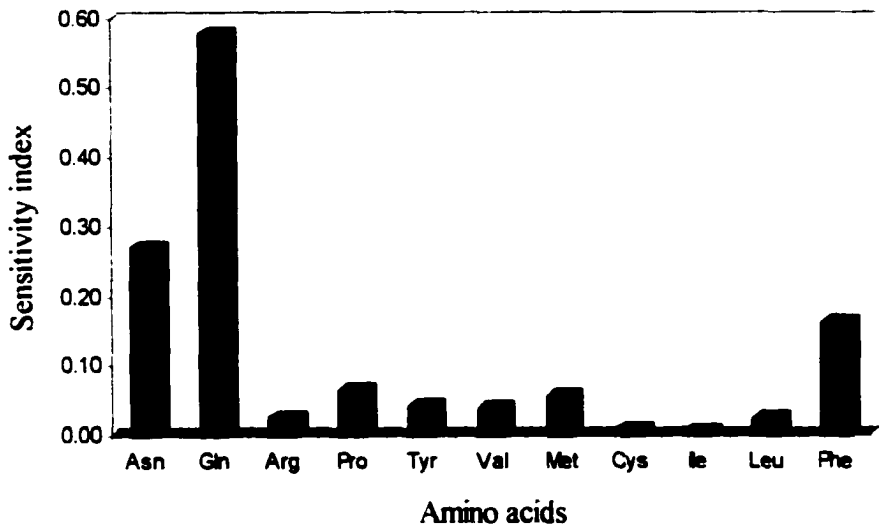

Figure 5.3 Training and testing NN results using the concentration of Asn, Gln, Arg, Pro, Tyr, Val, Met, Cys, Ile, Leu, Phe as inputs and the concentration of apoptotic cells as NN output.

To understand the relationship between amino acid deprivation and PCD, it is noteworthy to emphasize that the rate of cell growth of cultured mammalian cells is

proportional to the rate of protein synthesis minus the rate of protein degradation (Robinson et al., 1976). As mentioned by Stanners et al., the overall rate of protein synthesis depends on the functional amounts of the constituent components of the translational machinery including mRNA, ribosomes,, tRNA, initiation factors, etc. (Stanners et al., 1978). In other words, a change in the concentration of any these components would affect the cellular machinery of protein synthesis, and ultimately, cellular proliferation. During translation, molecules such as mRNA, tRNA, and amino acids, essential to protein synthesis, are brought together on the ribosome. The role of amino acyl-tRNA synthetase enzymes is to couple the correct amino acid to the correct tRNA molecule. As the mRNA is read, the specific tRNA is recognized and its amino acid is added to the growing peptide chain. When the ribosome reaches the stop codon, translation is terminated.

Stanners et al. (1978) suggested that the decline in the translational machinery could represent the first event for PCD. This view was later corroborated by Fukushima et al. (1996) who stated, as a result of their work with tsBN268 cells, that a defect in amino acyl-tRNA synthetase turned on the apoptotic machinery. The link between amino acid deprivation and PCD was given by Stanners et al. (1978) who proposed the following mechanism:

$$Enzyme\ \ AA\ \ (active) \underset{-AA + drug \text{ or } mutation}{\rightleftharpoons} Enzyme\ \ (reversibly\ \ inactive) \rightarrow Enzyme\ \ (permently\ \ inactive)$$

i.e., in the conformational state corresponding to no bound AA (amino acid), the enzyme (specific amino acyl-tRNA synthetase) has a high probability of becoming permanently

inactivated. This effect has to do with transcriptional regulation via feedback of substrate levels. In other words, a reduction in amino acid concentration leads to PCD. To explain why only certain cells in the bioreactor are affected by this mode of death, Franek and Sramkova (1996) proposed a negative control of population size, a theory in which cells die by apoptosis in a starvation-induced environment so that each member in the population efficiently utilizes the nutrient available in the environment.

Environmental control of homologous mammalian cells may operate in a manner similar to the operator *lacO* and repressor *lacI* system in the regulation of gene expression (Hu and Davidson, 1987). It is possible that either glutamine and asparagine alone was insufficient in retarding programmed cell death, but the presence of both amino acids hypothetically could be required for induction of required protein(s) that postpone apoptosis. Two cases are proposed : 1) two domains anologous to "*lacO*" regulate the transcription of two operons through binding of glutamine to one repressor protein and asparagine to another; 2) both glutamine and asparagine are required to activate one repressor protein, which regulates the transcription of a single operon.

Dual regulation concepts with reference to apoptosis can be found in the work of Fussenegger (2001). In considering the production of therapeutic proteins using mammalian cells, controlled proliferation technology is essential to higher specific productivies. Multigene metabolic engineering allows controlled proliferation by simultaneous and coordinated regulation of several transgenes. It is possible that nature has developed the same concept with regulation by two amino acids.

5.9.2 Prediction of X_{da} Using X_v, Asn, and Gln as NN Inputs

A neural network was built to predict the concentration of apoptotic cells, based on the concentrations of viable cells, asparagine, and glutamine. Data collected for the first 5 days of the fermentation were used in this section of the study. During that time, the cells were in the lag, logarithmic, or the stationary phase. The NN topology was similar to the one sketched in Fig. 5.1. The main differences were: the dimension of the input vector (n = 3) and the number of nodes in the input layer (m = 5). Additional nodes did not improve the performance of the NN. The nodes were added while monitoring the mean squared error (MSE). The MSE value did not improve significantly for additional nodes in the hidden layer. The network training function updates weights and biases according to a resilient backpropagation algorithm. This algorithm is mainly used because the steepest descent approach to train a multilayer network is not very efficient for error gradient of small magnitude. Small changes in the weights and biases usually occur even though the weights and biases are far from their converged optimal values. Resilient backpropagation training algorithm eliminates this problem since only the sign of the derivative is used to determine the direction of the weight update. The complete algorithm can be found in the work of Reidmiller and Braun (1993). Forty thousand epochs were initially chosen to train the network. After 2000 epochs, the training would stop if the network performance on the testing set failed to improve or remained the same. As before, the data were filtered and augmented to provide additional points for the training and testing phases. After randomizing the input set, an equal number of exemplars (71 components of the input vector) were used for training and testing. The NN results are shown in Fig. 5.4. The NN predicts very well the concentration of

apoptotic cells as indicated by the line "y=x". The mean squared error obtained at the end of the training was 5.50×10^{-5}.

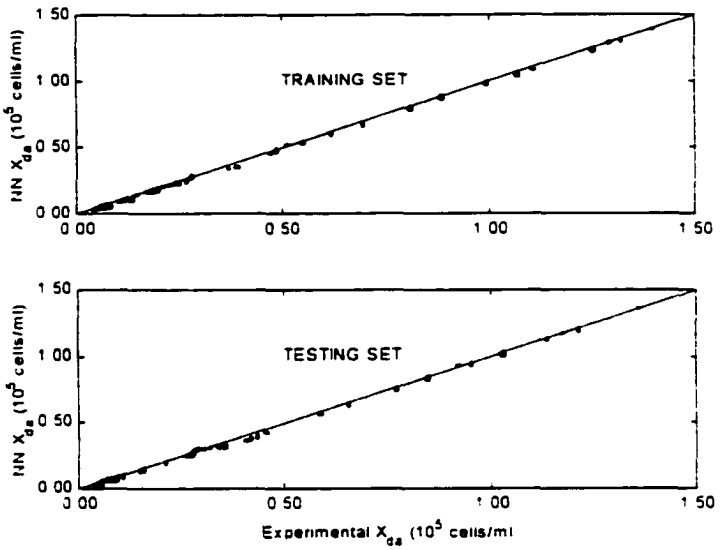

Figure 5.4. Training and testing NN results using the concentrations of viable cells, Asn, and Gln as inputs and the concentration of apoptotic cells as NN output. The line y=x is represented by "-".

5.9.3 Estimation of State Variables

The state variables are estimated to allow the calculation of the concentrations of viable cells, glutamine, and asparagine in the bioreactor. The estimation of these variables is important for an estimation of the concentration of apoptotic cells. The UKF was applied to the on-line estimation of the state variable vector $\mathbf{x}(k)$. The components of $\mathbf{x}(k)$ are $X_T(k)$, $X_v(k)$, $X_{dn}(k)$, $Gln(k)$, $Am(k)$, $Lac(k)$, $Glc(k)$, $Asn(k)$, and $P(k)$. They were

obtained after a mathematical description of the dynamic behavior of the CHO cells in the bioreactor. Eqs. (22) and (23) represent the state and output equations.

The state noise covariance vector is indicated by $\Omega = \left[10^{-2}, 10^{-2}, 10^{-4}, 1.0, 1.0, 10^{-4}, 10^{-4}, 1.0, 10^{-2}\right]$. The measurement noise covariance is given by $R = 10^{-26}$ (the oxygen uptake rate is in the order of 10^{-12} mole/ml.h). The initial covariance matrix is $\mathbf{P}(0) = 100 \times \mathbf{I}$; $\mathbf{I}$ is the identity matrix of order 9. The simulation time for the run was 150 hrs. The UKF results are shown in Figures 5.5, 5.6, and 5.7. The symbols UN and NC represent the unscented filter and noise containing signals, respectively.

The UKF performed well on the tested data. The filter tracked the concentrations of the viable cells, glutamine, ammonia, and lactate, asparagine, and t-PA fairly accurately. The estimations of necrotic cells, and glucose concentration were biased. This might be due to the size of the noises injected into the system. However, there was no evidence of divergence of the filter.

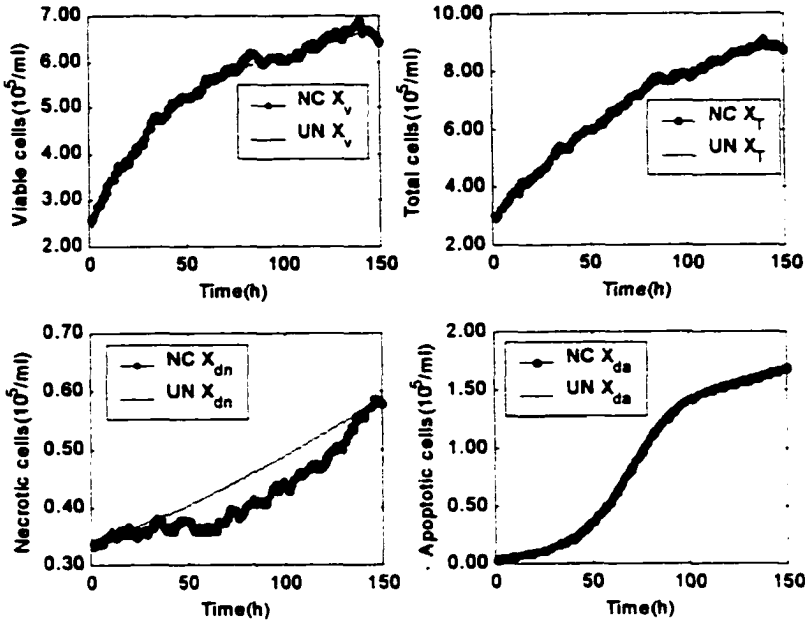

Figure 5.5 Estimation of viable, apoptotic, necrotic, and total cells by the unscented Kalman filter. NC, UN, and NF represent the noise-containing, unscented, and non-filtered (true process) signals respectively. The apoptotic cell concentration was calculated using the NN.

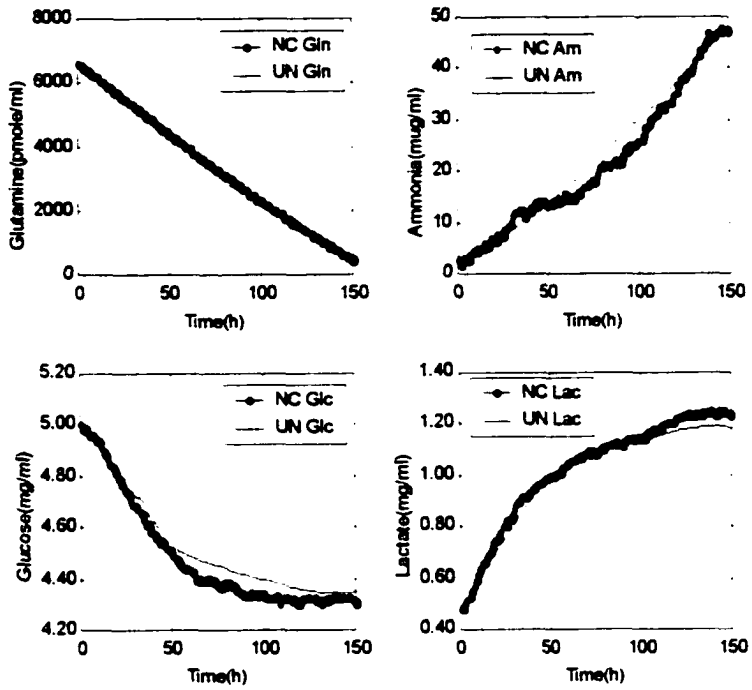

Figure 5.6 Estimation of glutamine, ammonia, glucose, and lactate by the unscented Kalman filter. NC, UN, and NF represent the noise-containing, unscented, and non-filtered (true process) signals respectively.

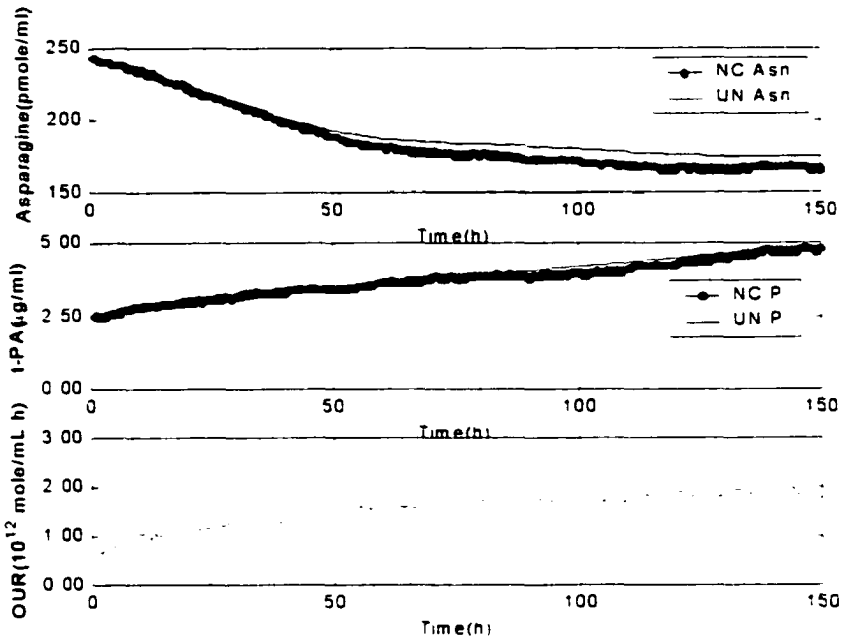

Figure 5.7 Estimation of asparagine, t-PA, by the unscented Kalman filter. NC, UN, and NF represent the noise-containing, unscented, and non-filtered (true process) signals respectively. OUR is the oxygen uptake rate.

5.9.4 Model Predictive Control of Apoptosis

The simulated MPC control of apoptotic cells implies the following experimental setup for DO control. The fed-batch fermentation of CHO cells takes place in a bioreactor with air in the head space and through a sparger located at the bottom of the fermentor. The concentration of dissolved oxygen is being controlled by manipulation of the mole fraction of oxygen through the sparger (Simon and Karim, 2000b). From Eqs. (19), (20), and (21), OUR can be computed by calculating the equilibrium concentration of oxygen for the bubble feed (C^*_{in}). C^*_{in} is calculated using Henry's law. C_{in} remains at a steady state value during the fermentation. A schematic of the process in shown in Fig. 5.8. The UKF uses the oxygen uptake rate measurement to determine the state variables of the process. The concentrations of viable cells, asparagine, and glutamine are fed to an optimal neural network in order to calculate the concentration of apoptotic cells. This value is compared to a desired set point and the error is fed to a model predictive controller. The controller activates 3 pumps connected to feed streams of glucose, asparagine, and glutamine.

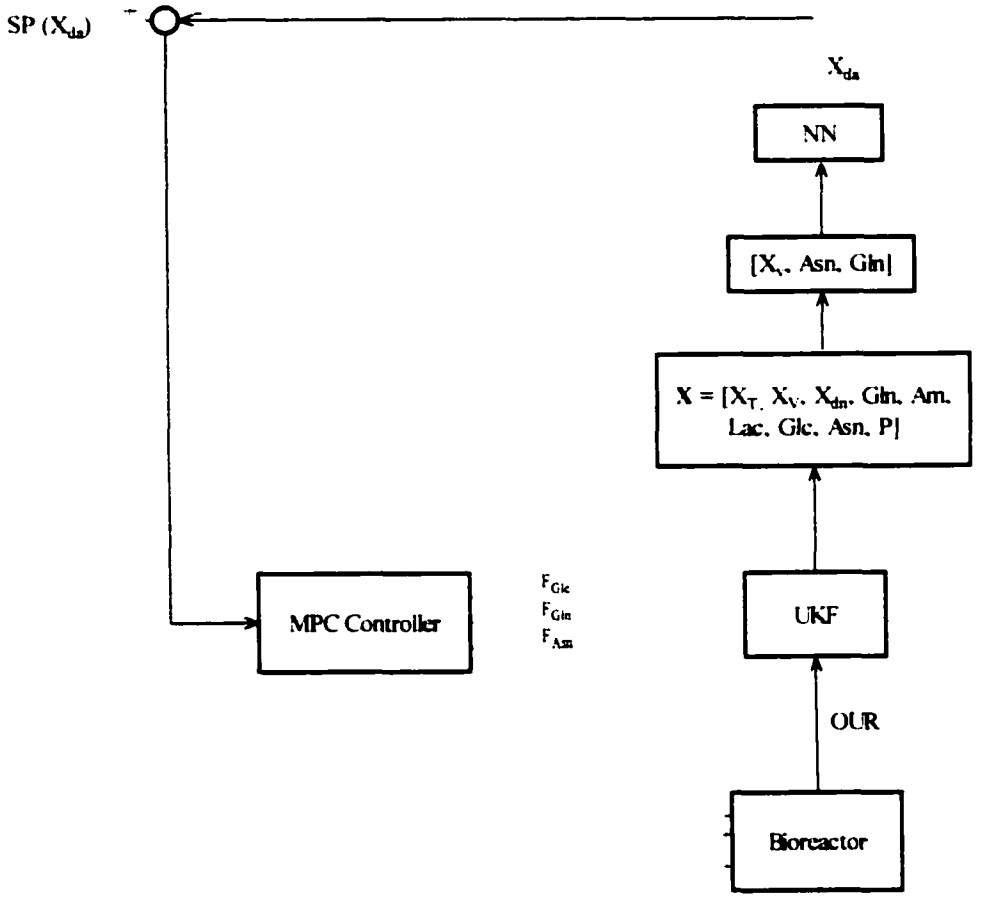

Figure 5.8 Model predictive control of apoptosis

The cells were initially cultivated in a batch bioreactor until the apoptotic cells reached a concentration of 1.15×10^{4} cells/ml. This value was predicted offline by a neural network based on the concentration of viable cells, glutamine and asparagine. The UKF outlined above was directly implemented for the batch case with the output signals (OUR) previously computed and stored in the memory of the computer. For the purpose of the fed-batch simulation, the UKF signals were assumed to be fairly accurate. This would be the case for small variation in the kinetic parameters. In real-time fermentation runs, the parameters of the model will vary. However, inclusion of the process noise in the UKF algorithm should minimize their contribution to the overall model. This assumption is necessary since the OUR data were no longer available. The methodology can be easily extended to a real time fed-batch system. Such an application can be found in the work of Dubach and Märkl (1992), who used the extended Kalman filter to monitor the cultivation of *Escherichia coli*. It should be noted that the nominal plant represented by Eqs. (3), (4), (6), (12), (13), (14), (15), (16), and (17) were reconstructed for the fed-batch simulation case to account for inlet flow rates of glucose, asparagine and glutamine.

The UKF estimations of the state variables were fed to a computer in which a constrained MPC algorithm was stored. The minimization of the objective function (27) was carried out using the following parameters: N2 = 3, Nu = 1, Γ= 0.5, β = 0. The minimization was subject to hard constraints on the input vector $\mathbf{u}$ ([0 0 0] < $\mathbf{u}$ < [1 1 1]). A sampling time (k) of 1 h was used. The MPC tuning parameters were not optimized;

their values were selected by trial and error. Once X_{da} reached a value of 1.15×10^{4} cells/ml or more, the computer activated glutamine, asparagine, and glucose tanks which were connected to the bioreactor. The flow rates of glutamine, asparagine and glucose were used as manipulated variables. Apoptotic cells were controlled at 1.15×10^{-4} cells/ml for about two weeks. The set point was then decreased to at 1.10×10^{-4} cells/ml in order to test the performance of the controller. The concentrations of Gln, Asn, and Glc in the inlet feed were 8.00 mM, 8.00 mM, and 6.00 g/l respectively. These concentrations were chosen so as to reduce the total volume of liquid added to the fermentor. The MPC was able to track the desired concentration of apoptotic cells. It should be noted that the set point change would not be implemented in real-time because the objective is to keep the apoptotic cells at a minimum value set by the accuracy of the instrument used to measure apoptotic cells. As shown in Fig. 5.9, the inlet glucose flow rate was insignificant using a set point of 1.5×10^{4} cells/ml. This observation is different from previous simulations in which F_{Glc} reached a maximum flow rate of 0.12 ml/h (results not shown). These results are evidence that addition of glucose to the bioreactor is not necessary to control apoptotic cells. This is due to the fact that the concentration of apoptotic cells is independent of glucose concentration. In practice, cell proliferation would be severely affected by glucose concentration in the long run. The accumulation of toxins in the bioreactor would also contribute to cell death.

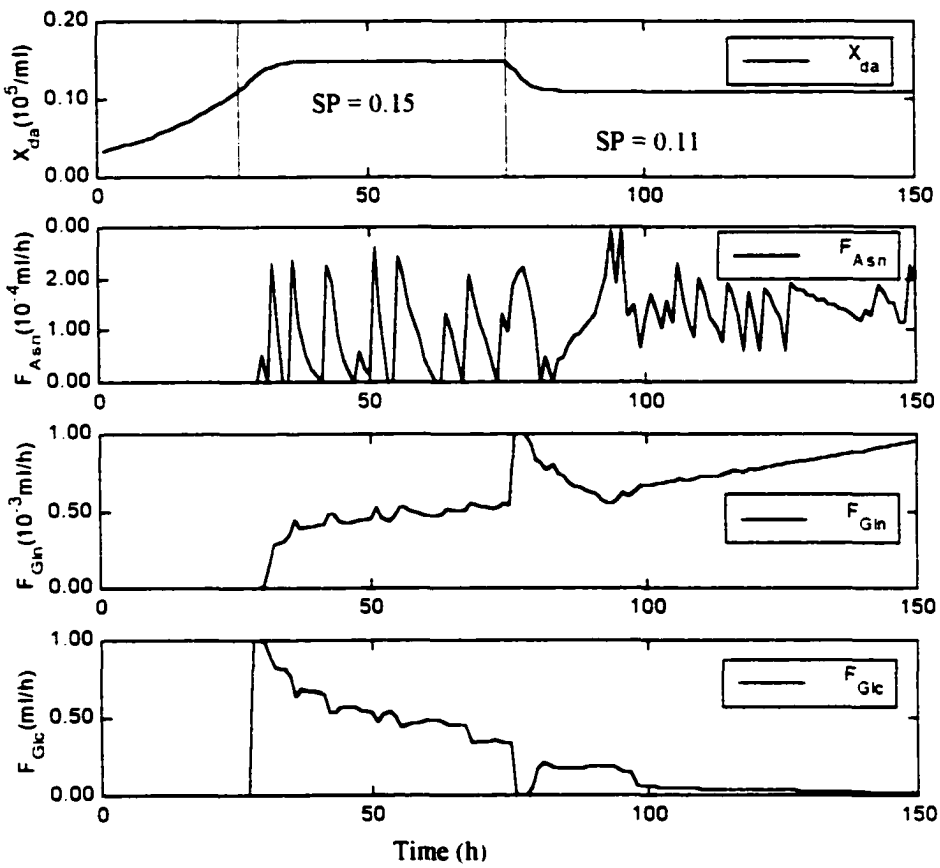

Figure 5.9 MPC Control of apoptotic CHO cell. The apoptotic cells were controlled at a setpoint (SP) of 1.50×10^4 cells/ml from 26 to 350 h. The apoptotic cells were then controlled at SP = 1.10×10^4 cells/ml for the rest of the simulation. F_{Gln}, F_{Asn} and F_{Glc} are the inlet flow rates of glutamine, asparagine, and glucose, respectively.

Activation of the PCD machinery is mainly controlled by a series of endogenous signals. One way to control PCD is by metabolic engineering which mainly considers genes involved in PCD. Genes such as *p*53 are being studied because they can potentially increase the sensitivity of the cells to activation of PCD. *bcl*-2 genes, on the other hand, decrease the sensitivity of the cells to apoptosis caused by damaging agents (Denmeade and Isaacs, 1996). Singh et al. (1997) used *bcl*-2 gene to delay the onset of apoptosis in mammalian cells. However, starvation-induced apoptosis may be easier to control than regulation via bcl-2 genes. Stability of bcl-2 transfected cultures may also become an issue in repetitive fed-batch operations. There has also been evidence that bcl-2 over-expression failed to protect NSO cells from apoptosis (Murray et al., 1996).

The present study offers a framework for real-time control of apoptosis based on manipulation of certain amino acids. The choice of apoptosis-preventing amino acids is cell-type specific. However, the technique developed can be extended to any mammalian cell culture subjected to starvation-induced apoptosis. The amino acids would initially be screened for their role in the onset or delay of apoptosis. The control scheme may involve a filter or an on-line HPLC to estimate the concentrations of these amino acids. Stoll et al. (1994) offered a simple HPLC method without any prederivatization to determine the

concentrations of glucose, lactate, glutamine, glutamate, pyrroboxylic carboxylic acids and alanine from hybridoma batch culture.

In conclusion, a methodology to control apoptotic cells via manipulation of certain amino acids was proposed. A kinetic model describing cell growth, substrate uptake and product formation was derived. The model included an apoptotic death rate as a function of asparagine, glutamine and viable cells. The selection of these amino acids was the result of a neural network based sensitivity analysis. An unscented Kalman filter was then successfully implemented for state estimations. A nonlinear model predictive control was applied to a simulated fed-batch bioreactor with flows of Gln, Asn, and Glc as manipulated variables. A NN predicted the concentration of apoptotic cells in the bioreactor. This hybrid model approach is different from methodologies that use the NN as the predictor in a MPC scheme. With nutrient controlled apoptosis research gaining momentum, this work offers a new perspective applicable to real-time control of apoptosis in bioreactors, different from genetic manipulation of the cells. The present approach may provide a way to increase the final titer of protein by minimizing death in the bioreactor.

5.10 Acknowledgements

The presented work was supported by the National Science Foundation (BES-9622526), the UNCF-Merck Graduate Science Research Dissertation Fellowship, and the Colorado State University Agricultural Experiment Station.

5.11 Nomenclature

S_k sensitivity index for input k

y_{ip} ith output of the NN for the pth pattern before input pertubation

$\bar{y}_{ip}$ ith output of the NN for the pth pattern after input pertubation

$\hat{y}$ NN estimation of y

xi input vector fed to the NN

w NN weight matrix

p NN bias vector

C_{O_2} concentration of dissolved oxygen in the liquid phase (mol/l^{-1})

$C^*_{O_2-H}$ liquid phase concentration of oxygen in equilibrium with the headspace (mol/ml^{-1})

$C^*_{O_2-B}$ liquid phase concentration of oxygen in equilibrium with the bubble phase (mol/ml^{-1})

$K_L a_B$ volumetric mass transfer coefficients in the bubble phase (h^{-1})

$K_L a_H$ volumetric mass transfer coefficients in the headspace (h^{-1})

OUR oxygen uptake rate (mol/ml.h)

q_{O_2-g} specific oxygen uptake rate for growth requirement (mol/cell.h)

q_{O_2-m} specific oxygen uptake rate for maintenance (mol/cell.h)

x state vector of Kalman filter

$\hat{\mathbf{x}}$ state vector estimated of Kalman filter

z observation vector of Kalman filter

K Kalman gain

P covariance of the innovation error

u manipulated variable vector

X translated state vector

Greek symbols

σ standard deviation

Γ output error weighting matrix

β input weighting matrix

5.12 References

Adams, JM, Cory, S. 1998. The Bcl-2 protein family: arbiter of cell survival. Sci 281:1322-1326.

Baughman, DR, Liu, YA 1995. Neural Networks in Bioprocessing and Chemical Engineering. San Diego, CA: Academic Press.

Bharath, R, Drosen, J 1994. Neural Network Computing. New York, NY: McGraw-Hill.

Caldwell, RB. 1995. Three methods of neural network sensitiviy analysis for input variable reduction: A case study in forcasting the S P 500 index (part 1). Neurove$t J 4:22-25.

Caldwell, RB. 1996. Three methods of neural network sensitiviy analysis for input variable reduction: A case study in forcasting the S P 500 index (part 2). Neurove$t J 4:17-22.

Clarke, DW, Mohtad, C, Tuffs, PS. 1987. Genelarized Predictive Control - Part I. The basic algorithm. Automatica 23:137-148.

Cowger, NL, O'Connor, KC, Hammond, TG, Lacks, DJ, Navar, GL. 1999. Characterization of bimodal cell death of insect cells in a rotating-wall vessel and shaker flask. Biotechnol Bioeng 64:14-26.

Darzynkiewicz, Z, Bruno, S, Del Bino, G, Gorczyca, W, Hotz, MA. 1992. Features of apoptotic cells measured by flow cytometry. Cytometry 13:795-808.

Darzynkiewicz, Z, Juan, G, Li, X, Gorczyca, W, Murakami, T, Traganos, T. 1997. Cytometry in cell neurobiology: Analysis of apoptosis and accidental cell death (necrosis). Cytometry 27:1-20.

Denmeade, SR, Isaacs, JT. 1996. Programmed cell death (apoptosis) and cancer chemotherapy. Cancer Control 3:306-309.

Distefano, DJ, Mark, GE, Robinson, DK. 1996. Feeding of nutrients delays apoptosic death in fed-batch cultures of recombinant NSO myeloma cells. Biotechnol Lett 18:1067-1072.

Dubach, AC, Markl, H. 1992. Application of an extended kalman filter method for monitoring high density cultivation of *Escherichia coli*. J Ferment Bioeng 73:396-402.

Ducommun, P, Ruffieux, PA, Furter, MP, Marison, I, Von Stockar, U. 2000. A new method for on-line measurement of the volumetric oxygen uptake rate in membrane aerated animal cell cultures. J Biotechnol 78:139-147.

Eikens, B, Karim, MN. 1999. Process identification with multiple neural network models. Int J Control 72:576-590.

Franek, F, Sramkova, K. 1995. Apoptosis and nutrition: Involvement of amino acid transport system in repression of hybridoma cell death. Cytotechnol 18:113-117.

Franek, F, Sramkova, K. 1996. Protection of B lymphocyte against starvation-induced apoptosis: survival-signal role of some amino acids. Immunol Lett 52:139-144.

Franek, F. 1995. Starvation-induced programmed death of hybridoma cells: Prevention by amino acid mixtures. Biotechnol Bioeng 45:86-90.

Fukushima, K, Motomura, S, Kuraoka, A, Nakano, H, Nishimoto, T. 1996. A single point mutation of hamster aminoacyl-tRNA synthetase causes apoptosis by deprivation of cognate amino acid residue. Genes to cells 1:1087-1099.

Fussenegger, M. 2001. The Impact of Mammalian Gene Regulation Concepts on Functional Genomic Research, Metabolic Engineering, and Advanced Gene Therapies. Biotechnology Progress, 17: 1-51.

Glacken, MW, Huang, C, Sinskey, AJ. 1989. Mathematical descriptions of hybridoma culture kinetics. III. Simulation of fed-batch bioreactors. J Biotechnol 10:39-66.

Hermann, JE. 1986. Enzyme-linked immunoassays for the detection of microbial antigens and their antibodies. Adv Appl Microbiol 31:271-289.

Hu MC, Davidson N. 1987. The inducible Lac operator-repressor system is functional in mammalian cells. Cell 48: 555-566.

Jackson, JE 1991. A User's Guide to Principal Components. New York, NY: John Wiley & Sons.

Julier, J, Uhlmann, JK, Durrant-Whyte, HF 1995. A new approach for filtering nonlinear systems. In: Pages 1628- 1632Proceedings of the 1995 American Control Conference, Seattle, Washington.

Karim, MN, Rivera, S. 1992. Artificial neural networks in bioprocess state estimation. Adv Bioechem Eng Biotechnol 46:2-33.

Karim, MN, Yoshida, T, Rivera, SL, Saucedo, VM, Eikens, B, Oh, GS. 1997. Global and local neural network models in Biotechnology. J Ferment Bioeng 83:1-11.

Korsmeyer, SJ. 1995. Regulators of cell death. Trends in Genetics 11:101-105.

Lund, P. 1974. Determination with glutaminase and glutamate dehydrogase. In H. U. Bergmeye: editors. Methods of enzymatic analysis, Verlag Chemie International, Deerfield Beach, FL 4, pp. 1719-1722.

Muller, HJ, Boos, J. 1998. Use of L-asparaginase in Childhood ALL. Critical Reviews in Oncology/Hematology 28:97-113.

Murray, K, Ang, CE, Gull, K, Hickman, JA, Dickson, AJ. 1996. NS0 myeloma cell death: influence of bcl-2 overexpression. Biotechnol Bioeng 51:298-304.

Nunez, G, Clarke, MF. 1994. The Bcl-2 family of proteins: regulators of cell death and survival. Trends Cell Biol 4:399-403.

Oltvai, ZN, Korsmeyer, SJ. 1994. Checkpoints of dueling dimers foil death wishes. Cell 79:189-192.

Phillips, NJ. 1973. Dye exclusion tests for cell viability. In: PF Kruse, Jr. And MK Patterson (Eds.), Tissue Culture: Methods and Applications, Academic Press, New York, pp. 406-408.

Principe, JC, Euliano, NR, Lefebvre, WC 2000. Neural and Adaptive Systems. New York, NY: John Wiley & Sons, Inc..

Reed, JC. 1994. Bcl-2 and the regulation of programmed cell death. Journal of Cell Biology 124:1-6.

Reid, S., Randerson, DH, Greenfield, PF. 1987. Amino acid dtermination in mammalian cell culture supernatants. J Biotechnol 1:68-72.

Riedmiller, M, Braun, H 1993. A direct adaptive method for faster backpropagation learning: The RPROP algorithm. In: Pages 586-591Proceedings of the IEEE International Conference on Neural Networks, San Francisco.

Robinson, JH, Smith, JA, Dee, LA. 1976. Synthesis and degradation of proteins in cultured, androgen-responsive tumor cells. Exp Cell Res 102:117-126.

Sakagami, H, Satoh, M, Yokote, Y, Takano, H, Takahama, M. 1998. Amino acid utilization during cell growth and apoptosis induction. Anticancer Research 18:4303-4306.

Sanfeliu, A, Stephanopoulos, G. 1999. Effect of glutamine limitation of the death of attached Chinese Amster Ovary cells. Biotechnol Bioeng 64:46-53.

Sargantanis, JG, Karim, MN. 1994. Multivariate iterated extended kalman filter based adaptive control: Case study of solid substrate fermentation. Ind Eng Chem Res 33:878-888.

Simon, L, Karim, MN 2000b. Identification and control of dissolved oxygen in hybridoma cell under shear sensitive environment. In: AIChE Annual Meeting, Los Angeles, CA.

Simon, L, Karim, MN, Schreiweis, A. 1998. Prediction and classification of different phases in a fermentation using neural networks. Biotechnol Tech 12:301-304.

Simon, L, Karim, MN. 2000a. Probabilistic neural networks using Bayesian decision strategies and a modified Gompertz model for growth phase classification. Biochem Eng J 7:41-48.

Singh, RP, Simpson, NH, Perani, A, Goldenzon, C, Al-Rubeai, M. 1997. Essential amino acid deprivation of hybridoma cells results in the induction of high levels of apoptosis, which is suppressed by bcl-2 over-expression. The Genetic Engineer and Biotechnologist 17:121-124.

Stanners, CP, Wightman, TM, Harkins, JL. 1978. Effect of extreme amino acid starvation on the protein synthetic machinery of CHO cells. J Cell Physiol 95:125-138.

Stoll, T, Pugeaud, P, von Stokar, U, Marison, IW. 1994. A simple HPLC technique for accurate monitoring of mammalian cell metabolism. Cytotechnol 14:123-128.

Telford, WG, King, LE, Fraker, PJ. 1994. Rapid quantification of apoptosis in pure and heteregeneous cell population using flow cytometry. Cytometry 172:1-16.

Winters, R, Matthews, R, Krishnan, K. 1994. Glutamine protects chinese hamster ovary cells from radiation killing. Life Sci 55:713-720.

Wu, X, Bellgardt, K. 1998. Fast on-line data evaluation of flow-injection analysis signals based on parameter estimation by an extended Kalman Filter. J Biotechnol 62:11-28.

Wyllie, AH, Kerr, JFR, Currie, AR. 1980. Cell death: The significance of apoptosis. Int Rev Cytol 68:251-306.

Yu, C, Roy, RJ, Kaufman, H, Bequette, BW. 1992. Multiple-model adaptive predictive control of mean arterial pressure and cardiac output. IEEE Trans Biomed Eng 39:765-777.

Chapter 6

ADVANCED PROCESS CONTROL IN CHO CELL CULTURE PROCESSES : EXPERIMENTAL STUDIES

6.1 Introduction

Classical control algorithms are currently used in different disciplines to control a range of processes including mechanical, electrical, chemical, and bioengineering processes. The switch from classical methods to advanced control design techniques has been latent and difficult, due in part to the complexity of proposed algorithms and the need of training programs to operate advanced sensors and control equipment. Additional challenges include a lack of sufficiently accurate sensors necessary to provide adequate measurements, a poor understanding of plant dynamics and constraints, and communication problems between researchers, operator, and equipment suppliers. As noted by Bogaerts (1999), sensors are expensive, and can potentially degrade the hydrodynamic properties of complex bioreactors. As a result, advanced control theories are tested on a simulated process while On-Off and PID controllers are still very popular in industrial settings. Williams et al. (1986) noticed that most computer-controlled processes only provide data acquisition and sequential control facilities. This trend is still predominant today.

Advanced control design technologies, although seemingly restricted to simulated plants, are suitable to solve a broad class of problems including non-linear and nonstationary systems and can significantly improve the performance of these physical processes. Pharmaceutical and biotechnological companies, for instance, are particularly interested in process optimisation and control of their inherently time-varying and nonlinear systems. A few percent changes in the final titer and product yield may, in fact, result in major cost benefits for large-scale production (Patarinska et al., 2000).

This article is restricted to the control of starvation-induced apoptosis in mammalian cells. The type of apoptosis investigated occurs as a result of deprivation of key amino acids. The two mechanisms of cell death reported in the literature are necrosis and apoptosis (Wyllie et al., 1980). Necrosis is a passive process that occurs when the cells are exposed to extreme environmental or physiologic stresses. Under these conditions, the cells are no longer able to maintain homeostatis, which leads to a cellular edema, extracellular ions and the eventual osmotic lysis of the cell. The contents of the cytoplasm leak out, leading to an intensive inflammation of surrounding tissues (Van Furth and Van Zwet, 1988). In necrotic death, the cells respond to pathologic changes initiated outside of the cells. These changes can be elicited by any of a large series of factors that triggers a change in the permeability of the plasma membrane. The cells play a passive role in initiating the process of death. On the contrary, in PCD the cells participate actively in the death mechanism (Wyllie et al., 1980).

Apoptotic cells are induced to commit suicide under normal physiological conditions. PCD is crucial to the normal development and homeostatis of multicellular organisms and can be used to kill virus-infected and cancer cells (Reed, 1994; Oltvai and Korsmeyer,

1994; Nunez and Clarke, 1994; Korsmeyer, 1995). PCD occurs normally at different stages of morphogenesis - in the growth and development of metazoans and in normal turnover in adult tissue. Once initiated, PCD leads to a cascade of biochemical and morphological events that result in irreversible degradation of the genomic DNA and fragmentation of the cell (Wyllie et al., 1980), (Cohen, 1993; Steller, 1995). The chromatin condenses and migrates to the nuclear membrane. Internucleosomal cleavage, that leads to laddering of DNA at the junction of nucleosomes, is noticed (Reed, 1994). The cytoplasm shrinks without membrane rupture. Blebbing of plasma and nuclear membranes is observed. The cell contents are then packaged in vesicles called apoptotic bodies which are immediately engulfed by phagocytic cells (Savill et al., 1989). Epitopes appear on the plasma membrane marking the cells as a phagocytic membrane.

The lack of available nutrients such as amino acids and glucose has been cited as a potential inducer of apoptosis in cell cultures (Mercille and Massie, 1994). Regardless of the type of bioreactors used, the nutritional demand of mammalian cells often exceeds the available supply (Mercille and Massie, 1994). Nutrient deprivation can also occur in microporous beads (De la Broise et al., 1992) and hollow fibers (Piret and Cooney, 1990). In the human body, nutrient deprivation may cause the cells to die by apoptosis. Ischemia, for instance, has been implicated in many cases as an agent for the onset of PCD (Dragunow et al., 1993). Heart tissues clinically exposed to ischemic insults and kidney cells during transplantation undergo apoptosis. Nutrient deprivation can also occur in tumors as a result of insufficient blood supply. D5 hybridoma cells were also found to be prone to the induction of apoptosis by incubation in methionine-deficient medium (Perreault and Lemieux, 1994). Arginine deprivation induced apoptosis in leukemia

L1210 cells (Ormerod et al., 1994). Using human promyelocytic leukemia (*HL-60*), human oral squamous carcinoma (*HSC-2, HSC-4, NA*), human salivary gland tumour (*HSG*) and rat neuron cells (*PC-12*), Sakagami *et al.* (1998) noted that serine depletion accumulated the *G1* arrested cells and a large number of apoptotic cells were produced. Addition of serine to the media prolonged the logarithmic cell growth phase (Sakagami et al., 1998). Sanfeliu and Stephanopoulos (1999) found that in the case of CHO cells, the depletion of both glutamine and glutamic acid caused the cells to die by apoptosis. They further observed that the presence of protective factors such as serum in the culture medium, the availability of essential nutrients, and the over-expression of antideath genes can help in preventing apoptosis in cell culture. However, no systematic method has been proposed to control starvation-induced apoptosis. This contribution explores the application of model-predictive control, Kalman filters, and artificial NNs to control apoptotic death in a bioreactor as a result of deprivation on amino acids.

The first part of the paper describes Kalman filter techniques, model predictive controls and artificial NNs. Materials and methods are summarized in the second part. The last section deals with the results and discussions.

6.2 The Extended Kalman Filter

6.2.1 Kinetic Equations for the Model

The state equations in the Kalman filter are based on a mathematical model of the growth of CHO cells, product formation, and substrate consumption. The reactor model is given by the balances:

$$\frac{d(X_v(t))}{dt} = (\mu - k_d)X_v(t) - \frac{F}{V}X_v(t) \tag{1}$$

$$\frac{d(X_{da}(t))}{dt} = k_{da}X_v(t) - \frac{F}{V}X_{da}(t) \tag{2}$$

$$\frac{d(X_{dn}(t))}{dt} = k_{dn}X_v(t) - \frac{F}{V}X_{dn}(t) \tag{3}$$

$$\mu = \frac{\mu_{max}Glc(t)Gln(t)}{(k_{Glc} + Glc(t))(k_{Gln} + Gln(t))K_{inh}} \tag{4}$$

$$K_{inh} = \left(\frac{Glc(t)}{k_{Glc}} + 1\right)\left(\frac{Lac(t)}{k_{Lac}} + 1\right)\left(\frac{Am(t)}{k_{Am}} + 1\right) \tag{5}$$

$$k_d = k_{dn} + k_{da} \tag{6}$$

$$k_{dn} = const \tag{7}$$

$$k_{da} = f_{VV}(Gln, Ans) \tag{8}$$

$$\frac{d(Gln(t))}{dt} = \frac{F_{Gln}Gln_o}{V} - k_{deg}Gln(t) - q_{Gln}X_v(t) - \frac{F}{V}Gln(t) \tag{9}$$

$$\frac{d(Am(t))}{dt} = k_{deg}Gln(t) + q_{Am}X_v(t) - \frac{F}{V}Am(t) \tag{10}$$

$$\frac{d(Lac(t))}{dt} = \frac{\mu}{Y_{\frac{X_v}{Lac}}}X_v - \frac{F}{V}Lac(t) \tag{11}$$

$$\frac{d(Glc(t))}{dt} = \frac{F_{Glc}Glc_o}{V} - \frac{\mu}{Y_{\frac{X_v}{Glc}}}X_v(t) - \frac{F}{V}Glc(t) \tag{12}$$

$$\frac{d(Asn(t))}{dt} = \frac{F_{Asn}Asn_o}{V} - \frac{\mu}{Y_{\frac{X_v}{Asn}}}X_v(t) - \frac{F}{V}Asn(t) \tag{13}$$

$$\frac{d(P(t))}{dt} = \alpha\mu X_v(t) + \beta X_v(t) - \frac{F}{V}P(t) \tag{14}$$

$$\frac{dV}{dt} = F \tag{15}$$

$$F = F_{Asn} + F_{Glc} + F_{Gln} \tag{16}$$

The definitions of the variables and the parameter values are listed in Table 6.1. The relative sensitivities of the model parameters were also computed (Table 6.1). The sensitivity values were calculated based on a 5% change in the process parameters at a fermentation time of 100 hours. Eqs (2) and (8) are combined into one equation

$$X_{Ab}(t) = f_{NN}(X_v(t) - X_v(0), Gln(t) - Gln(0), Asn(t) - Asn(0)) + X_{Ab}(0) \tag{17}$$

where f_{NN} is a NN mapping. The parameters of the model are obtained by fitting the batch data to Eqs. (1), (3), (9), (10), (11), (12), (13), and (14) with F = 0. These model equations were later used in the Kalman filter. The measured variables are the concentrations of total and viable cells, lactate and glucose.

Variable and Parameter	Definition	Numerical value	Unit	Relative Sensitivity
X_T	Total cell concentration	—	10^5 cells/ml	—
Xv	Viable cell concentration	—	10^5 cells/ml	—
X_{da}	Apoptotic cell concentration	—	10^5 cells/ml	—
X_{dn}	Necrotic cell concentration	—	10^5 cells/ml	—
Glc	Glucose concentration	—	g/l	—
Asn	Asparagine concentration	—	pmole/ml	—
Gln	Glutamine concentration	—	pmole/ml	—
Lac	Lactate concentration	—	g/l	—
Am	Ammonium concentration	—	µg/ml	—
P	tPA concentration	—	µg/ml	—
μ_{max}	Maximum specific growth rate	0.18	h^{-1}	$(\Delta X_T/X_T)/(\Delta\mu_{max}/\mu_{max}) = 9.18\times10^{-1}$
k_{dn}	specific necrotic death rate	3.00×10^{-3}	h^{-1}	$(\Delta X_{dn}/X_{dn})/(\Delta k_{dn}/k_{dn}) = 3.81\times10^{-1}$
k_{da}	specific apoptotic death rate	—	h^{-1}	—
k_{Glc}	Glucose Monod constant	2.09	g/l	$(\Delta X_T/X_T)/(\Delta k_{Glc}/k_{Glc}) = -1.41\times10^{-1}$
k_{Gln}	Glutamine Monod constant	2.79×10^{4}	pmole/ml	$(\Delta X_T/X_T)/(\Delta k_{Gln}/k_{Gln}) = -8.15\times10^{-1}$
ki_{Lac}	Lactate inhibition constant	1.07×10^{4}	g/l	$(\Delta X_T/X_T)/(\Delta ki_{Lac}/ki_{Lac}) = -3.46\times10^{-2}$
ki_{Glc}	Glucose inhibition constant	2.04[1]	g/l	$(\Delta X_T/X_T)/(\Delta ki_{Glc}/ki_{Glc}) = 7.43\times10^{-1}$
ki_{Am}	Ammonium inhibition constant	16.45	µg/ml	$(\Delta X_T/X_T)/(\Delta ki_{Am}/ki_{Am}) = 3.24\times10^{-1}$
k_{deg}	Glutamine decomposition constant	4.32×10^{-3}	h^{-1}	$(\Delta Gln/Gln)/(\Delta k_{deg}/k_{deg}) = 2.43\times10^{-1}$
q_{Gln}	Specific glutamine uptake rate	4.81	pmole/(10^5 cells.h)	$(\Delta Gln/Gln)/(\Delta q_{gln}/q_{gln}) = 1.51\times10^{-1}$
q_{Am}	Specific ammonium uptake rate	5.43×10^{-2}	µg/(10^5 cells.h)	$(\Delta Am/Am)/(\Delta q_{Am}/q_{Am}) = 7.72\times10^{-1}$
Y_{XvGlc}	Glucose yield coefficient	4.90	(10^5 cells)/g	$(\Delta Glc/Glc)/(\Delta Y_{XvGlc}/Y_{XvGlc}) = 2.18\times10^{-}$
Y_{XvLac}	Lactate yield coefficient	4.70	(10^5 cells)/g	$(\Delta Lac/Lac)/(\Delta Y_{XvLac}/Y_{XvLac}) = -7.39\times10^{-1}$
Y_{XvAsn}	Asparagine yield concentration	4.69×10^{-2}	(10^5 cells)/pmole	$(\Delta Asn/Asn)/(\Delta Y_{XvAsn}/Y_{XvAsn}) = 5.72\times10^{-1}$
α	Growth associated coefficient	4.34×10^{-1}	µg/(10^5 cells.h)	$(\Delta P/P)/(\Delta\alpha/\alpha) = 2.64\times10^{-1}$
β	Non-growth associated coefficient	5.58×10^{-2}	µg/h	$(\Delta P/P)/(\Delta\beta/\beta) = 7.17\times10^{-1}$

Table 6.1. Nomenclature and parameter values for solving the model equations

6.2.2 Kalman filters

The Kalman filter gives the optimal mean-squared error (MMSE) linear estimate of a state vector $\mathbf{x}(k)$ (Kalman and Bucy, 1999; Sargantanis and Karim, 1994). Initial values of estimated state variables are updated via a Kalman gain to provide a better estimate. The prior estimate $\hat{\mathbf{x}}(k-1)$ and the current observation $\mathbf{z}(k)$ are assumed to be Gaussian random variables. Kalman filters approximate a state variable that converges towards the true state of the process. For discrete-time non-linear systems, the state and output equations are:

$$\dot{\mathbf{x}}(t) = \mathbf{f}\left[\mathbf{x}(t), \mathbf{u}(t)\right] + \mathbf{v}(t) \tag{18}$$

$$\mathbf{z}(k) = \mathbf{h}\left[\mathbf{x}(k), \mathbf{u}(k)\right] + \mathbf{w}(k) \tag{19}$$

where $\mathbf{x}(t)$ is the state vector (10×1) of the system at time t obtained from Eqs. (1), (3), (9), (10), (11), (12), (13), (14), and (15) after adding a white noise $\mathbf{v}(k)$. The manipulated variable vector $\mathbf{u}(t_{k-1})$ is $\mathbf{0}$ for the batch fermentation case. $\mathbf{f}(\mathbf{x}(t), \mathbf{u}(t))$ is the 10×1 state function vector model. $\mathbf{z}(t_k)$ is the output observation scalor at time step k given by (19). The components of $\mathbf{x}(t)$ are $X_T(t)$, $X_v(t)$, $X_{dn}(t)$, $Gln(t)$, $Am(t)$, $Lac(t)$, $Glc(t)$, $Asn(t)$, $P(t)$, $V(t)$. The components of $\mathbf{z}(t_k)$ is given by $X_T(t)$, $X_v(t)$, $Lac(t)$, and $Glc(t)$. The measurement white noise (4×1) is given $\mathbf{w}(k)$. Eq. (19) can be written as

$$\mathbf{z}(k) = \mathbf{M}\mathbf{x}(k) + \mathbf{w}(k) \tag{20}$$

where

$$M = \begin{bmatrix} 1 & 0 & 0 & 0 & 0 & 0 & 0 & 0 & 0 & 0 \\ 0 & 0 & 1 & 0 & 0 & 0 & 0 & 0 & 0 & 0 \\ 0 & 0 & 0 & 0 & 0 & 1 & 0 & 0 & 0 & 0 \\ 0 & 0 & 0 & 0 & 0 & 0 & 1 & 0 & 0 & 0 \end{bmatrix} \quad (21)$$

and

$$\mathbf{x}(k) = \begin{bmatrix} X_T(k) & X_V(k) & X_{dn}(k) & \mathrm{Gln}(k) & Am(k) & Lac(k) & Glc(k) & Asn(k) & P(k) & V(k) \end{bmatrix}^T \quad (22)$$

In this work, a discrete-discrete Kalman filter algorithm was used as summarized below:

- Prediction of states

$$\hat{\mathbf{x}}_{k|k-1} = \mathbf{f}_k(\hat{\mathbf{x}}_{k-1}, \mathbf{u}) \quad (23)$$

- Prediction of the covariance matrix of states

$$\mathbf{P}_{k|k-1} = \frac{\partial \mathbf{f}_k}{\partial \mathbf{x}_k} \mathbf{P}_{k-1} \frac{\partial \mathbf{f}_k}{\partial \mathbf{x}_k}^T + \mathbf{Q}_{k-1} \quad (24)$$

- Kalman gain matrix

$$\mathbf{K}_k = \mathbf{P}_{k|k-1} \mathbf{M}_k^T \left(\mathbf{M}_k \mathbf{P}_{k|k-1} \mathbf{M}_k^T + \Lambda_k \right)^{-1} \quad (25)$$

- Update of the state estimation

$$\hat{\mathbf{x}}_k = \hat{\mathbf{x}}_{k\,k-1} + \mathbf{K}_k\left(\mathbf{z}_k - \mathbf{M}_k\hat{\mathbf{x}}_{k\,k-1}\right) \tag{26}$$

- Update of the covariance matrix of states

$$\mathbf{P}_k = (\mathbf{I} - \mathbf{K}_k\mathbf{M}_k)\mathbf{P}_{k\,k-1} \tag{27}$$

- Initialization

$$\mathbf{P}_{0\,0} = \Lambda_{x_0}, \qquad \hat{\mathbf{x}}_{0\,0} = E\left[\mathbf{x}_0\right] \tag{28}$$

6.3 Model Predictive Control

Multistep Model Predictive controllers (MPCs) have been used as an advanced control technique in industry (Yamamoto and Hashimoto, 1991). Dynamic Matrix Control (DMC) (Cutler and Ramaker, 1980), and Model Algorithm Control (MAC) are algorithms related to MPC based on deterministic impulse or step response models. Autoregressive moving average (ARMA) has been used for long-range model predictive controllers (De Tremblay et al., 1992; De Keyser and Van Cauwenberghe, 1982). Adaptive Generalized Predictive Controllers (GPC) (Bitmead et al., 1990) have also been proposed to account for variability in system parameters.

MPCs compute a sequence of manipulated variables by solving an on-line optimization problem. MPC was initially applied to power plants and petroleum refineries. For a decription of MPC algorithms and progress in the field, the reader is encourage to read the works of Bequette (1991), Muske and Rawlings (1993), and Proll and Karim (1994) to mention a few. Richalet *et al.* (1978) published their work on Model Predictive Heuristic Control (MPHC). They used a solution software called IDCOM (Identification and Command) and a descrete-time Finite Impluse Response (FIR) model in which the output at a specific time is a weighted linear combination of past inputs. The weights are the impulse response coefficients h_i.

$$y_{k-j} = \sum_{i=1}^{N} h_i u_{k-j-i} \tag{1.29}$$

To identify the finite impulse response, Richalet et al. minimized distance between plant test and predicted data. They used a Fluid Catalytic Cracking Unit (FCCU), a Poly-Vinyl Chloride (PVC) plant and a power plant steam generator as potential applications of the MPHC algorithm. DMC was also presented as a MPC (Cutler and Ramaker 1980). Both the MPHC and the DMC drive the output as close as possible to a predefined reference trajectory. In the MPHC, the trajectory is defined as a first order path from the current output value to the desired setpoint. The DMC uses a penalty term on the manipulated variable moves. In the DMC algorithm, a step response model is used:

$$y_{k-j} = \sum_{i=1}^{N-1} s_i \Delta u_{k-j-i} + s_N u_{k-j-N} \tag{1.30}$$

The penalty terms are used to provide robustness in the presence of model error. The IDCOMM and DMC algorithms had a lot of industrial applications but mainly for unconstrained multivariate processes. The constraints did not appear explicitly in their formulation. The DMC problem was then solved using quadratic programming (QDMC) which allows the input and output constraints to be included (Garcia and Morshedi, 1986). The QDMC algorithm is referred to as a second generation MPC because the QP algorithm allows the explicit inclusion of input and output constraints. However, the plant model is still a linear step response. The popularity of the QDMC may stem from the fact that the Hessian of the QP is usually positive definite. The optimization problem is therefore convex and standard optimization codes can then be used to solve the problem. Muske and Rawlings (1993) point out limitations of existing industrial MPC technology. In their views, the impulse and step response models are over-parametrized. Moreover the impulse and step response are only applicable to stable processes. The use of an auto-regressive parametric model (ARX) can help (Sargantanis and Karim, 1999). The MPC traditionally assumes a constant output disturbance for all future time. A model for disturbances would improve the feedback immensely. Muske and Rawlings (1993) have used a state space model and an optimal observer to improve the performance of the controller. A major problem remains for nonlinear plant models. The QP is no longer convex for a nonlinear plant. The solution is a global optimization problem. Bequette (1991) describes several approaches that can be used. Another solution is to use an adaptive MPC algorithm such as the GPC introduced by Clarke *et al.* (1987). One can then use a linear or nonlinear model and update the model parameters.

However, questions on nominal stability, robust stability and performance still need to be addressed. The bottom line is, in the case of linear systems, the stabilty of MPC is insured by choices of prediction and control horizons and weighting matrices in the objective function (Sistu and Bequette, 1996). Biochemical engineering processes are mainly nonlinear. Classical control linearizes the model equation before implementing control. If the system dynamics are very nonlinear, these approaches will fail. Variable transformation is another alternative that converts the set of nonlinear differential equations into a set of differential equations. However, such an approach is very sensitive to model error. Besides, it is not always possible to come up with a tranformation model. The alternative is to use MPC. In MPC, the process can still be linear. MPCs can be used for control problems with constraints on state and manipulated variables. The plant is initially modeled and the task is to calculate manipulated variable moves U over a control horizon which optimizes a performance objective over some prediction horizon: V sampling periods with V greater than U. With this arrangement, one obtains tight control of the process, better constraint handling and robustness in the presence of unusual dynamics and time-delays. The first method is to solve the differential equation and to implement the optimization. The manipulated variable is initially guessed, and the differential equations are solved numerically to obtain the control profile. The objective function is calculated. The control profile is updated using some optimization algorithm and the process is repeated until the optimal control values are obtained. This gives a sequential solution and optimization strategy in which there is not a lot of programming effort. The incorporation of plant constraints is very difficult. A better strategy is to use a simultaneous solution and optimization strategy (NLP).

The advantages of MPC are as follows: the ability to bring the controlled variable to its set-point quickly and smoothly, and the explicit inclusion of plant constraints. Because the manipulated variable tracks the constraints when error in the model parameter are incorporated, a reasonable MPC performance can be obtained while the process is brought to its set-point with no steady-state offset. Even for an open-loop unstable system, the MPC is able to bring the controlled variable to its set-point with no steady-state offset. An open-loop optimal control strategy is sometimes unable to accomplish this because even small deviations from the optimal profile cause the controlled variable to reach an open-loop stable steady state. Thus, feedback control is crucial (Patwardhan et al., 1990).

MPCs have been around for the last 30 years. The algorithm involves a repeated optimization of an open-loop performance objective over a finite horizon from the current time to a prediction horizon. Since 1970, Kleinman (1970) used a finite horizon to compute a state feedback gain that stabilizes a linear system. MPC is distinguished from standard feedback control because the methodology explicitly incorporate plant constraints in the control law equation (Eaton and Rawlings, 1992). In an example using a DMC on an system represented by an all-pass function, Eaton and Rawlings (1992) showed that an open-loop control action that achieves zero tracking error for the plant on any bounded interval produced a feedback loop that is internally unstable. Such a controller, indeed inverts the RHP zero and tries to use unstable pole cancellation with the plant. Increasing the horizon also improves performance and when the RHP zero is closer to the origin, a longer prediction horizon improves the performance of the controller. Choosing the control horizon to be less than the prediction horizon is like placing an

infinite penalty on the last manipulate variable move. The need for selecting a penalty on the manipulated variable in the objective function is removed. Also, under these conditions, the controller avoids an output that would give an unstable system. However, a small time of suboptimal behavior persists at the end of the control horizon and the beginning of the prediction horizon. This problem can be eliminated by choosing a larger prediction horizon or by adding an extra term of the form $R(u-u_{ref})^2$ to the objective function. R can be adjustable and u_{ref} is the manipulated variable obtained by solving the objective function without the extra term. For plants with time delay, the only requirement is that the prediction horizon must be at least as long as the delay. MPC is also able to handle unstable plants. MPC also forecasts any constraint violations and takes current action to reduce errors caused by constraints. Choosing a small control horizon while a large prediction horizon is used may deteriorate performance because the controller is being asked to predict the required control action for a changing profile while also being forced to predict one relatively long constant control move over the final portion of the prediction horizon. The difference between an optimal controller and the MPC is that for the optimal controller, model parameter error will effect the performance of the controller and the plant may drift away from the trajectory since the estimated model bears no resemblance to the true model. One way to handle this problem is to reset the initial conditions at each sampling time. On the other hand, the MPC has the advantage that it does this automatically for a wide assortment of problems and most importantly handles feedback.

6.4 Neural Networks

During the last ten years, NNs have emerged as an accepted tool for modeling nonlinear processes (Baughman and Liu, 1995; Bharath and Drosen, 1994; Eikens and Karim 1999; Simon et al., 1998; Simon and Karim, 2000). Due to their approximation capabilities as well as their inherent adaptive features, artificial NNs offer an appealing alternative to classical methods of modeling nonlinear dynamic systems. NN models consist of a set of weights, **w**, a set of basis functions $f(.)$, and a set of parameters **p** (biases, centers, etc.). The general equation can be written as:

$$\hat{y} = f(\mathbf{xi}, \mathbf{w}, \mathbf{p}) \tag{31}$$

where $\hat{y}$ denotes the NN estimation and **xi** is the input vector. Parameters **w** and **p** are adjusted during a "training" procedure in order to minimize some kind of error measure. Different architectures of NNs have been implemented in the literature (Eikens and Karim, 1999; Karim et al., 1997; Karim and Rivera, 1992; Simon et al., 1998; Simon and Karim, 2000). The development of a NN model requires a training set made up of known input and output patterns. In the training phase, examples representative of the problem are propagated to the network. The weights are adjusted to minimize a performance criterion such as the squared error between the experimental or measured output and the output predicted by the network. The network learns the underlying relationship based on the given set using an iterative error-minimization procedure. On-line or off-line learning is

used for training. In on-line training, the input-output data pairs (also called exemplars) presented to the network are stored and can be accessed repeatedly. In off-line training, the weights are updated after each exemplar is feed to the network. The exemplar is then discarded. Off-line learning offers several advantages over on-line learning. The former allows the networker to monitor the objective function for a particular set of weights. Different techniques, such as multiple random initializations or genetic algorithms (GAs), can then be tested to improve the performance of the network. Freeman (1994) presented a brief introduction to the use of GAs in the optimization of NN weights.

A validation set is either used to refine the topology (also called architecture or structure) of the network or to serve as a stopping criterion. Parameters such as the number of units in a hidden layer or the number of hidden layers determine the structure of the network. In the first methodology, the NN designer assesses the performance of different trained networks by evaluating an objective function using the validation set. The network with the smallest error is selected. In the second approach, training and validating take place concurrently. The network stops learning once the sum of residuals based on the validation set start to increase beyond a user-specified number of iterations. A testing set is later used to avoid overfitting. A common practice among networks is to use training and testing sets, especially when the number of experimental data is limited.

6.5 Experimental Procedure

At the beginning of the experiment, the specific apoptotic death rate was assumed to be zero. Except for the concentration of total and viable cells, glucose, and lactate, the state variables took on values based on previous fermentation runs, at the same condition

and medium compositions. A trained NN subroutine was then passed to the main program. The arguments of the network were the concentrations of viable cells, glutamine and asparagine; the output was the concentration of apoptotic cells. The original input and output patterns were expressed in deviation forms, that is, in terms of deviations measured from their initial concentrations. The elements of the covariance matrix of states were then defined. The state equations were integrated forward in time with the concentration of apoptotic cells and the specific apoptotic death rate and evaluated at each time step. The upper time limit for the integration corresponded to the next sampling time. After saving the end values of the state variables, the initial states were fed into a discrete version of the system equation. It should be noted that the differential equations, representative of the system, were converted to a continuous state space representation by using the function "jacobian" in Matlab^{R}:

$$\mathbf{P}_{k,k-1} = \frac{\partial \mathbf{f}_k}{\partial \mathbf{x}_k} \mathbf{P}_{k-1} \frac{\partial \mathbf{f}_k^T}{\partial \mathbf{x}_k} + \mathbf{Q}_{k-1} \tag{32}$$

Eq. (32) was then converted to a discrete state space model using the Matlab^{R} function "c2d."

$$\mathbf{x}(k+1) = \mathbf{A}\mathbf{x}(k) + \mathbf{B}\mathbf{u}(k) \tag{33}$$

Equations (24) and (25) were used to predict the covariance matrix and to calculate the Kalman gain. The concentrations of total and viable cells, glucose and lactate are

measured analytically at a time corresponding to the upper time limit of the integration. These variables represented the output vector y of Eq. (26). The state vector and covariance matrix were updated according to Equations (26) and (27), respectively. The concentrations of apoptotic cells were calculated based on the updated state values. The updated covariance and state vector were saved and used at the next sampling time. The state variable vector, estimated concentration of apoptotic cells, specific apoptotic death rates, volume, and the flow rates of glucose, glutamine and asparagine were then passed to a constrained MPC controller ("constr" in Matlab^{R}). A network was used to approximate the concentration of apoptotic cells during implementation of the controller. The control and prediction horizons were 1 and 45 respectively. A prediction horizon of 45 corresponded to an average of 3 sampling times (a average sample time of 15 hours was used). The controller outputs the flow rates of glucose, glutamine, and asparagines to keep apoptotic cells at a concentration of 1.0×10^{5} cells. The procedure was repeated at the next sampling time.

6.6 Materials and Methods

6.6.1 Cell Line and Culture Medium

The CHO cell line, CHO 1-155500, obtained from ATCC (American Type Culture Collection, Manassas, VA) was used in this research. The cells produce recombinant tissue-type plasminogen activator (t-PA) that has clinical applications as a thrombolytic agent. The cells were initially thawed and diluted ten-fold (1 ml of culture and 9 ml of 90% HAMS F-12 medium and 10% fetal bovine serum). These were then transferred to a 75 ml T-flask containing 95% selection medium (Dulbecco's Modified Eagle Medium)

and 5% dialyzed fetal bovine serum. The flask was placed in an incubator (VWR Scientific Products, model 2325, West Chester, PA) set at 37°C and 8 % carbon dioxide overlay. For subsequent studies, the cells grew in a 3-l bioreactor (New Brunswick, Scientific, CO., Inc., Edison, NJ). The pH (Cole-Parmer Instrument Company, Vernon Hills, Illinois) was controlled at 7.2 by addition of 1 M NaOH and carbon dioxide. The dissolved oxygen (Cole-Parmer Instrument Company, Vernon Hills, Illinois) was controlled at a concentration of 40% saturated air. The agitation speed was set at 80 RPM. The temperature was maintained at 37°C.

6.6.2 Sample Analysis

The concentration of total cells was measured using a hemacytometer. The samples were initially diluted to 2,000-20,000 cells per ml. Cell viability was assessed by trypan blue Trypan blue (Sigma Product No. T0776), exclusion . Flow cytometry was the methodology employed to detect and quantify apoptotic cells (Darzynkiewicz et al., 1992; Telford et al., 1994; Darzynkiewicz et al., 1997). Ammonia was assayed enzymatically. The concentrations of lactate and glucose were determined using a YSI analyzer. The compositions of amino acids were determined by HPLC method. The product, t-PA, was analyzed via ELISA.

6.6.3 Bioreactor

Cultures were run in a 3-L temperature-controlled stirred vessel (Applikon, Foster City, CA) with a 1.4 liter working volume for the batch mode. A schematic representation of the system is shown in Fig. 6.1. The bioreactor was fitted with one marine impeller

(Impeller), two spargers (Sparger 1 and Sparger 2) and sterilizable dissolved oxygen (DO), and pH probes (Ingold). Dissolved oxygen readings were recorded as percent saturation. One hundred percent saturation corresponds to the saturation of DO in air at 37°C. DO was controlled at 40 % by manipulating the flow rate of oxygen through Sparger 2. The oxygen was initially passed though a set of two sterile filters (Filter 2, 0.2 μm) before flowing through Sparger 2. The stirring speed was maintained at 80 RPM via a motor (Speed controller, Applikon). The pH was controlled at 7.2 by manipulating the flow rates of carbon dioxide (CO_2) and 1 N sodium hydroxide (Base). Air flew into the reactor headspace after passing through Filter 3 (0.2, μm). Carbon dioxide circulated through Filter 1 into the vessel via Sparger 1. The flow rate of each gas entering the reactor can be read and further adjusted with flowmeters (Flowmeter 1 through 3). The gas mixture composed of air, oxygen, and carbon dioxide left the bioreactor through a condenser (Condenser). Peristaltic pumps (Pump 1 through 4, Matsterflex, Cole-parmet Instrument Company) were used for addition of glucose, glutamine, asparagine, and sodium hydroxide into the vessel. The temperature was maintained at 37°C (Heating tape).

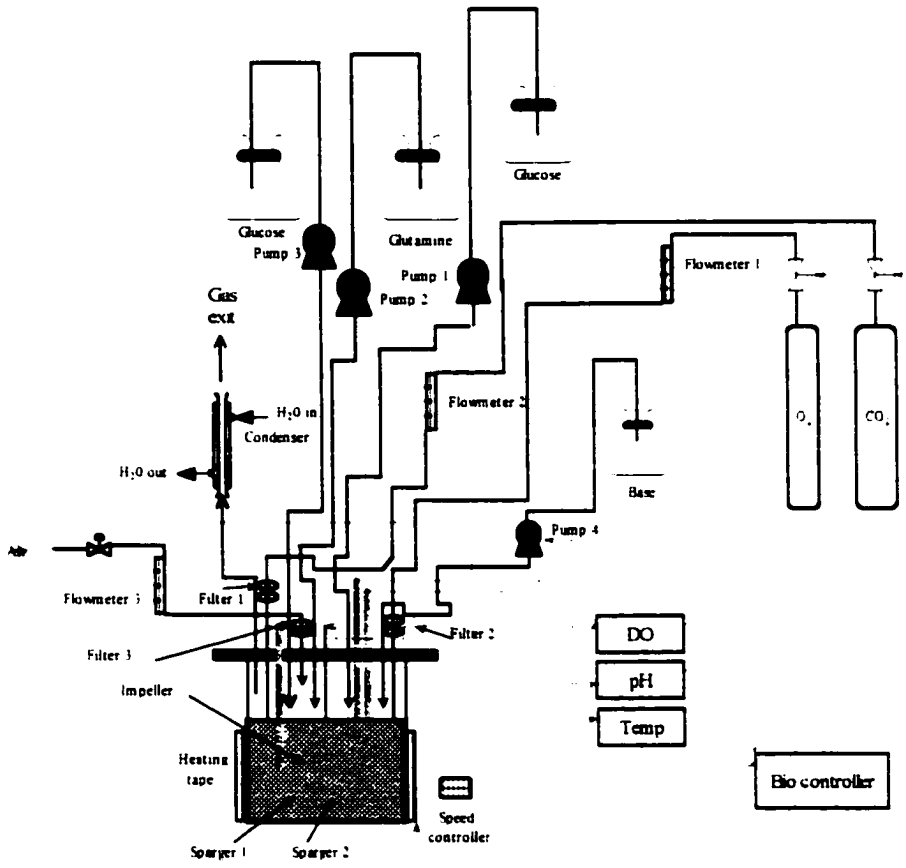

Figure 6.1. Schematic representation of the system

6.7 Results and Discussions

The controller implemented (Fig. 6.2) was able to control the concentration of apoptotic cells. The concentrations of viable cells, total cells, lactate and glucose are shown in Figures 6.3 though 6.6. The predicted (Eq. 23) and updated estimates (Eq. 26) from the Kalman filter agreed very well with the concentrations obtained by forward integration of the model equations. For instance, the glucose concentrations obtained from the filter agrees better with the measured values than with the concentrations

predicted by the kinetic model. Fig. 6.7a shows the feeding policy. Flow rates of 1.0 ml/h are not plotted. In Fig 6.7b, the scale is adjusted to show the whole plot. It should be noted that the flow rate of glucose remained at zero most of the time. The reason is that, in the model proposed, PCD is only a function of viable cells, glutamine, and asparagine.

The concentration of apoptotic cells is shown in Fig 6.8. The calculated concentration of apoptotic cells was slow to converge to the measured value. The problem is that the Kalman filter technique was not used to directly update the concentration of apoptotic cells. Its value was a function of viable cells, asparagine and glutamine. The error in the measured concentration of apoptotic cells at 250 h was probably due to cell debris which makes the precise determination of apoptotic cells difficult by flow cytometry method. This leads to the analysis of the observability Grammian. A system is observable iff

$$rank\left[C^T, C^T A^T, \ldots, C^T \left(A^{n-1}\right)^T\right]^T = n \tag{34}$$

where $C = M$ and n = 10 in linear CHO cell model. Eq. (34) was implemented at each time step. The results of the analysis clearly showed that the initial concentrations of asparagine, total protein, necrotic cells and the working volume (except for the fed-batch case) could not be reconstructed from the measured variables. This matrix is of rank 6 for the batch case and 7 for the fed-batch. The Grammian is shown for the first sampling time (Table 6.2). This result was expected since the measured outputs do not influence the non-observable part of the linear system, given by the state and measurement equations (33), and (20), respectively. It should be noted that these findings are simple artifacts of model linearization. For instance, the concentration of asparagine is a function of viable

cells (Eq. (13)). Furthermore, a change in glucose concentration would affect the accumulation rate of viable cells as evidenced by Equations (1) and (4), which would result in a change in the concentration of asparagine in the bioreactor. A similar argument can be made for necrotic cell and product concentrations. A more rigorous analysis using Lie derivatives could be pursued to show that asparagine is, in fact, observable. The reader is encouraged to read the work of Isidori for an in-depth analysis of nonlinear control systems (Isidori, 1989).

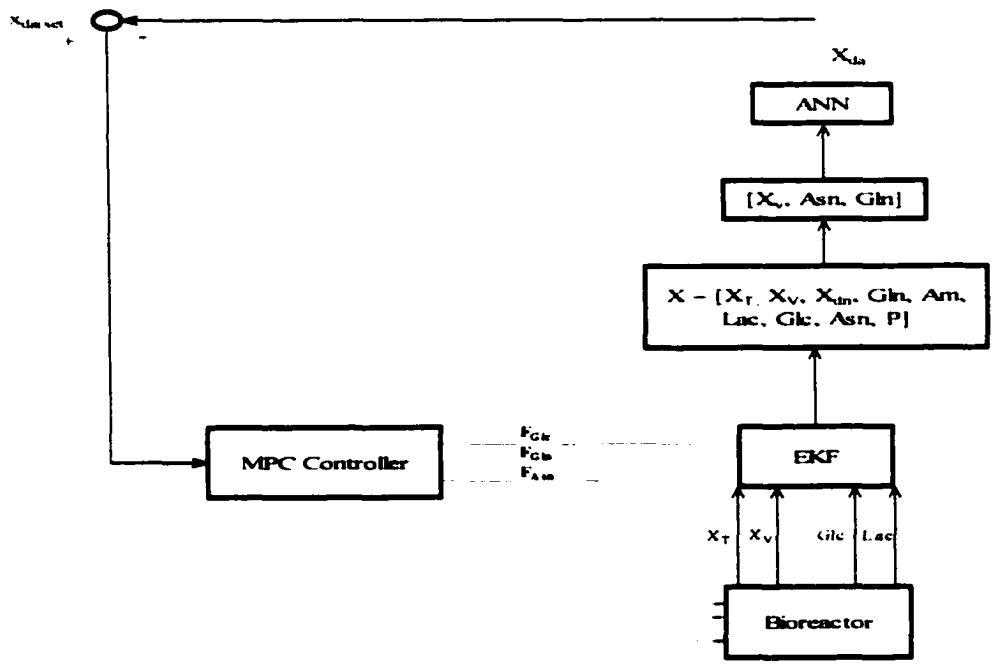

Figure 6.2. Model predictive control of apoptosis diagram

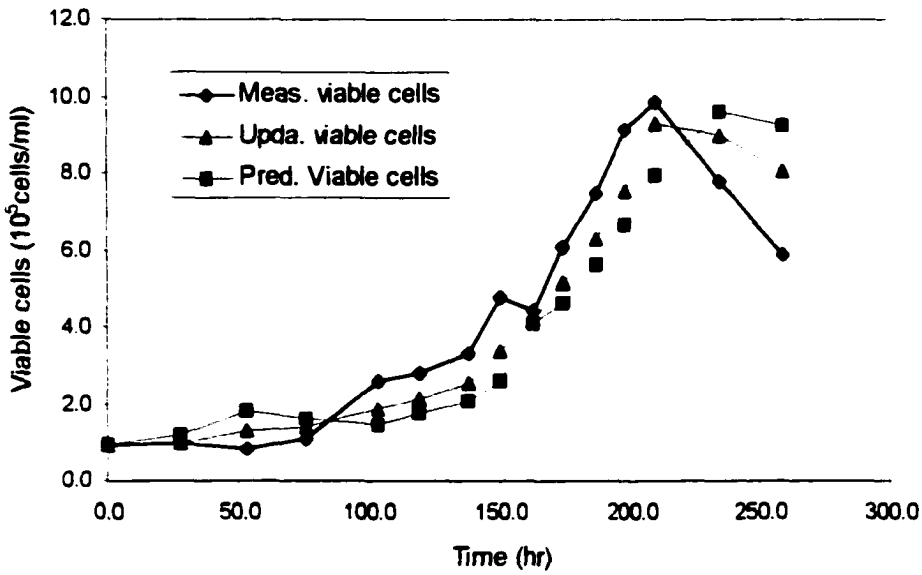

Figure 6.3. Profiles of viable cells

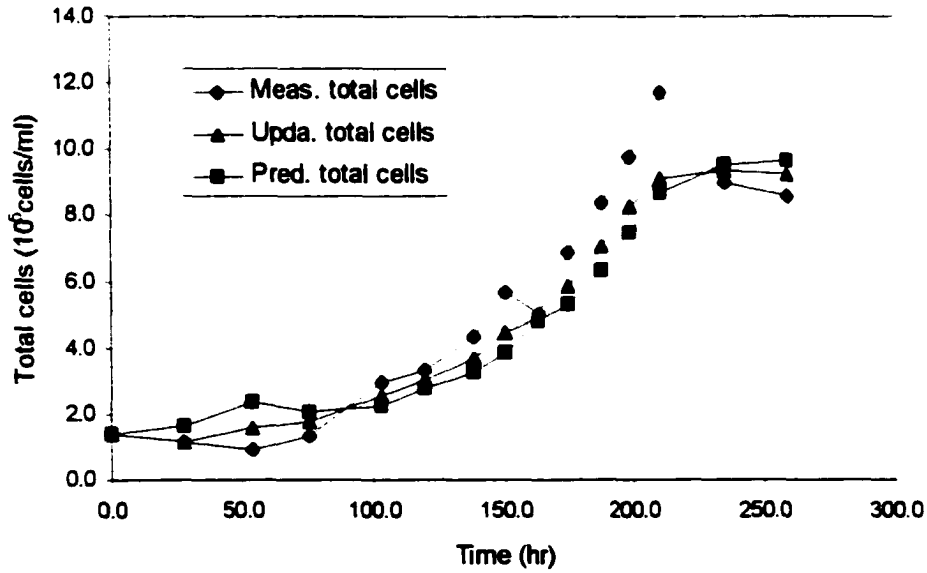

Figure 6.4. Profiles of total cells

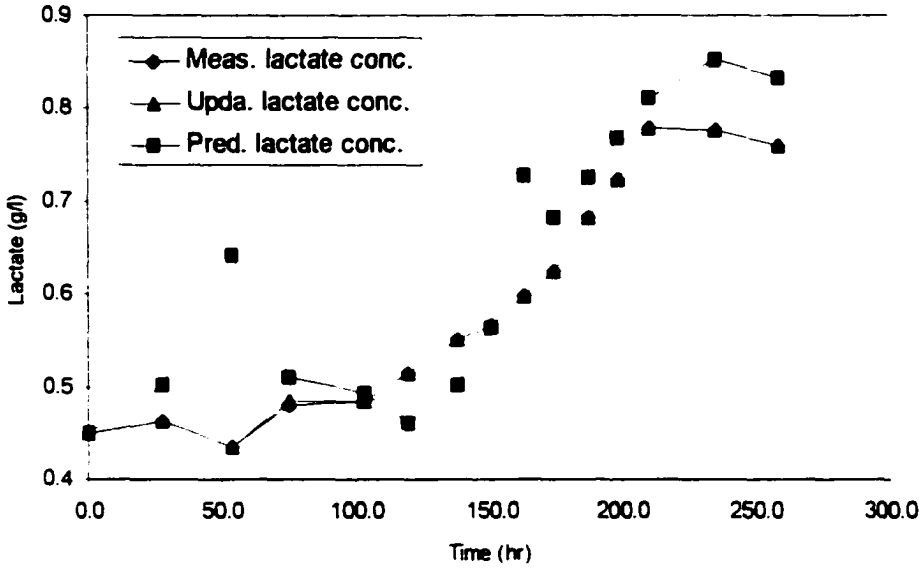

Figure 6.5. Profiles of lactate production

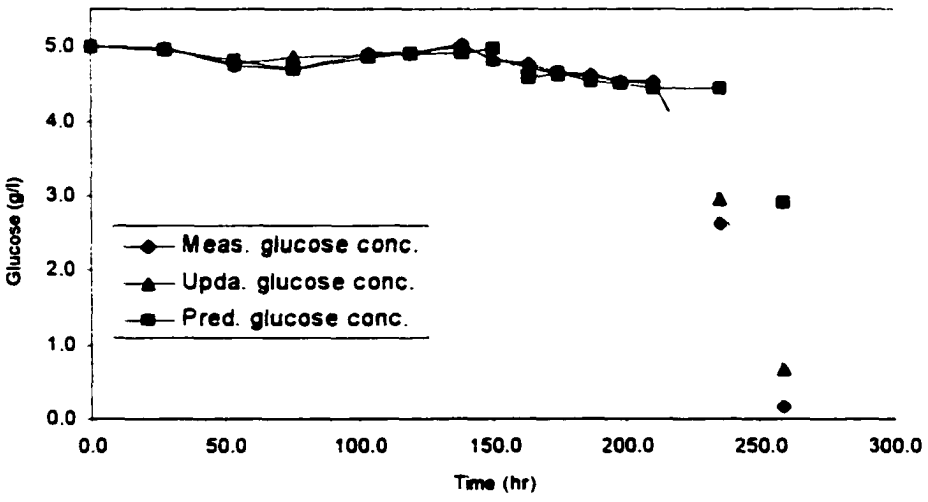

Figure 6.6. Profiles of glucose consumption

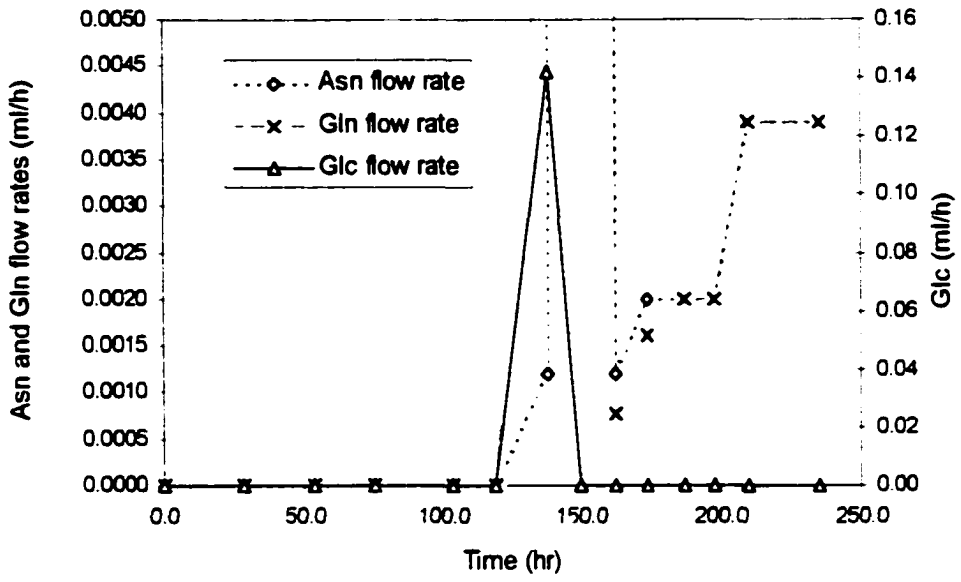

Figure 6.7a. Nutrient feeding flow rates

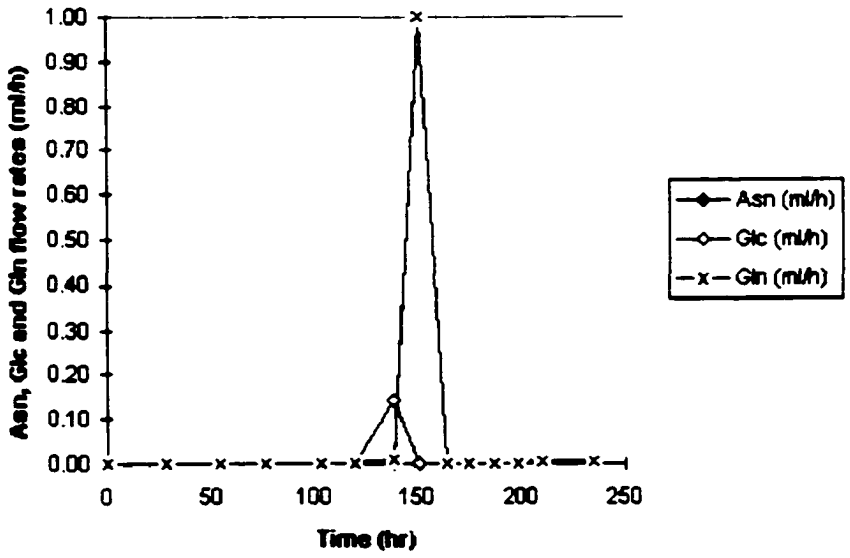

Figure 6.7b. Nutrient feeding flow rates

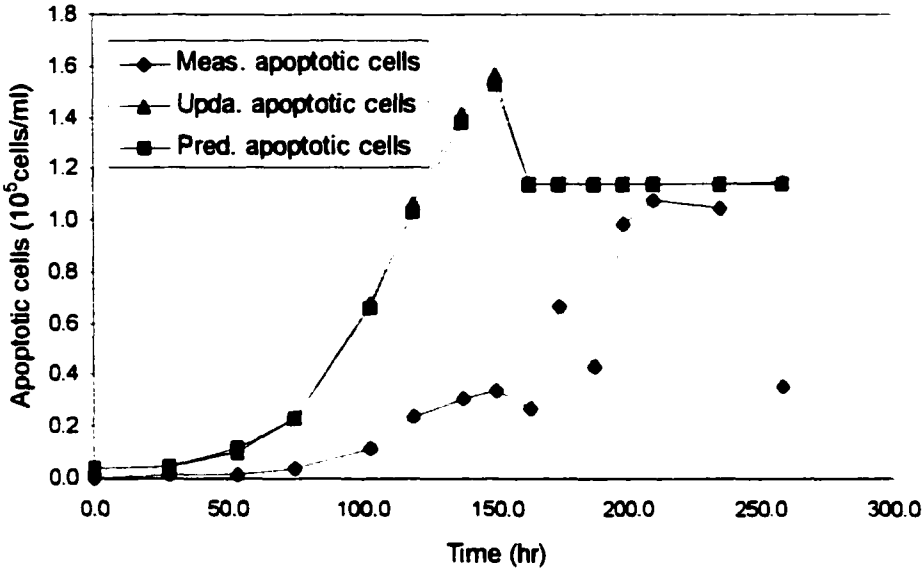

Figure 6.8. Profiles of apoptotic cells

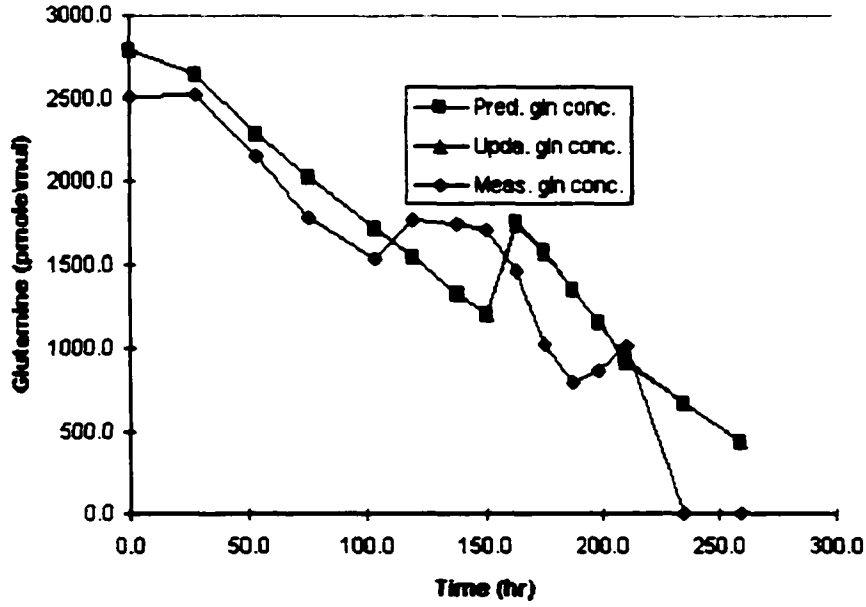

Figure 6.9. Profiles of glutamine consumption

1.00E+00	0.00E+00	0.00E+00	0.00E+00	0.00E+00	0.00E+00	0.00E+00	0.00E+00	0.00E+00	0.00E+00
0.00E+00	0.00E+00	1.00E+00	0.00E+00	0.00E+00	0.00E+00	0.00E+00	0.00E+00	0.00E+00	0.00E+00
0.00E+00	0.00E+00	0.00E+00	0.00E+00	0.00E+00	1.00E+00	0.00E+00	0.00E+00	0.00E+00	0.00E+00
0.00E+00	0.00E+00	0.00E+00	0.00E+00	0.00E+00	0.00E+00	1.00E+00	0.00E+00	0.00E+00	0.00E+00
1.00E+00	0.00E+00	1.98E-02	7.95E-06	-2.90E-03	-8.30E-03	0.00E+00	0.00E+00	0.00E+00	0.00E+00
0.00E+00	0.00E+00	1.02E+00	7.95E-06	-2.90E-03	-8.30E-03	0.00E+00	0.00E+00	0.00E+00	0.00E+00
0.00E+00	0.00E+00	-3.80E-03	-1.62E-06	6.00E-04	1.00E+00	0.00E+00	0.00E+00	0.00E+00	0.00E+00
0.00E+00	0.00E+00	4.00E-03	1.69E-06	-6.00E-04	-1.80E-03	1.00E+00	0.00E+00	0.00E+00	0.00E+00
1.00E+00	0.00E+00	3.97E-02	1.61E-05	-5.80E-03	-1.69E-02	0.00E+00	0.00E+00	0.00E+00	0.00E+00
0.00E+00	0.00E+00	1.04E+00	1.60E-05	-5.80E-03	-1.68E-02	0.00E+00	0.00E+00	0.00E+00	0.00E+00
0.00E+00	0.00E+00	-7.60E-03	-3.27E-06	1.20E-03	1.00E+00	0.00E+00	0.00E+00	0.00E+00	0.00E+00
0.00E+00	0.00E+00	8.00E-03	3.41E-06	-1.20E-03	-3.60E-03	1.00E+00	0.00E+00	0.00E+00	0.00E+00
1.00E+00	0.00E+00	5.99E-02	2.43E-05	-8.80E-03	-2.55E-02	0.00E+00	0.00E+00	0.00E+00	0.00E+00
0.00E+00	0.00E+00	1.06E+00	2.42E-05	-8.80E-03	-2.55E-02	0.00E+00	0.00E+00	0.00E+00	0.00E+00
0.00E+00	0.00E+00	-1.15E-02	-4.95E-06	1.80E-03	1.01E+00	0.00E+00	0.00E+00	0.00E+00	0.00E+00
0.00E+00	0.00E+00	1.20E-02	5.15E-06	-1.90E-03	-5.40E-03	1.00E+00	0.00E+00	0.00E+00	0.00E+00
1.00E+00	0.00E+00	8.03E-02	3.26E-05	-1.18E-02	-3.44E-02	0.00E+00	0.00E+00	0.00E+00	0.00E+00
0.00E+00	0.00E+00	1.08E+00	3.26E-05	-1.18E-02	-3.43E-02	0.00E+00	0.00E+00	0.00E+00	0.00E+00
0.00E+00	0.00E+00	-1.54E-02	-6.65E-06	2.40E-03	1.01E+00	0.00E+00	0.00E+00	0.00E+00	0.00E+00
0.00E+00	0.00E+00	1.61E-02	6.93E-06	-2.50E-03	-7.30E-03	1.00E+00	0.00E+00	0.00E+00	0.00E+00
1.00E+00	0.00E+00	1.01E-01	4.11E-05	-1.49E-02	-4.35E-02	0.00E+00	0.00E+00	0.00E+00	0.00E+00
0.00E+00	0.00E+00	1.10E+00	4.10E-05	-1.49E-02	-4.34E-02	0.00E+00	0.00E+00	0.00E+00	0.00E+00
0.00E+00	0.00E+00	-1.94E-02	-8.37E-06	3.00E-03	1.01E+00	0.00E+00	0.00E+00	0.00E+00	0.00E+00
0.00E+00	0.00E+00	2.02E-02	8.73E-06	-3.20E-03	-9.20E-03	1.00E+00	0.00E+00	0.00E+00	0.00E+00
1.00E+00	0.00E+00	1.22E-01	4.98E-05	-1.81E-02	-5.27E-02	0.00E+00	0.00E+00	0.00E+00	0.00E+00
0.00E+00	0.00E+00	1.11E+00	4.96E-05	-1.81E-02	-5.26E-02	0.00E+00	0.00E+00	0.00E+00	0.00E+00
0.00E+00	0.00E+00	-2.34E-02	-1.01E-05	3.70E-03	1.01E+00	0.00E+00	0.00E+00	0.00E+00	0.00E+00
0.00E+00	0.00E+00	2.44E-02	1.06E-05	-3.80E-03	-1.12E-02	1.00E+00	0.00E+00	0.00E+00	0.00E+00
1.00E+00	0.00E+00	1.43E-01	5.86E-05	-2.14E-02	-6.22E-02	0.00E+00	0.00E+00	0.00E+00	0.00E+00
0.00E+00	0.00E+00	1.13E+00	5.84E-05	-2.13E-02	-6.19E-02	0.00E+00	0.00E+00	0.00E+00	0.00E+00
0.00E+00	0.00E+00	-2.74E-02	-1.19E-05	4.30E-03	1.01E+00	0.00E+00	0.00E+00	0.00E+00	0.00E+00
0.00E+00	0.00E+00	2.86E-02	1.24E-05	-4.50E-03	-1.32E-02	1.00E+00	0.00E+00	0.00E+00	0.00E+00
1.00E+00	0.00E+00	1.64E-01	6.75E-05	-2.47E-02	-7.18E-02	0.00E+00	0.00E+00	0.00E+00	0.00E+00
0.00E+00	0.00E+00	1.15E+00	6.72E-05	-2.46E-02	-7.15E-02	0.00E+00	0.00E+00	0.00E+00	0.00E+00
0.00E+00	0.00E+00	-3.15E-02	-1.37E-05	5.00E-03	1.01E+00	0.00E+00	0.00E+00	0.00E+00	0.00E+00
0.00E+00	0.00E+00	3.28E-02	1.43E-05	-5.20E-03	-1.52E-02	1.00E+00	0.00E+00	0.00E+00	0.00E+00
1.00E+00	0.00E+00	1.85E-01	7.66E-05	-2.80E-02	-8.16E-02	0.00E+00	0.00E+00	0.00E+00	0.00E+00
0.00E+00	0.00E+00	1.17E+00	7.62E-05	-2.79E-02	-8.12E-02	0.00E+00	0.00E+00	0.00E+00	0.00E+00
0.00E+00	0.00E+00	-3.56E-02	-1.56E-05	5.70E-03	1.02E+00	0.00E+00	0.00E+00	0.00E+00	0.00E+00
0.00E+00	0.00E+00	3.71E-02	1.62E-05	-5.90E-03	-1.73E-02	1.00E+00	0.00E+00	0.00E+00	0.00E+00

Table 6.2. Observability matrix

Fig 6.9 shows the concentration of glutamine in the bioreactor. The concentration of asparagine (not shown) was for the most part below the detection level of the HPLC. Fig. 6.10 shows the concentration of viable cells, apoptotic cells, and total protein concentration for the batch bioreactor. Fig 6.11 shows the protein concentration when the proposed fed-batch methodology was used to control PCD. It was possible to increase

the final concentration of total proteins with the fed-batch policy (26.8 vs 67.2). In the batch system, the concentration of apoptotic cells reached a concentration of 1.5×10^5 cells/ml while in fed-batch operation, the maximum concentration of apoptotic cells was less than 1.1×10^5 cells/ml. At the maximum protein concentration, the productivity for the batch system is 0.014 mg/(viable cells).h. In this computation, the maximum cell density was also used. For the fed-batch system, the productivity was 0.054 mg/(viable cells .h). This clearly shows that the new methodology increases protein productivity and reduces the concentration of apoptotic cells.

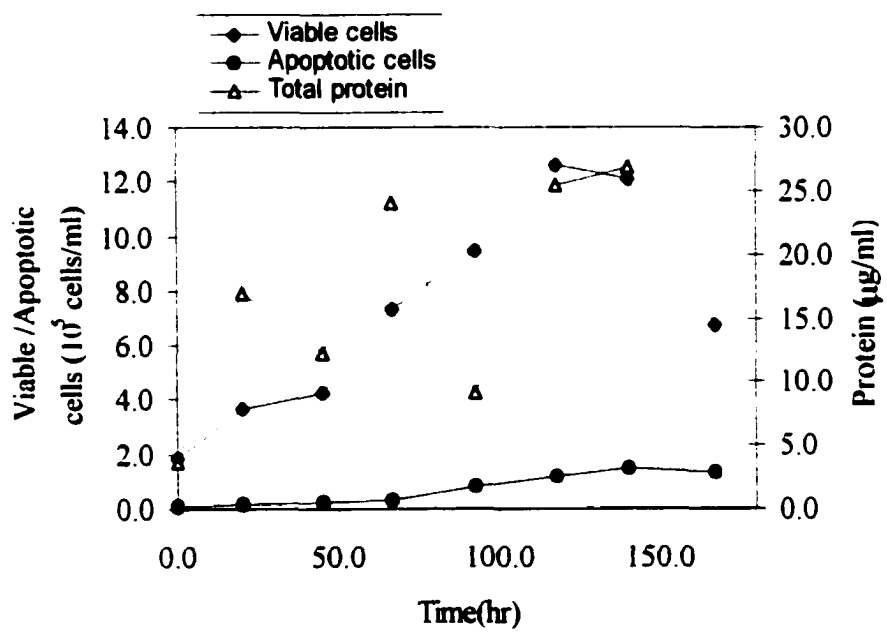

Figure 6.10 Batch fermentation results

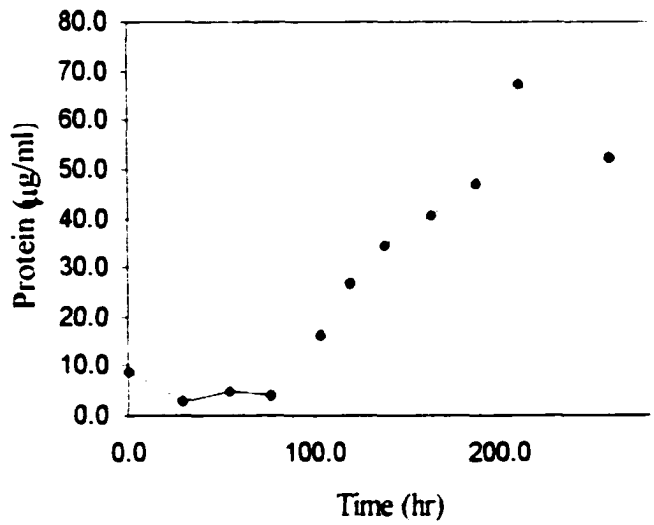

Figure. 6.11 Fed-batch fermentation

6.8 Conclusions

The methodology was proposed to control PCD and increased the protein production in a bioreactor. After estimating the state variables using an extended Kalman filter, a neural network was then used to approximate the concentration of apoptotic cells in the bioreactor based on the concentrations of viable cells, glutamine and asparagine. Based on the concentration of apoptotic cells, a model predictive controller was used to maintain control PCD at a concentration $1.0x10^5$ cells/ml. The maximum concentration of apoptotic cells was reduced from $1.5x10^5$ cells/ml to $1.1x10^5$ cells/ml. A higher protein

productivity was also obtained: 0.054 mg/(viable cells .h) for the fed-batch as compared to 0.014 mg for the batch operation.

6.9 References

Baughman, DR, Liu, YA 1995. Neural Networks in Bioprocessing and Chemical Engineering. San Diego, CA: Academic Press.

Bequette, BW. 1991. Nonlinear control of chemical processes: A review. Industrial & Engineering Chemistry Research 30:1391-1413.

Bharath, R, Drosen, J 1994. Neural Network Computing. New York, NY: McGraw-Hill.

Bitmead, R, Gevers, M, Wertz, V 1990. Adaptive optimal control: The thinking man's GPC. Englewood Cliffs, NJ: Prentice Hall.

Bogaerts, P. 1999. A hybrid asymptotic-Kalman observer for bioprocesses. Bioprocess Engineering 20:249-255.

Clarke, DW, Mohtad, C, Tuffs, PS. 1987. Genelarized Predictive Control - Part I. The basic algorithm. Automatica 23:137-148.

Cohen, JJ. 1993. Apoptosis. Immunology Today 14:126-130.

Cutler, CR, Ramaker, BL 1980. Dynamic Matrix Control - A computer control algorithm. In: Procedures of Automatic Control Conference, San Francisco, paper WP5-B.

Darzynkiewicz, Z, Bruno, S, Del Bino, G, Gorczyca, W, Hotz, M A. 1992. Features of apoptotic cells measured by flow cytometry. Cytometry 13: 795-808.

Darzynkiewicz, Z, Juan, G, Li, X, Gorczyca, W, Murakami, T, Traganos, T. 1997. Cytometry in cell neurobiology: Analysis of apoptosis and accidental cell death (necrosis). Cytometry 27:1-20.

De Keyser, RMC, Van Cauwenberghe, AR 1982. Typical application possibilities for self-tuning predictive control. In: Pages 975-980IFAC Symposium of Identification and System Parameter Estimation, Washigton, DC.

De Tremblay, M, Perrier, M, Chavarie, C, Archambault, J. 1992. Optimization of fed-batch culture of hybridoma cells using dynamic programming: single and multi feed cases. Bioprocess Engineering 9:229-234.

De la Broise, D, Noiseux, M, Massie, B, Lemieux, R. 1992. Hybridoma perfusion systems: a comparison study. Biotechnology and Bioengineering 40:25-32.

Dragunow, M, Young, D, Hughes, P, MacGibbon, G, Lawlor, P, Singleton, K, Sirimanne, E, Beilharz, E, Gluckman, P. 1993. Is c-Jun involved in nerve cell death following status epilepticus and hypoxic-ischaemic brain injury? Brain Research 4:347-352.

Eaton, JW, Rawlings, JB. 1992. Model predictive control of chemical processes. Chemical Engineering Science 47:705-720.

Eikens, B, Karim, MN. 1999. Process identification with multiple neural network models. International Journal of Control 72:576-590.

Freeman, JA 1994. Simulating neural networks with Mathematica. New York: Addison-Wesley Publishing Company.

Garcia, CE, Morshedi, AM. 1986. Quadratic programming solution of dynamic matrix control. Chemical Engineering Communications 46:73-87.

Isidori, A 1989. Nonlinear Control Systems. New York: Springer Verlag.

Kalman, RE, Bucy, RS. 1999. New results in linear filtering and prediction. Trans. ASME, Journal of Basic Eng. 20:249-255.

Karim, MN, Rivera, S. 1992. Artificial neural networks in bioprocess state estimation. Advances in Biochemical Engineering and Biotechnology 46:2-33.

Karim, MN, Yoshida, T, Rivera, SL, Saucedo, VM, Eikens, B, Oh, GS. 1997. Global and local neural network models in Biotechnology. Journal of Fermentation and Bioengineering 83:1-11.

Kleinman, DL. 1970. An easy way to stabilize a linear constant system. IEEE Transactions on Automatic Control 15:692-1000.

Korsmeyer, SJ. 1995. Regulators of cell death. Trends in Genetics 11:101-105.

Mercille, S, Massie, B. 1994. Introduction of apoptosis in nutrient-deprived cultures of hybridoma and myeloma cells. Biotechnology and Bioengineering 44:1140-1154.

Muske, KR, Rawlings, JB. 1993. Model predictive control with linear models. AIChE Journal 39:262-287.

Nunez, G, Clarke, MF. 1994. The Bcl-2 family of proteins: regulators of cell death and survival. Trends in Cell Biology 4:399-403.

Oltvai, ZN, Korsmeyer, SJ. 1994. Checkpoints of dueling dimers foil death wishes. Cell 79:189-192.

Ormerod, MG, Orr, RM, Peacock, JH. 1994. The role of apoptosis in cell killing by cisplatin: A flow cytometry study. British Journal of Cancer 69:93-100.

Patarinska, T, Dochain, D, Agathos, SN, Ganovski, L. 2000. Modelling of continuous microbial cultivation taking into account the memory effects. Bioprocess Engineering 22:517-527.

Patwardhan, AA, Rawlings, JB, Edgar, TF. 1990. Nonlinear model predictive control. Chemical Engineering Communications 87:123-141.

Perreault, J, Lemieux, R. 1994. Essential role of optimal protein synthesis in preventing the apoptotic death of culture *B* cell hybridomas. Cytotechnology 13:99-105.

Piret, JM, Cooney, CL. 1990. Model of oxygen transport limitations in hollow fiber bioreactors. Biotechnology and Bioengineering 37:80-92.

Proll, T, Karim, MN. 1994. Model-predictive pH control using real-time NARX approach. AIChE Journal 40:269-282.

Reed, JC. 1994. Bcl-2 and the regulation of programmed cell death. Journal of Cell Biology 124:1-6.

Richalet, J, Rault, A, Testud, JL, Papop, J. 1978. Model predictive heuristic control. Automatica 14:413-428.

Sakagami, H, Satoh, M, Yokote, Y, Takano, H, Takahama, M. 1998. Amino acid utilization during cell growth and apoptosis induction. Anticancer Reseach 18:4303-4306.

Sanfeliu, A, Stephanopoulos, G. 1999. Effect of glutamine limitation of the death of attached Chinese Hamster Ovary cells. Biotechnology and Bioengineering 64:46-53.

Sargantanis, IG, Karim, MN. 1999. Variable structure NARX models: Application to dissolved-oxygen bioprocess. AIChE Journal 45:2034-2045.

Sargantanis, JG, Karim, MN. 1994. Multivariate iterated extended kalman filter based adaptive control: Case study of solid substrate fermentation. Industrial & Engineering Chemistry Research 33:878-888.

Savill, JS, Wyllie, AH, Henson, JE, Walport, MJ, Henson, PM, Hasiett, C. 1989. Macrophage phagocytosis of aging neutrophilis in inflammation. Journal of Clinical Investigation 83:865-875.

Simon, L, Karim, MN, Schreiweis, A. 1998. Prediction and classification of different phases in a fermentation using neural networks. Biotechnology Techniques 12:301-304.

Simon, L, Karim, MN. 2000. Probabilistic neural networks using Bayesian decision strategies and a modified Gompertz model for growth phase classification. Biochemical Engineering Journal 7:41-48.

Sistu, PB, Bequette, BW. 1996. Nonlinear model-predictive control: Closed-loop stability analysis. AIChE Journal 42:3388-3402.

Steller, H. 1995. Mechanisms and genes of cellular suicide. Science 267:1445-1449.

Telford, WG, King, LE, Fraker, PJ. 1994. Rapid quantification of apoptosis in pure and heteregeneous cell pupulation using flow cytometry. Cytometry 172:1-16.

Van Furth, R, Van Zwet, TL. 1988. Immucytochemical detection of 5-bromo-2-deoxyuridine incorporation in individual cells. Journal of Immunological Methods 108:45-51.

Williams, D, Montgomery, PA. 1986. Multivariable adaptive control of baker's yeast fermentation. IEE Proceedings 133:247-264.

Wyllie, AH, Kerr, JFR, Currie, AR. 1980. Cell death: The significance of apoptosis. International Review of Cytology 68:251-306.

Yamamoto, S, Hashimoto, M 1991. Present status and future needs: The view from Japenese Industry. In: Proc. of CPC-IV, San Padre Island, Texas.

Chapter 7

CONCLUDING REMARKS AND ORIENTATIONS FOR FUTURE WORKS

7.1 Contributions

Pharmaceutical companies are interested in apoptosis research because PCD plays a key role in diseases such as cancer, stroke, Parkinston's and Huntington's diseases (Defrancesco, 2001). Understanding and controlling of apoptosis will, in fact, be accompanied by the discovery of new drugs and therapeutics (Agres, 2001). Metabolic engineering approaches have been used to increase or decrease the sensitivity of mammalian cells to PCD (Denmeade and Isaacs, 1996). Sing et al., for instance, used *bcl-2* gene to delay the onset of apoptosis in mammalian cells (Singh et al., 1997). However, transfected cultures may become unstable in repetitive fed-batch operations. There has also been evidence that *bcl-2* over-expression failed to protect NSO cells from apoptosis (Murray et al., 1996).

This contribution offers an alternative approach to control starvation-induced apoptosis as a result of amino acid deprivation. Neural network input sensitivity analysis was used to select amino acids (asparagine and glutamine) that could delay the onset of apoptosis. This information was used to maintain apoptotic cells at a concentration of 1.0

$\times 10^5$ cells/ml and to increase protein productivity. The methods outlined can be applied to industrial mammalian cell cultivations.

Additional contributions of this research are the applications of statistical tools and advanced process control algorithms to improve the performance of fermentation processes. After the selection of amino acids by NN sensitivity analysis, model predictive controllers were used to control PCD. A first principle model was initially derived to allow for step-ahead predictions of the state variables. Corrective control actions were then taken to force apoptotic cells to follow a desired trajectory. This approach proved that sophisticated instrumentations are not necessary for real-time control implementation. Off-line measurements of the concentrations of total and viable cells, lactate and glucose were used to update the fermentation state variables. Matlab^R was then used to calculate the flow rates of glucose, asparagine, and glutamine. The pumps were activated manually to supply the required flow rates.

In this work, we have extended classical mammalian cell kinetic models to account for PCD. An apoptotic death rate was defined as a NN function of viable cells, glutamine and asparagine. This approach also allows the inclusion in the cellular growth model of additional factors that may be responsible for apoptosis. Thus, the present methodology can be applied to reduce apoptotic cell death in different mammalian cell lines. The pro-apoptotic elements would be identified by a neural network-based sensitivity analysis and fed-back into the medium at flow rates set by an MPC controller.

7.2 Suggestions for Future Works

Several aspects of this study can be investigated further. The process can be completely automated by using an HPLC for real-time measurements of the amino acids that play a key role on the onset of apoptosis. With a sensor for viable cells, one can approximate the concentration of apoptotic cells.

Observability of nonlinear systems is very important for biological processes. In the paper entitled "Advanced Process Control in CHO Cell Culture Processes: Experimental Studies," it was shown that the concentration of asparagine was not observable after linearization of the model equations. However, it is obvious from the original nonlinear model that the concentration of asparagine is a function of viable cells. Additional research should be done in the area of observability of nonlinear systems because of the wide use of filters to estimate fermentation states due to a lack of biosensors. Theories of Lie derivatives can be further studied to address this issue.

The use of MPC to control biological processes such as apoptotic death has tremendous benefits. The algorithm can be formulated to include plant constraints and nonlinearity. However, for biological systems, MPC designers need to take into account the time varying nature of kinetic growth models. The calculation of the key parameters such maximum specific growth rate, protein yield may vary in the course of the fermentation. Thus, the applications of Robust MPC to biotechnology are a promising area of research.

A linear time-varying system of the form

$$\begin{aligned} &\mathbf{x}(k+1) = \mathbf{A}(k)\mathbf{x}(k) + \mathbf{B}(k)\mathbf{u}(k), \\ &\mathbf{y}(k) = \mathbf{C}\mathbf{X}(k), \\ &[\mathbf{A}(k) \quad \mathbf{B}(k)] \in \Omega \end{aligned} \tag{1}$$

can be used to approximate the kinetic model of the CHO cells. The components of $\mathbf{x}(k)$ are $X_T(k)$, $X_v(k)$, $X_{dn}(k)$, Gln(k), Am(k), Lac(k), Glc(k), Asn(k), P(k), V(k). The components of $\mathbf{u}(k)$ are the flow rates of glucose, asparagine, and glutamine. The vector $\mathbf{y}(k)$ is made up of the concentrations of total and viable cells, lactate and glucose. Ω is a family of plant. Following the work of Kothare M.V. et al., an unconstrained infinite horizon MPC can be formulated as (Kothare et al., 1996)

$$\min_{u(k+i|k), i=0,1,\ldots,m-1} \quad \max_{[A(k+i) \quad B(k+i)] \in \Omega, i \geq 0} J_\infty(k) \tag{2}$$

with

$$J_\infty(k) = \sum_{i=0}^{\infty} \left[x(k+i|k)^T Q_1 x(k+i|k) + u(k+i|k)^T R u(k+i|k) \right] \tag{3}$$

in which Q_1 and R are symmetric weighting matrices, m is the input or control horizon, $J_\infty(k)$ is the cost function over an infinite prediction horizon, Ω is a set defined by

$$\begin{aligned} &\Omega = Co\{[A_1 \quad B_1], [A_2 \quad B_2], \ldots, [A_L \quad B_L]\} \\ &[A \quad B] = \sum_{i=1}^{L} \lambda_i [[A_i \quad B_i] \\ &\lambda_i > 0 \\ &\lambda_1 + \lambda_2 + \ldots + \lambda_L = 1 \end{aligned} \tag{4}$$

where Co denote the convex hull. In the current research A_i, and B_i are the coefficient of the growth model obtained after linearizing around different operating points. Kothare et al. have shown that the system (2), (3), and (4) can be converted to a Linear Matrix Inequalities (LMI) problem of the form (Kothare et al., 1996):

$$u(k+i|k) = Fx(k+i|k), \quad i \geq 0 \tag{5}$$

$$F = YQ^{-1} \tag{6}$$

LMI formulation

$$\min_{\gamma, Q, Y} \gamma \tag{7}$$

Subject to

$$\begin{bmatrix} 1 & x(k|k)^T \\ x(k|k) & Q \end{bmatrix} \geq 0 \tag{8}$$

and

$$\begin{bmatrix} Q & QA_j^T + Y^T B_j^T & QQ_1^{1/2} & Y^T R^{1/2} \\ A_jQ + B_jY & Q & 0 & 0 \\ Q_1^{1/2}Q & 0 & \gamma I & 0 \\ R^{1/2}Y & 0 & 0 & \gamma I \end{bmatrix} \geq 0, \tag{9}$$

$$j = 1, 2, \ldots, L$$

Additional derivations are provided for the case of constrained MPC. LMI methodologies can be used to solve Equations (7) to (9).

Bioprocesses are characterized by changes in operating conditions as a result of variation in the metabolism of the cells. Moreover, these processes exhibit nonlinear behavior even in the neighborhood of the operating range and they are usually subjected to physical constraints. As a result, robust controllers will play a key role in validation and

control of bioprocesses. Additional research needs to be done to formulate a user-friendly framework for the applications of robust control algorithms to mammalian cell culture-type processes. LMI is a good starting point.

7.3 References

Agres, T. 2001. Drug makers on the apoptotic trail. The Scientist 15:18-19.

Defrancesco, L. 2001. Death in the balance. The Scientist 15:17-17.

Denmeade, SR, Isaacs, JT. 1996. Programmed cell death (apoptosis) and cancer chemotherapy. Cancer Control 3:306-309.

Kothare, MV, Balakrishnan, V, Morari, M. 1996. Robust constrained model predictive control using linear matrix inequalities. Automatica 32:1361-1379.

Murray, K, Ang, CE, Gull, K, Hickman, JA, Dickson, AJ. 1996. NS0 myeloma cell death: influence of bcl-2 overexpression. Biotechnology and Bioengineering 51:298-304.

Singh, RP, Simpson, NH, Perani, A, Goldenzon, C, Al-Rubeai, M. 1997. Essential amino acid deprivation of hybridoma cells results in the induction of high levels of apoptosis, which is suppressed by bcl-2 over-expression. The Genetic Engineer and Biotechnologist 17:121-124.

Chapter 8

APPENDIX

8.1 Cultivation Conditions

The CHO cell line, CHO 1-155500, obtained from ATCC (American Type Culture Collection, Manassas, VA) was used in this research. The cells produce recombinant tissue-type plasminogen activator (t-PA) that has clinical applications as a thrombolytic agent. The cells were initially thawed and diluted ten-fold (1 ml of culture and 9 ml of 90% HAM'S/F-12 medium and 10% fetal bovine serum). These were then transferred to a 75 ml T-flask containing 95% selection medium (Dulbecco's Modified Eagle Medium) and 5% dialyzed fetal bovine serum. The flask was placed in an incubator (VWR Scientific Products, model 2325, West Chester, PA) set at 37°C and 8 % carbon dioxide overlay. For subsequent studies, the cells grew in a 3-l bioreactor (New Brunswick, Scientific, CO., Inc., Edison, NJ). The pH (Cole-Parmer Instrument Company, Vernon Hills, Illinois) was controlled at 7.2 by addition of 1 M NaOH and carbon dioxide. The dissolved oxygen (Cole-Parmer Instrument Company, Vernon Hills, Illinois) was controlled at a concentration of 40% saturated air. The agitation speed was set at 80 RPM. The temperature was maintained at 37°C.

8.2 Sample Analysis

The concentration of total cells was measured using a hemacytometer. The samples were initially diluted to 2,000-20,000 cells per ml. Cell viability was assessed by the trypan blue exclusion method. Flow cytometry (Coulter EPICS V, Beckman Coulter Inc., Miami, FL) was the methodology employed to detect and quantify apoptotic cells. To quantify the percentage of apoptotic cells, a sample was initially centrifuged at 5000 RPM for 10 min. The sample was then washed twice in phosphate-buffered saline (PBS) (Sigma, St. Louis, MO), centrifuged and vortexed. They were then fixed in 2.5 mL of 70% ethanol and stored at -20°C. The cells were later incubated for 45 min at room temperature with 2.5 μg mL^{-1} RNase (Boehringer Mannheim, Indianapolis, IN). They were then washed twice in PBS. Propidium iodine (Sigma, St. Louis, MO) in the concentration of 50 μg mL^{-1} in PBS, was added for a 20-min staining period. After staining by propidium iodide, these cells were quantified using flow cytometry.

8.3 Kinetic Equations for the Fed-Batch Model

$$X_T(t) = X_v(t) + X_{da}(t) + X_{dn}(t) \tag{1}$$

$$\frac{d(X_v(t))}{dt} = (\mu - k_d)X_v(t) - \frac{F}{V}X_v(t) \tag{2}$$

$$\frac{d(X_{da}(t))}{dt} = k_{da}X_v(t) - \frac{F}{V}X_{da}(t) \tag{3}$$

$$\frac{d(X_{dn}(t))}{dt} = k_{dn}X_v(t) - \frac{F}{V}X_{dn}(t) \tag{4}$$

$$\mu = \frac{\mu_{max} Glc(t) Gln(t)}{(k_{Glc} + Glc(t))(k_{Gln} + Gln(t)) K_{inh}} \tag{5}$$

$$K_{inh} = \left(\frac{Glc(t)}{k_{Glc}} + 1\right)\left(\frac{Lac(t)}{k_{Lac}} + 1\right)\left(\frac{Am(t)}{k_{Am}} + 1\right) \tag{6}$$

$$k_d = k_{dn} + k_{da} \tag{7}$$

$$k_{dn} = const \tag{8}$$

$$k_{da} = f_{VN}(Gln, Ans) \tag{9}$$

$$\frac{d(Gln(t))}{dt} = \frac{F_{Gln} Gln_o}{V} - k_{deg} Gln(t) - q_{Gln} X_v(t) - \frac{F}{V} Gln(t) \tag{10}$$

$$\frac{d(Am(t))}{dt} = k_{deg} Gln(t) + q_{Am} X_v(t) - \frac{F}{V} Am(t) \tag{11}$$

$$\frac{d(Lac(t))}{dt} = \frac{\mu}{Y_{\frac{X_v}{Lac}}} X_v - \frac{F}{V} Lac(t) \tag{12}$$

$$\frac{d(Glc(t))}{dt} = \frac{F_{Glc} Glc_o}{V} - \frac{\mu}{Y_{\frac{X_v}{Glc}}} X_v(t) - \frac{F}{V} Glc(t) \tag{13}$$

$$\frac{d(Asn(t))}{dt} = \frac{F_{Asn} Asn_o}{V} - \frac{\mu}{Y_{\frac{X_v}{Asn}}} X_v(t) - \frac{F}{V} Asn(t) \tag{14}$$

$$\frac{d(P(t))}{dt} = \alpha \mu X_v(t) + \beta X_v(t) - \frac{F}{V} P(t) \tag{15}$$

$$\frac{dV}{dt} = F \tag{16}$$

$$F = F_{Asn} + F_{Glc} + F_{Gln} \tag{17}$$

8.4 Experimental and Fitted Data for Batch Fermentation Model

Fig. 8.1 shows the experimental and predicted concentrations of viable, total, necrotic, and apoptotic cells. The concentration of total cells was obtained using Eq. 1. Good agreement between the predicted and actual fermentation state variables was obtained for cells in the lag and exponential phases. The simulation under-predicts the viable and total cells at the end of the exponential phase.

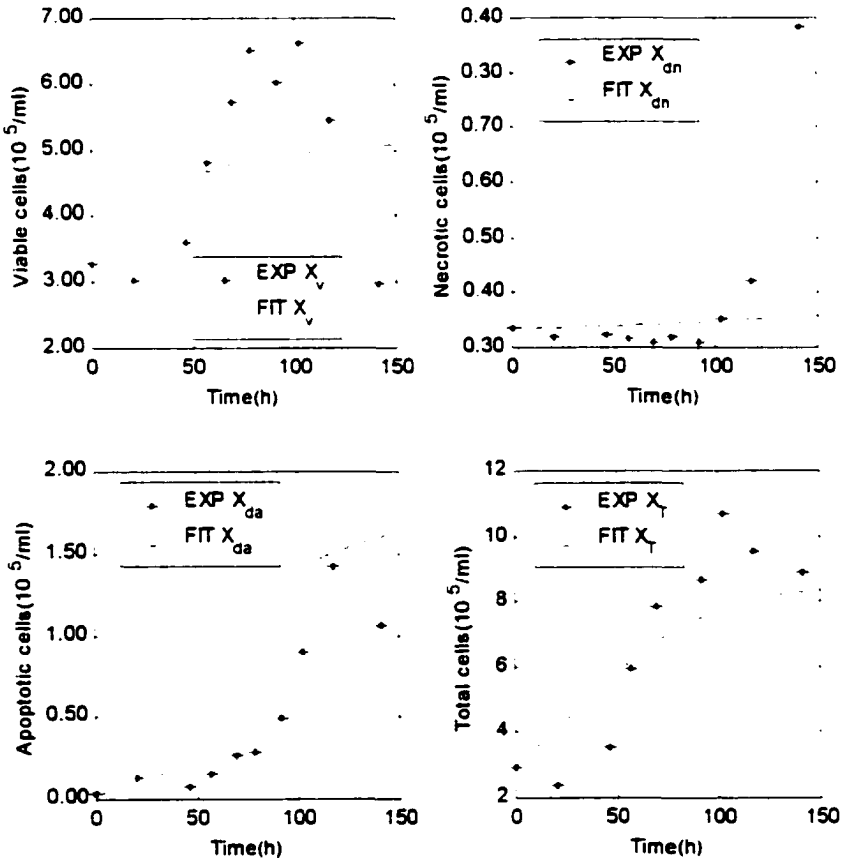

Fig 8.1 Experimental and fitted concentrations of viable, necrotic and apoptotic an total cells

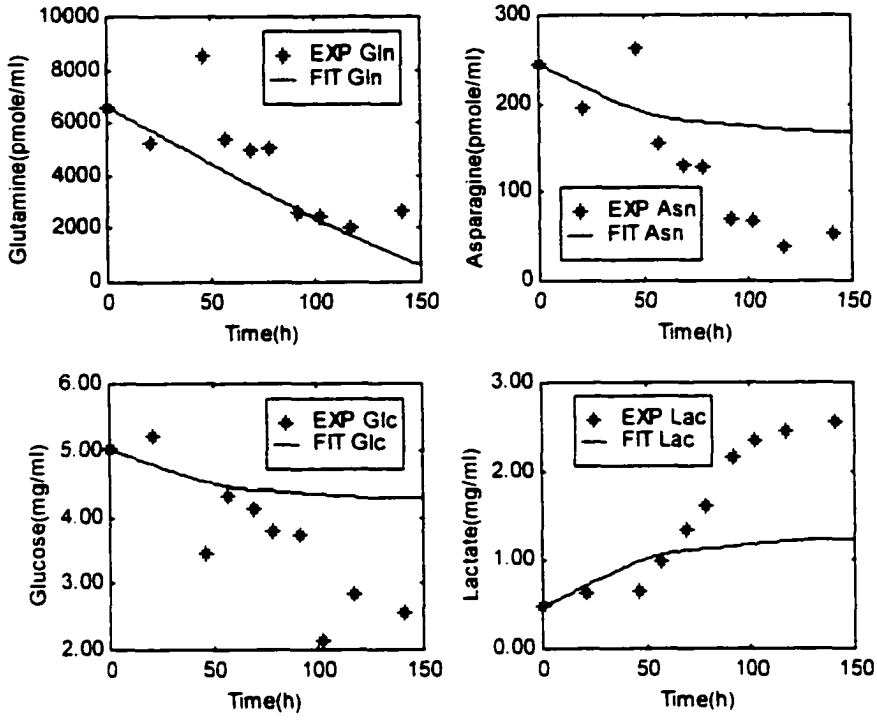

Fig 8.2 Experimental and fitted concentrations of glutamine, asparagine, glucose, and lactate

8.5 Open-loop Fed-batch Fermentation for Random Perturbation of Flow Rates

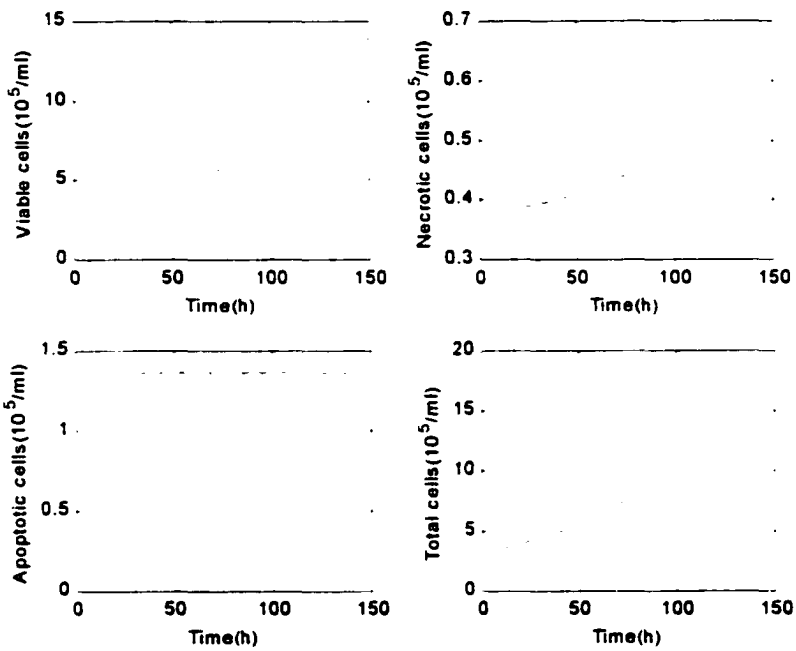

Fig 8.3 Concentrations of viable, necrotic, apoptotic and total cells for an open-loop fed-batch model of CHO cells

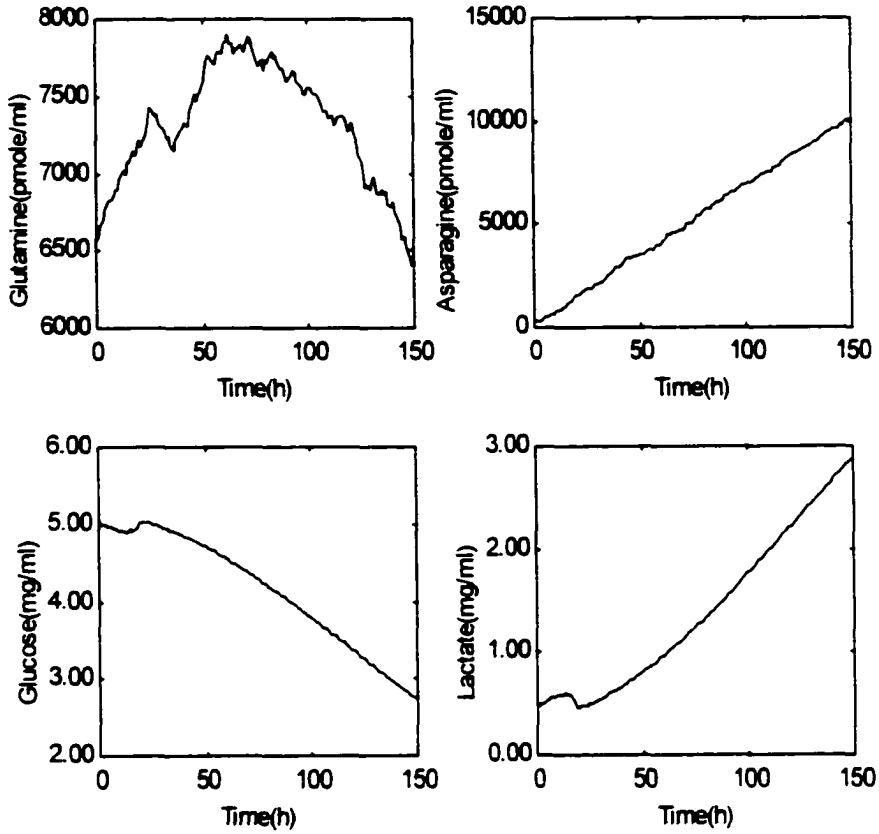

Fig 8.4 Concentrations of glutamine, asparagine, glucose, and lactate for an open-loop fed-batch model of CHO cells

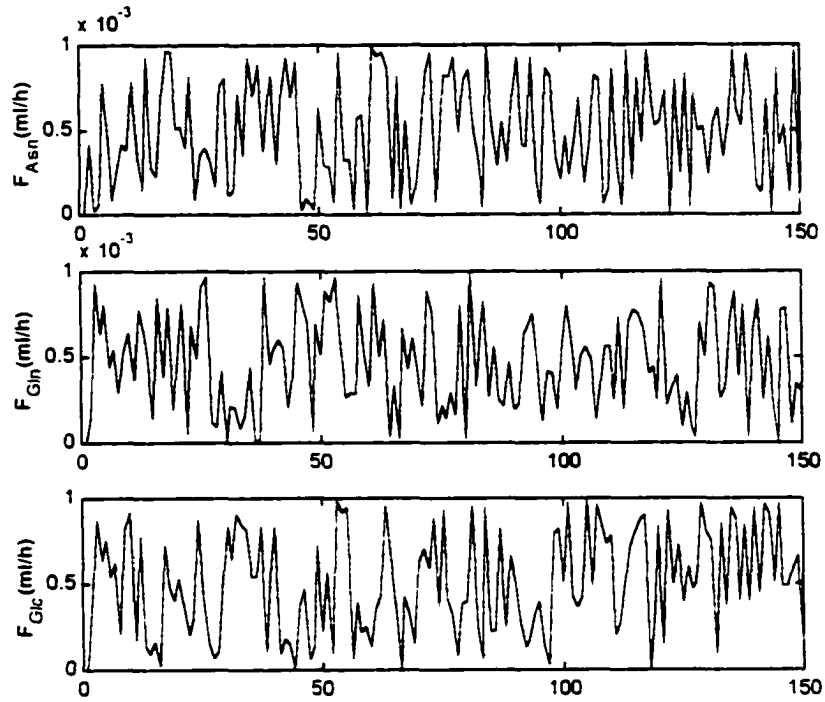

8.5 Flow rates of asparagine, glutamine and glucose lactate for an open-loop fed-batch model of CHO cells